BULLETIN OF THE EARTHQUAKE RESEARCH INSTITUTE,
UNIVERSITY OF TOKYO. Vol. 38, Part 4. December, 1960.

東京大学
地震研究所彙報

第 38 号　第 4 册

昭和 35 年 12 月

目　次

論文及報告

頁

29. 不均質な媒質内を伝る弾性波の安定性について 一見掛けの内部摩擦係数— (英文) ..... 吉山良一 467
30. 山形県関根・梓山地方の花崗質岩に含まれる捕獲岩 (英文) ..... 市村毅 479
31. 噴火予知に関する基礎的研究 (I) 火山活動に関連する地震と地殻変動 (英文) ..... 水上武 497
32. 電磁式地震計の磁気回路について (邦文) ..... 嶋悦三 545

所報

索引

(The titles in occidental languages are given on the back cover.)

地震研究所彙報は，年4回定期に（ただし，第1号より第6号までは不定期に，第7号は3冊として刊行された），彙報別冊は不定期に刊行される．

この彙報に載せられた論文及び報告についての責任は，すべてその著者のみにある．

この彙報についての照会通信は，すべて東京大学地震研究所長にあてられたい．

The Bulletin is published quarterly. (Vols. 1–6 were published at irregular intervals and Vol. 7 consisted of three parts.)
Supplementary Volume is published at irregular interval.

The authors of the papers alone are responsible for the statements and opinions contained in their respective papers.

All communications relating to this Bulletin should be addressed to the Director of the Earthquake Research Institute, University of Tokyo, Japan.

Earthquake Research Institute, University of Tokyo
Address:
No. 1, Motofuji-cho, Bunkyo-ku,
Tokyo Metropolis, Japan.
Telephone: 921-3161-Extension 6506
Cable address: ZISINKEN, TOKYO.

東京大学地震研究所
所在地
東京都文京区本富士町一番地
電話　小石川 921—3161 (代) 構内 6506
電略　ブンケウ　トウダイ　ヂシン

BULLETIN OF THE EARTHQUAKE RESEARCH INSTITUTE
Vol. 38 (1960), pp. 467-478

29. *Stability of Waves through a Heterogeneous Medium and Apparent Internal Friction.*

By Ryoichi YOSHIYAMA,

Earthquake Research Institute.

(Read Sept. 27, 1960.—Received Sept. 27, 1960.)

1. Introduction

The attenuation of seismic waves has been studied by many authors[1], and the present writer[2], too, has obtained some results in that sphere. Though the numerical precision of the information obtained is still questionable, it seems that the attenuation coefficient is almost inversely proportional to the period of the wave, and not to the square of the period, but, at the same time, it is slightly large for the waves with short period and, perhaps also, for the waves with a period in certain range. And examining various points noticed in the course of those studies, it seems necessary to find out some other mechanism of the attenuation of waves, in addition to the generally accepted ones. In this paper, an idea is presented for the elucidation of the above-mentioned relationship of the attenuation coefficient to the period from the stability of the wave through a heterogeneous medium, a preliminary reasoning of which was once explained in a previous paper[3]. Some allied problem was treated by Lord Rayleigh[4] soon after Hill studied the differential equation that is called after his name. However, besides that the main point of the problem, or in other words, manner of applying the mathematical results to the physical interpretation, is

1) M. EWING and F. PRESS, "An Investigation of Mantle Rayleigh Waves." *B.S.S.A.*, **44** (1954), 127-147; "Mantle Rayleigh Waves from the Kamchatka Earthquake of November 4, 1952." *B.S.S.A.*, **44** (1954), 471-479.

Y. SATÔ, "Attenuation, Dispersion, and the Wave Guide of the G Wave." *B.S.S.A.*, **48** (1958), 231-251.

2) R. YOSHIYAMA, "Maximum Amplitude and Epicentral Distance." *Bull. Earthq. Res. Inst.*, **37** (1959), 389-404; "Propagation of Surface Waves and Internal Friction." *Bull. Earthq. Res. Inst.*, **38** (1960), 361-368.

3) R. YOSHIYAMA, "Waves through a heterogeneous medium." (in Japanese). *Zisin*, I-**14** (1941), 363-366.

4) Lord Rayleigh, "Maintenance of vibrations by forces of double frequency, and propagation of waves through a medium with a periodic structure." *Sci. Papers.* Vol. 3. 1-14.

different, the mathematical method is somewhat improved in the writer's studies by a reformation of the differential equation.

2. Recapitulation from previous studies with some extension

For simplicity's sake in the mathematical treatment, it is assumed that the property of the medium changes in one direction x, and a plain wave is propagated in that direction: propagation of P-wave or SH-wave of normal incidence applies to this case. The equation of motion of the wave is given by,

$$\rho\frac{\partial^2 u}{\partial T^2}=\frac{\partial}{\partial x}\left(E\frac{\partial u}{\partial x}\right), \tag{1}$$

where T is time-coordinate. E, elastic constant, stands for $\lambda+2\mu$ in the case of P-wave, for μ in the case of SH-wave, and is a function of x; whether density ρ may be a function of x or a constant, it does not affect the main part of the results of the discussion in this paper. u is a component of displacement: x-component in the case of P-wave, and a transverse component perpendicular to x in the case of SH-wave. The velocity of propagation of the wave is

$$c(x)=\sqrt{\frac{E}{\rho}}\,. \tag{2}$$

Following the method of mathematical treatment developed in a previous paper, the travel time, t, of the wave is used for space co-ordinate in place of x, where t is defined by,

$$t=\int\frac{dx}{c(x)}\,. \tag{3}$$

And putting $\sqrt{\rho c}\,u=\phi(t, T)$, we obtain, from (1), a differential equation for ϕ as follows:

$$\frac{\partial^2\phi}{\partial T^2}=\frac{\partial^2\phi}{\partial t^2}-\alpha^2\phi\,, \tag{4}$$

where

$$\alpha^2=c^2\left\{\frac{1}{\sqrt{E}}\frac{d^2\sqrt{E}}{dx^2}-\frac{1}{\sqrt{c}}\frac{d^2\sqrt{c}}{dx^2}\right\},$$

or, putting $K=\rho c$,

$$=c^2\left\{\frac{\sqrt{\rho}}{K}\frac{d^2}{dx^2}\frac{K}{\sqrt{\rho}}-\sqrt{\frac{\rho}{K}}\frac{d^2}{dx^2}\sqrt{\frac{K}{\rho}}\right\}. \tag{5}$$

In a heterogeneous medium, α^2 is originally a function of x, and is transformed into a function of t in virtue of (3), and α^2 vanishes when the medium is homogeneous. If we neglect the change of α^2 from place to place, the solution of the equation (4) is obtained,

$$\phi(t, T)=\exp i(pT\pm\sqrt{p^2-\alpha^2}t) . \tag{6}$$

So that,

$$u=\frac{1}{\sqrt{\rho c}}\exp i(pT\pm\sqrt{p^2-\alpha^2}t) , \tag{7}$$

$K=\rho c$ is called in acoustics specific acoustic impedance, and, when it is constant, α^2 vanishes, even if the medium is heterogeneous; the results from such an assumption, however, will have little importance in the application to the study of seismic bodily waves. On the other hand, in some cases, for example, when $\rho=$const. and $c=a+bx$, α^2 turns out a constant, and (7) is a rigorous solution of the equation of motion (1); since these assumptions are conventionally used and the solution is rigorous, (7) will be useful in some future studies. α^2 effects a non-dissipative attenuation of the wave, arising in nature from selective reflection: reflection of this kind was studied by Matuzawa[5].

One of the important problems related to the study of seismic waves occurs when the medium has a periodic, or, in general, fluctuating structure in a certain direction; though it is assumed in this paper to set about the mathematical study of the problem that $\rho=$const. and $c(x)=a(1+b\cos\gamma x)$, the simplest of oscillatory functions, we may be able to deduce some fundamental properties of the wave through the medium in consideration.

3. Reasoning to apparent internal friction

Putting $c(x)=a(1+b\cos\gamma x)$ in (2),

$$t=\frac{2}{a\gamma\sqrt{1-b^2}}\tan^{-1}\frac{\sqrt{1-b^2}}{1+b}\tan\frac{\gamma x}{2} ,$$

$$x=\frac{2}{\gamma}\tan^{-1}\frac{1+b}{\sqrt{1-b^2}}\tan\frac{\gamma at\sqrt{1-b^2}}{2} . \tag{8}$$

And, if we assume ρ constant, we have from (5),

5) T. MATUZAWA; "Reflexion und Refraktion der seismischen Wellen durch eine kontinuierlich verändernde Schicht," *Bull. Earthq. Res. Inst.*, **33** (1955), 543–548.

$$\alpha^2=\frac{\sqrt{c}}{3}\frac{d^2}{dx^2}c^{\frac{3}{2}}\,. \tag{9}$$

Assuming $c(x)=a(1+b\cos\gamma x)$, applying $x-t$ relation given by (8), and denoting $\gamma at\sqrt{1-b^2}/2$ by z, we obtain from (9),

$$c(x)=a(1+b\cos\gamma x)=\frac{a(1-b^2)}{1-b\cos 2z}\,,$$

$$\alpha^2=\frac{\gamma^2a^2(1-b^2)}{4(1-b\cos 2z)^2}\,b\left\{\frac{5}{2}b-2\cos 2z-\frac{b}{2}\cos 4z\right\}\,. \tag{10}$$

So that, putting $\phi(t,\,T)=\phi_1(t)\exp(ipT)$ in (4), p being a circular frequency of the wave, a differential equation for $\phi_1(t)$ is obtained as follows:

$$\frac{d^2\phi_1}{dz^2}+\left\{q^2+\frac{b(-5b+4\cos 2z+b\cos 4z)}{2(1-b\cos 2z)^2}\right\}\phi_1=0\,, \tag{11}$$

$$q=\frac{2p}{a\gamma\sqrt{1-b^2}}\,;\qquad z=\frac{\gamma at\sqrt{1-b^2}}{2}\,,$$

which is clearly on the lines of Hill's equation, and, assuming that b is small, (11) is transformed approximately to Mathieu's equation. Since,

$$\frac{b(-5b+4\cos 2z+b\cos 4z)}{2(1-b\cos 2z)^2}=b\left\{-\frac{b}{2}+2\cos 2z+\frac{5}{2}b\cos 4z+\mathrm{O}(b^2)\right\}\,,$$

it is approximately

$$\frac{d^2\phi_1}{dz^2}+\left\{q^2+2b\cos 2z\right\}\phi_1=0\,. \tag{12}$$

Then we have a solution of $\phi_1(z)$, when z is large, in the form,

$$\phi_1(z)=\psi(z)\exp(-\mu z)\,, \tag{13}$$

where $\psi(z)$ is a periodic function of z. Therefore, the attenuation of ϕ_1, which consequently applies to that of the wave is determined by μ in (13). According to the theory of Mathieu's equation, when b is fixed, μ is a function of q^2, and the largest real value of μ, for a range of $q^2\geq 0$, is

$$\mu_m\fallingdotseq\frac{1}{2}|b|\,,\qquad \text{when } q^2\fallingdotseq 1-\frac{1}{8}b^2\,. \tag{14}$$

Under these conditions, the attenuation of the wave is given by

$\exp(-|b|z/2)$. So that the apparent or mean attenuation constant of the wave is $|b|z/2x$, which is equal to $|b|\gamma at\sqrt{1-b^2}/4x$, or approximately to $|b\gamma|/4$.

Suppose a wave of a certain period, then p is specified. And γ-value which satisfies (14) for the specified p is approximately given by,

$$q\simeq 1\ ; \qquad \gamma=2p/a\ . \tag{15}$$

If the wave length of the periodic structure of the medium is L, $\gamma=2\pi/L$. So that, from (15), the L-value that effects the largest attenuation to the wave whose period is $\tau=2\pi/p$ is given by,

$$L=a\tau/2\ . \tag{16}$$

It is a debatable point whether we have the L-value represented by (16) in the actual structure of the earth for the wave of an assigned period τ. If we assume that there is always, that means for any period of the wave, or, at least, for a certain range of period of the wave, such L-value that satisfies (16) in the structure, the attenuation constant of the wave of the period of that range is $|b\gamma|/4$, or, putting $\gamma=2p/a$, $|b|\pi/a\tau$. Consequently, apparent, or say, equivalent, internal friction on account of heterogeneity, $1/Q'$ is

$$1/Q'=|b|\ . \tag{17}$$

$1/Q'$ diminishes the wave amplitude in the course of its propagation, and the attenuation effect is clearly additive to the genuine internal friction, if any. The mechanism of the attenuation caused by $1/Q'$ is not, however, dissipative; it means that some part of the energy of the wave is transformed into harmonic waves. Those circumstances will be understood, also, from the results obtained in a previous paper[6] which proves that there is a generation of a characteristic stationary wave and diminution of the amplitude of the first shock. In this case, the harmonic waves generated are given by each term in the infinite harmonic series $\psi(z)$ of (13). Those harmonic waves will be studied in the near future, and until the study is finalised some doubtful points will remain unsolved, from a theoretical point of view, in the acceptance of formula (17), because the solution of Mathieu's equation is too complicated to be easily adapted to the mathematical description of the propagation of waves. In spite of some uncertainties, we can assume that the order of magni-

6) R. YOSHIYAMA, "Elastic Waves from a Point in an Isotropic Heterogeneous Sphere. Part 2," *Bull. Earthq. Res. Inst.*, **18** (1940), 41-56.

tude of $1/Q'$ can not be much different at any rate from that set down in (17), and the effect of the heterogeneity of the medium in the apparent attenuation of the waves will not be negligible, since the internal friction computed from the observations of seismic waves is also a small quantity and does not exceed 9.10^{-3}. Of course, the above stated results are worked out to apply to special bodily waves, but will be applicable to some extent even to surface waves; at least, if it is said generally, the attenuation effect will not be less than for bodily waves. And the magnitude of b, that is a measure of the irregularities of structure in the horizontal direction, as large as 10^{-2} will be reasonably presumable in any district, if it is expected to cover some hundred kilometres, and if it is expected, also, in some range to have an arbitrary wave length, to effect the largest attenuation to the wave with a certain period. On the other hand, the present writer expects the effect of the heterogeneity of the earth's crust of the order of magnitude $3-5\times10^{-3}$, at the largest, in $1/Q'$, to fill up some part of the difference between the two internal frictions, one being obtained from the computation of a surface wave with a long period which ranges from fifty seconds to some hundreds of seconds, and the other from the study of "Maximum amplitude and the Epicentral distance relation" of large earthquakes in Japan, in which the period of the seismic waves ranges from a few seconds to several seconds.

For a given small b-value, real μ decreases very rapidly either for $q^2>1$ or for $q^2<1$, and, for a certain range of q^2, μ is a pure imaginary. So that, the attenuation of the wave, whose period is τ, by the periodic structure of a wave length other than that which exerts the largest effect and is obtained above in (16), is negligible.

4. Theoretical calculation and some remarks

As already mentioned, it seems to the writer that the solution of Mathieu's equation, hitherto obtained, is not satisfactory for a straightforward study of the propagation of waves; the solution implies inseparable two sets of waves, primary waves and reflected waves. Though the co-existence of the two sets of waves will be an important property, utterly natural in itself, of waves through the medium with a periodic structure, it gives rise to some theoretical difficulties, when we try to interpret physically the solution for the elucidation of a progressive wave. To remove those difficulties completely, analytical study of the

solution, or reformation of the infinite series of the solution will be necessary. However, it is not a problem to be solved easily. And, in this paper, to remove a part of those difficulties and to arrive at formula (17), the following example is studied.

A three layered medium is assumed as shown in Fig. 1; two of the three, I and III, are homogeneous, and the intermediate medium, II, is the one that is considered with a special interest in this paper, having a periodic structure. A sinusoidal wave with a period $\tau=2\pi/p$ is propagated from medium I to medium III through medium II; $\boldsymbol{A}_1$, $\boldsymbol{A}_2$ and $\boldsymbol{A}_3$ are the displacement vectors in each medium caused by the wave propagated in x-direction, x-direction being assumed from medium I to medium III; $\boldsymbol{B}_1$ and $\boldsymbol{B}_2$ are those from the wave in the opposite direction; clearly $\boldsymbol{B}_3$ is zero. Then it follows;

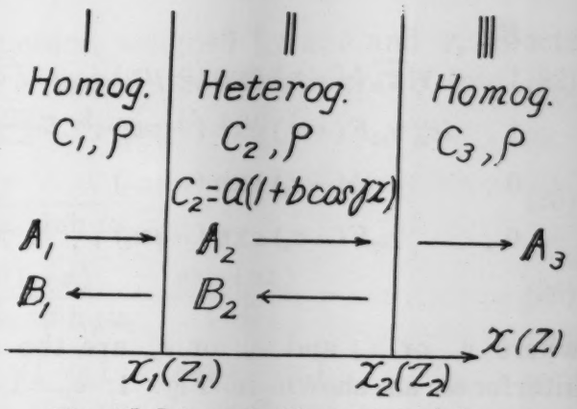

Fig. 1. Schematic illustration of the assumption and the notations.

$$\text{I.}\quad \boldsymbol{A}_1=\frac{A_1}{\sqrt{\rho_1 c_1}}\exp(ipT)\exp\{-ik_1(x-x_1)\}\,, \tag{18}$$

$$\boldsymbol{B}_1=\frac{B_1}{\sqrt{\rho_1 c_1}}\exp(ipT)\exp\{ik_1(x-x_1)\}\,,$$

$$\text{II.}\quad \boldsymbol{A}_2+\boldsymbol{B}_2=\frac{1}{\sqrt{\rho_2 c_2}}\exp(ipT)\{A_2\psi(-z)\exp(-\mu z)+B_2\psi(z)\exp(\mu z)\}\,, \tag{19}$$

$$\text{III.}\quad \boldsymbol{A}_3=\frac{A_3}{\sqrt{\rho_3 c_3}}\exp(ipT)\exp\{-ik_3(x-x_2)\}\,, \tag{20}$$

c_1 and c_3 are constant respectively, while $c_2=a(1+b\cos\gamma x)$. There will be no necessity to explain the notations in (18) and (20). The formula in the bracket of (19) is the complete solution of Mathieu's equation (12); in (13), one of the two terms, which diverges at $x=\infty$, was discarded and the study of theoretical basis of such discarding is one of the subjects in this section.

When $q^2\fallingdotseq 1$ and b is small, the function in the complete solution of Mathieu's equation is given by,

$$\psi(z)\fallingdotseq\sin(z-\sigma)+s_3\sin(3z-\sigma) \tag{21}$$

where $\sigma=\pi/4$, $s_3=b/8$ and $\mu=b/2$, regardless of the sign of b. $\psi(-z)$ is obtained by putting $\sigma=-\pi/4$. Boundary conditions at the two interfaces, that imply continuity of displacement and stress, assign four simultaneous equations to determine B_1, A_2, B_2 and A_3 in A_1. Those equations are obtained in the following, being only assumed that density ρ is constant throughout the whole medium:

$$\begin{array}{rrrrr} B_1 & +A_2 & +B_2 & +A_3=A_1 & \\ -1\,, & \sqrt{c_{12}}\psi(-z_1)\exp(-\mu z_1)\,, & \sqrt{c_{12}}\psi(z_1)\exp(\mu z_1)\,, & 0\,, & 1\,. \\ 1\,, & ic_{21}^{3/2}\gamma_{12}F(-z_1)\exp(-\mu z_1)\,, & ic_{21}^{3/2}\gamma_{12}F(z_1)\exp(\mu z_1)\,, & 0\,, & 1\,. \\ 0\,, & \psi(-z_2)\exp(-\mu z_2)\,, & \psi(z_2)\exp(\mu z_2)\,, & -\sqrt{c_{23}}\,, & 0\,. \\ 0\,, & \gamma_{32}F(-z_2)\exp(-\mu z_2)\,, & \gamma_{32}F(z_2)\exp(\mu z_2)\,, & ic_{32}^{3/2}\,, & 0\,. \end{array} \tag{22}$$

where x_1, or z_1, and x_2, or z_2, are the x- or z-co-ordinates of the two interfaces as shown in Fig. 1; $c_{12}=1/c_{21}=c_1/c_2$ at $x_1(z_1)$, $c_{23}=1/c_{32}=c_2/c_3$ at $x_2(z_2)$; $\gamma_{12}=\gamma a\sqrt{1-b^2}/2k_1c_2(x_1)$, $\gamma_{32}=\gamma a\sqrt{1-b^2}/2k_3c_2(x_2)$;

$$F(z)=\left\{\frac{2c_2}{\gamma a\sqrt{1-b^2}}\cdot\sqrt{c_2}\frac{d}{dx}\frac{1}{\sqrt{c_2}}+\mu\right\}\psi(z)+\frac{d\psi(z)}{dz}$$

$$F(-z)=\left\{\frac{2c_2}{\gamma a\sqrt{1-b^2}}\cdot\sqrt{c_2}\frac{d}{dx}\frac{1}{\sqrt{c_2}}-\mu\right\}\psi(-z)+\frac{d\psi(-z)}{dz}\,. \tag{23}$$

Considering the limited purposes of our study at present, we may assume for the sake of mathematical simplicity the following: 1) origins of x- and z-co-ordinates are at the interface of the I and the II medium, i.e., $x_1=z_1=0$, then we may put $z_2=z_0$; 2) $c_1=c_3$; 3) velocity of propagation and its gradient are continuous at the interfaces. After all, our assumption on the velocity distribution throughout the whole medium is such as shown in Fig. 2; then the co-ordinates of the interface between II and III is $x_2=2n\pi/\gamma$, or $z_2(z_0)=n\pi$. From these assumptions, it follows, putting $z_1=0$, $z_2(z_0)=n\pi$;

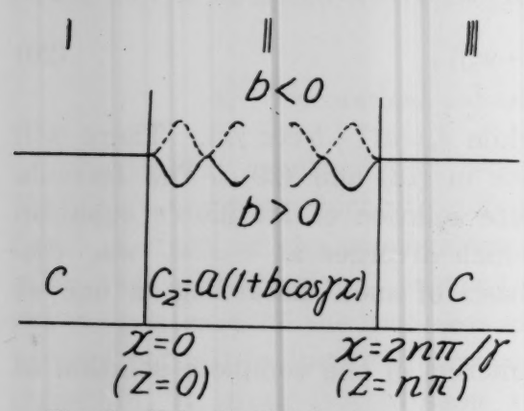

Fig. 2. Velocity distribution, assumed.

$$\begin{aligned}
&\psi(z_1)=-(1+s_3)/\sqrt{2}=-\psi(-z_1)\ ,\\
&\psi(z_2)=(-1)^{n+1}(1+s_3)/\sqrt{2}=-\psi(-z_2)\ ,\\
&F(z_1)=(1-s_3)/\sqrt{2}=F(-z_1)\ ,\\
&F(z_2)=(-1)^n(1-s_3)/\sqrt{2}=F(-z_2)\ , \qquad s_3=b/8\\
&\quad c_{12}=c_{21}=c_{23}=c_{32}=1\ ,\\
&\quad \gamma_{12}=\gamma_{32}=\gamma a\sqrt{1-b^2}/2p\ .
\end{aligned} \tag{24}$$

For the wave, to which this structure, assigned by a, b and γ, effects the largest attenuation, $\gamma a\sqrt{1-b^2}/2p \fallingdotseq 1$. Substituting (24) into (22) and solving the equations, we obtain A_3, A_2, B_2 and B_1:

$$\frac{A_3}{A_1}=\frac{(-1)^n}{\cosh \mu z_0-2is_3 \sinh \mu z_0} \tag{25}$$

$$\frac{A_2}{A_1}=\frac{(1-s_3)-i(1+s_3)}{\cosh \mu z_0-2is_3 \sinh \mu z_0}\cdot\frac{\exp(\mu z_0)}{\sqrt{2}} \tag{26}$$

$$\frac{B_2}{A_1}=\frac{-(1-s_3)-i(1+s_3)}{\cosh \mu z_0-2is_3 \sinh \mu z_0}\cdot\frac{\exp(-\mu z_0)}{\sqrt{2}} \tag{27}$$

$$\frac{B_1}{A_1}=\frac{-i \sinh \mu z_0}{\cosh \mu z_0-2is_3 \sinh \mu z_0}\ , \tag{28}$$

$$(\mu=b/2,\ s_3=b/8)$$

z_0 is proportional to the thickness of the medium II and, accordingly, to the distance over which the wave is propagated through the medium of a periodic structure. From (25), when $z_0=0$, $A_3/A_1=1$; and when z_0 is large,

$$\frac{A_3}{A_1}=\frac{2\exp(-|\mu|z_0)}{1-2is_3}\ . \tag{29}$$

Therefore, at large distances, $|A_3|$ decreases as $\exp(-|\mu|z_0)$; this result may be interpreted to support our reasoning based on (13). At the same time, however, we must notice, that if the amplitude at the origin is estimated by (13) from observations at large distances, it will be over-estimated almost twofold, chiefly because of the difference between $\exp(-|\mu|z_0)$ and $1/\cosh \mu z_0$; the non-dissipative attenuation concerned contrasts in this point with the ordinary dissipative one, in which we have two linearly independent particular solutions with $\exp(-|\mu|z)$ and none with $\exp(|\mu|z)$.

Concerning $\boldsymbol{A}_2+\boldsymbol{B}_2$, according as $b>0$ or $b<0$, there is a slight change of the notations in the following description, which clearly never

affects the main point of the discussion. We may assume, for the present, $b>0$. The wave motion in medium II, when z_0-z, which is always positive in medium II, is large, contribution to A_2+B_2 from B_2 vanishes, and the wave motion is expressed by A_2 only. So that, when z_0 is large, while z is fixed,

$$A_2+B_2=A_1\frac{\exp(ipT)}{\sqrt{\rho_2 c_2}}\cdot\frac{\sqrt{2}\{(1-s_3)-i(1+s_3)\}}{1-2is_3}\cdot\psi(-z)\exp(-\mu z), \tag{30}$$

A_2+B_2 in (30) expresses clearly a stationary wave, whose amplitude decreases as $\exp(-\mu z)$; it was already pointed out by Rayleigh that the wave propagated through the medium of a periodic structure is ultimately totally reflected back to the origin, and here obtained result also indicates the same conclusion. The behaviour of the primary wave apart from the reflected wave must be studied by the solution where z_0-z is not large, the intense effect of the reflected wave being avoided there. And, since $z_0>z_0-z>0$ in the medium, exponential factor of B_2 is transformed,

$$\exp(-\mu z_0)\cdot\exp(\mu z)=(1-\delta)\exp\mu(z_0-z)\ , \tag{31}$$

where $0<\delta<1$; $\delta=0$ when $\mu(z_0-z)=0$, $\delta=1$ when $\mu(z_0-z)=\infty$; and the problem to be studied is the case when $\delta\ll 1$. So that,

$$A_2+B_2=A_1\frac{\exp(ipT)}{\sqrt{\rho_2 c_2}}\cdot\frac{\exp\mu(z_0-z)}{\cosh\mu z_0-2is_3\sinh\mu z_0}$$

$$\times\left[\exp(-iz)-s_3\exp(iz)+s_3\exp(-i3z)+\frac{\delta}{\sqrt{2}}\{(1-s_3)+i(1+s_3)\}\psi(z)\right]. \tag{32}$$

We can see in (32) the primary wave progressing in $+x$ direction with a small quantity of its reflected wave, the 3rd harmonic wave in the same direction with the primary wave and stationary wave whose amplitude is proportional to δ; phase velocity of the 3rd harmonic wave is one third of the primary waves.

Concerning the reflected wave in medium I, as z_0 tends from zero to infinity, $|B_1/A_1|$ increases from zero to $1/\sqrt{1+4s_3^2}$, almost equal to unity, but that it is less than unity altogether implies that some energies are kept as a stationary wave in medium II. If we take simply $b=0$, $\sinh\mu z_0=0$ then $|B_1/A_1|=0$, but, if we take $z_0=1/b^2$ and $b\to 0$, then $|B_1/A_1|=1$. Here we have a special type of total reflection, the phase angle being shifted by $\pi/2$.

It is to be noted especially that we have harmonic waves neither in the refracted wave through medium III, nor in the reflected wave through

medium I. Therefore, considering the complicated structure of the earth, it will be understood that those harmonic waves are important not so much in themselves as in their absorbing effect on the energy of the primary wave. The energy absorbing mechanism is clearly one of those by resonance effect of oscillators, the wave-mechanical elucidation of which being given by the formulas (30) and (32). Examination of the transient aspects of the wave motion from $\boldsymbol{A}_2+\boldsymbol{B}_2$ to $\boldsymbol{A}_3$ by (30) and (32), also, seems important at this stage of the studies, in which a fundamental problem of the apparent internal friction is taken up. However, for the study of the principal part of the seismic waves, the formula of A_3 (25) will be more seismologically significant than (30) or (32).

From the results above obtained, we are lead to the conclusion, for the present, that the effect of the periodic structure on the amplitude A of a progressive wave is represented by $A=1/\cosh \mu z$ in stead of the simple exponential function which is used in (13). Therefore, apparent internal friction $1/Q'$ caused by the periodic structure should be estimated somewhat smaller than $|b|$ that is obtained by (17).

Approximate attenuation formula of the seismic waves with the period $\tau=4\pi/a\gamma$ through a medium with a periodic structure whose constant of internal friction is $1/Q$ will be represented by the expression,

$$A=\frac{1}{\cosh(\pi bx/a\tau)}\cdot\exp(-\pi x/Qa\tau)\,. \tag{33}$$

Estimation of b, or, generally b_n in the earth's crust when we put $c(x)=a(1+\sum_n b_n\cos\gamma_n x)$ is a problem to be studied from observation in future. If $|b_n|$ is equal to a constant $|b|$ for any γ_n-value in a certain range such that $\gamma_1<\gamma_n<\gamma_2$, then the apparent internal friction of the medium for the seismic waves with a period τ, such that $4\pi/a\gamma_1>\tau>4\pi/a\gamma_2$ is, at a large distance, approximately $|b|+\dfrac{1}{Q}$.

Acknowledgement: Financial support for these studies was granted from the Research Fund for Science of the Ministry of Education.

29. 不均質な媒質内を伝る弾性波の安定性について

—見掛けの内部摩擦係数—

地震研究所　吉山良一

弾性波の速度を $c(x)=a(1+b\cos\gamma x)$ として Mathieu の微分方程式によつてかかる媒質内を伝播する弾性波の安定性をしらべた．考えとしては古い問題であるが波動伝播の理論とむすびつけて具体的に取扱つた例はない様である．地震波の観測に現われるいわゆる内部摩擦の見掛値との関係をしらべると b の値がほとんど直接摩擦係数 $1/Q$ に相当することになるのでその影響は見逃し得ないものがある．媒質の internal friction を $1/Q$ とすればある特定の周期 $\tau=4\pi/a\gamma$ の波，波長で比較すれば媒質の構造上の波長 $2\pi/\gamma$ の 2 倍の波長の波に対する振巾減衰の式は結局

$$A=\frac{1}{\cosh(\pi bx/a\tau)}\cdot\exp(-\pi x/Qa\tau)$$

で表わされる．したがつてその様な構造がつづく限り遠いところでの傾向を見ればそのような波に対する媒質の見掛けの internal friction は $|b|+\frac{1}{Q}$ となる．今後調査すべきことは地殻内の弾性波の速度は場所によつてある平均値を上下しているであろうが，それを $c(x)=a(1+\sum_n b_n\cos\gamma_n x)$ の形においた時 $|b_n|$ の大いさが種々の γ_n に対してどのような値を取るかである．

BULLETIN OF THE EARTHQUAKE
RESEARCH INSTITUTE
Vol. 38 (1960), pp. 479-495

30. *Xenoliths Included in Granitic Rocks of the Sekine-Azusayama District, Yamagata Prefecture.**

By Takeshi ICHIMURA.

(Read March 24, 1959.—Received September 22, 1960.)

Introduction

The granitic area of the Sekine-Azusayama district now included in Yonezawa City is characterized by the high frequency of xenoliths which have different characteristics and modes of occurrence (Fig. 1). The xenoliths exposed here are occasionally found extensively and in intricate manner (Fig. 2) when compared with those of other granitic areas of Yamagata Prefecture. They are represented by several kinds of rock, and some of them pass into one another without showing any sharp boundary between them.

Such geological and petrological features can be observed along the Haguro-gawa and Kariyasu-gawa as well as along their tributaries. The most remarkable one is to be seen at the lowermost course of the Kariyasu-gawa where various kinds of xenolith are well exposed and traversed intricately by granitic rocks.

The writer's field work started at this place and was extended to other parts of the district. Thus, the writer could examine many exposures throughout the whole area. Among them, those of the limestone quarry were very attractive, since he obtained from here abundant contact minerals due to the granitic intrusion. During that time, his laboratory work was carried out on the specimens collected from different localities.

General Features of Mother Rocks

In the beginning, it is necessary to give some explanation of granitic rocks which are known as the mother rocks of xenoliths (Fig. 3). They are represented by biotite granite, biotite granodiorite and hornblende biotite granodiorite.

Of these, biotite granite is always found in close association with

* Communicated by H. TSUYA.

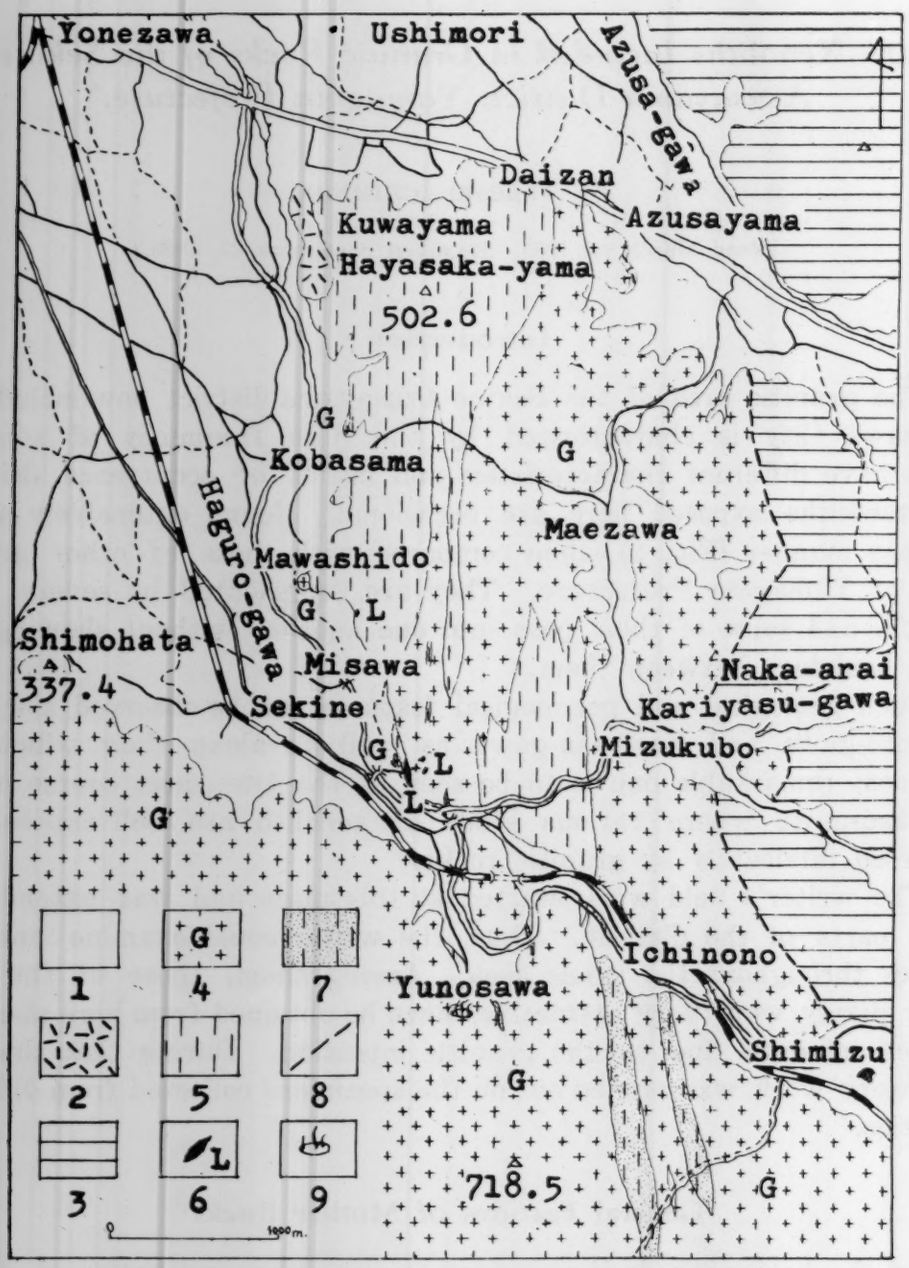

Fig. 1. Geological map of the Sekine-Azusayama district.

1. Quaternary fluviatile deposits, 2. Plagioliparite, 3. Miocene tuff, shale and sandstone, 4. Granite, granodiorite, pegmatite and aplite, 5. Quartz diorite and amphibolite associated with biotite schist and biotite gneiss, 6. Crystalline limestone, 7. Quartz diorite or biotite schist associated with biotite gneiss, 8. Fault, 9. Mineral spring.

xenoliths, and its occurrence is limited as comrared with that of granodiorite. It is a leaucocratic rock composed of quartz, orthoclase, microcline, plagioclase (oligoclase-andesine), biotite, magnetite, apatite, zircon, allanite, titanite, chlorite, sericite and limonite. One of the characteristic features of this rock is the high frequency of microcline and perthite.

Granodiorite is the most predominant rock in the Sekine-Azusayama district, it being first exposed near Daizan and extends southwards across the Ou Railway Line, forming the main part of the hilly land together with xenoliths and Miocene sediments, but on its eastern margin it is largely displaced against the Miocene formation (Fig. 1).

So far as is known at present, hornblende biotite granodiorite seems to pass into biotite granodiorite here and there without revealing any sharp boundary between them. Such a tendency can be observed at Misawa and the limestone quarry near Sekine as well as along the Haguro-gawa between Yunosawa and Ichinono. The same may be said of biotite granite, although it has not yet been confirmed by the writer.

Granodiorite is mostly a medium-grained or coarse-grained rock with such mineral ingredients as quartz, microcline, orthoclase, plagioclase (basic oligoclase—andesine), magnetite, apatite, zircon, titanite, epidote, goethite, limonite, chlorite and calcite (Table I, Fig. 7).

Table I. Essential mineral ingredients of granodiorite.

Quartz	Orthoclase	Microcline	Plagioclase	Biotite	Hornblende
Diameter =0.4mm. 1.8mm. Remarkably wavy extinction.	Very low in frequency. Occasionally shows a microperthitic structure. Smaller than plagioclase.	Low in frequency.	Abundant. Longer diameter=1.8mm −4.8mm. α(min.)=1.534 γ(max.)=1.556 An_{30-40} Partly alters to sericite. Inclusions= apatite, biotite, hornblende & magnetite.	Max. diameter on base=1.5 mm. γ=1.655± X=light yellow, $X=Z$= dark bown, Alters to chlorite. Inclusions= apatite, magnetite, zircon, allanite & titanite.	Max. diameter=14 mm. X=light yellow, Y=yellowish green, Z=green or bluish green. $Z>Y>X$. $Z\wedge c=15°-18°$. α=1.645 −1.667. γ=1.661−1.682. Partly changes into calcite, chlorite or epidote. Inclusions=apatite, magnetite, zircon, biotite & allanite.

Distribution and Modes of Occurrence of Xenoliths

The xenoliths of this granitic area are composed of amphibolite, biotite gneiss, biotite schist, crystalline limestone and quartz diorite. Of these, amphibolite and quartz diorite are found here and there through

the whole area, but the distribution of biotite schist or biotite gneiss seems to be restricted to the southern half.

(1) Xenoliths of amphibolite and quartz diorite: These kinds of rock form a main part of the xenoliths exposed here, showing gradual or sudden transition from one to another, and they pass into biotite schist or biotite gneiss further southwards. The largest exposure is to be seen at the northwestern corner of the area which includes Kuwayama, Hayasaka-yama (502.6 m.), Kobasama, Mawashido and Misawa. It is traceable southwards down to the opposite side of Sekine where limestone has once been quarried.

Separated by granitic rocks, there is another exposure of a large xenolith which extends southwards across the Kariyasu-gawa and Haguro-gawa. The northern half of this xenolith consists of amphibolite, crystalline limestone and quartz diorite, but it is characterized by the appearance of biotite schist and biotite gneiss to the south. The best exposure is to be seen at the lowermost course of the Kariyasu-gawa (Fig. 2). As is shown on the river-bed and the cutting of the truck road, the xenolith of amphibolite and quartz diorite is intricately traversed by biotite granite, biotite pegmatite and other leucocratic rocks. Exclusive of pegmatite, these leucocratic rocks have an aplitic appearance, consisting of quartz, plagioclase, biotite, hornblende, magnetite, zircon, titanite, apatite and allanite. They occur as veinlets or irregular masses which have a narrow zone (5 mm.—3 cm. in width) poor in ferromagnesian minerals along the contact parts. It is also noteworthy that many xenoliths of quartz diorite, 30 cm.—2 m. in diameter, are sporadically included in the mother rock exposed near Ichinono. They can be observed on the river-bed of the Haguro-gawa. The xenoliths of this place are rounded or angular in form and are always bordered sharply against the mother rock. The swarms of such xenoliths of amphibolite and quartz diorite can be investigated at several places.

(2) Xenoliths of biotite schist and biotite gneiss: These two kinds of rock are sometimes found together with amphibolite or quartz diorite and increase in frequency to the south. The occurrence of biotite schist is known at Kuwayama and near the junction of the Haguro-gawa and Kariyasu-gawa (Fig. 4) as well as along a tributary of the Haguro-gawa branching off at the opposite side of Shimizu. Biotite gneiss is, on the other hand, exposed at Misawa, the lowermost course of the Kariyasu-gawa and Ichinono. When biotite schist and amphibolite are associated, the former reveals a gradual transition to the latter.

Xenoliths of crystalline limestone: There are several xenoliths of crystalline limestone, large and small, which are sporadically distributed in the area between Mawashido and the lowermost course of the Kariyasu-gawa. They take a lenticular or irregular form, and some of them can be seen at the old limestone quarry near Sekine (Fig. 5). The largest one at this quarry is estimated to be about 300 m. in length, being included in granodiorite together with amphibolite, biotite schist and quartz diorite. It is intruded by hornblende pegmatite and biotite granite. The writer collected here various kinds of contact minerals. Moreover, the biotite granite of the same quarry contains three small xenoliths free of such contact minerals and amphibolite or quartz diorite (Fig. 6.). The occurrence of crystalline limestone is also noticed near Mawashido and along the tributaries of the Kariyasu-gawa branching off northwards or westwards. At these places, the main xenolithic rocks are amphibolite and quartz diorite.

Mineral Composition of Xenoliths

(1) Amphibolite: There are several types of amphibolite represented by compact and hard rocks with a black color. Some of them have a distinct schistosity and intricate structure, showing various textures under the microscope. They are composed of plagioclase, green hornblende, biotite, magnetite, epidote, titanite, zircon, rutile, apatite, limonite and tourmaline (Fig. 8). The frequency of these minerals varies to a remarkable extent in different specimens, with exclusion of green hornblende, plagioclase and magnetite.

One of the important ingredients is plagioclase with a subhedral or anhedral form. It ranges from basic andesine to acidic labradorite. When the mineral is not twinned but reveals a wavy extinction, its appearance resembles quartz to some extent.

In this rock, the most predominant mineral is the subhedral or anhedral hornblende with a long or stout prismatic habit. Frequently, it occurs in close association with biotite, although the latter is absent in the specimens collected from Kuwayama and Hayasaka-yama or elsewhere. The size of this mineral seems generally to increase along the contact parts where the rock passes into quartz diorite or granodiorite.

The quantity of biotite is subordinate as compared with green hornblende and has a tendency to decrease in the specimens from the northern half of the area. The relationship between this mineral and

green hornblende is clearly evident at the lowermost course of the Kariyasu-gawa. The amphibolite exposed here is mostly rich in biotite flakes and grades into biotite schist. A similar tendency can be seen at the old limestone quarry.

Magnetite is a mineral common to all specimens and takes generally an octahedral or irregular form. In the latter case, it is occasionally represented by a skeletal crystal. The writer has collected some specimens rich in magnetite from near Hayasaka-yama and Kuwayama as well as from the lowermost course of the Kariyasu-gawa. Some of it is included by hornblende or oligoclase or biotite and fills up the interstices between them. The crystal is usually 0.01 mm.—0.08 mm. in diameter.

The occurrence of epidote seems to be restricted to the specimens from Misawa and the valley entering westwards from Mizukubo. The crystal is subhedral or anhedral and prismatic or granular, producing some confused aggregates. The largest one is 0.43 m. long and 0.25 mm. across. In such a case, the angle between Z and (100) is estimated to be 30°.

Titanite is also one of the accessory ingredients frequently contained in the specimens from near Mizukubo and the lowermost course of the Kariyasu-gawa. Its minute crystal takes an irregular form, being intermixed with hornblende or biotite and being characterized by its high birefringence and relief. As can be observed in some thin sections, magnetite is surrounded by this mineral.

Besides them, a noteworthy feature is the presence of tourmaline in the specimens from the eastern side of Hayasaka-yama. The mineral is found as a phenoblast which is always anhedral in its crystal form. It is distinctly pleochroic from light yellowish brown (X) to yellowish brown (Z) at the periphery, but from light blue (X) to blue (Z) at the core. The largest crystal is 1.44 mm. long and 0.85 mm. across. The enclosure is magnetite, limonite and hornblende.

Table II. Essential mineral ingredients of amphibolite.

Plagioclase	Hornblende	Biotite
Mostly, 0.02mm.—0.08 mm. in longer diameter. $\alpha=1.551\pm$ $\gamma=1.560\pm$ $An_{45\pm}$	Generally, 0.7 mm. ± in longer diameter. The largest one is 1.02mm. long and 0.34 mm. across. $\alpha=1.648-1.660$ $\gamma=1.662-1.672$ X=light yellow. Y=yellowish green or green. Z=green or dark green. $Z\wedge c=18°-25°$	0.3 mm—0.5 mm. in diameter (base). $\gamma=1.650\pm$ Pleochroism is weaker than that of granodiorite.

Zircon, rutile, apatite and limonite are contained in minor quantity.

(2) Biotite schist: This rock is frequently exposed in close association with amphibolite or biotite gneiss and reveals occasionally a gradual transition between them. It has a black color and distinct schistosity, consisting of such mineral ingredients as quartz, microcline, orthoclase, plagioclase, biotite, muscovite, hornblende, magnetite, zircon, epidote, chlorite and limonite (Fig. 9).

One of the important minerals is quartz composed of irregular or somewhat round crystals which are found in a mosaic or interdented structure. Mostly, it shows a strain shadow and is characterized by an abundance of liquid inclusions. The largest crystal is 1.7 mm. in diameter.

Microcline and orthoclase are, on the other hand, very rare ingredients. The occurrence of these minerals are known only in the specimens obtained from near the junction of the Haguro-gawa and Kariyasu-gawa. They are represented by minute subhedral or anhedral crystals, the longer diameter of the largest one being 0.25 mm. in microcline and 0.29 mm. in orthoclase respectively. In the case of orthoclase, a microperthitic structure is usual.

Plagioclase is a common ingredient in almost all specimens and belongs to andesine or labradorite. The crystal is subhedral or anhedral, and its longer diameter is estimated to be 0.5 mm. in the largest crystal.

The tabular crystals or irregular flakes of biotite occur in a parallel arrangement. They are strongly pleochroic from light yellow or light brown (X) to dark brown or reddish brown (Y or Z). In this case, the index of refraction, γ, is 1.644—1.650. Such biotite crystals enclose mostly magnetite and are sometimes chloritized. The diameter of the largest one is 2 mm. on (001). Muscovite is, however, low in frequency when compared with biotite. Its crystal is scattered here and there in quartz layers and lenses, forming sporadically some confused aggregates.

Hornblende is always absent in type specimens, but begins to appear in those exposed close to amphibolite. It has a pleochroism which changes from light yellow (X) to yellowish green (Y) or deep green (Z).

Octahedral or skeletal magnetite is a noticeable mineral in the specimens from the limestone quarry near Sekine, but it is almost or entirely absent in other cases. The crystal has a diameter of 0.01 mm. —0.08 mm., and some of it passes into limonite.

Zircon and apatite are present to a negligible degree. The same may be said of epidote which traverses the rock as a veinlet.

(3) Biotite gneiss: This rock has a coarse banded structure due to

the repetition of the parts rich in biotite and quartzose layers. At a glance, it looks like the Ryōke or Tsukuba metamorphosed sediments. Under the microscope, the rock is composed of quartz, microcline, orthoclase, biotite, muscovite, magnetite and zircon.

Of these, quartz is the predominant mineral, showing a mosaic or interdented structure. The crystal is 0.85 mm. in the maximum diameter and indicates a strain shadow in each grain. It is usually rich in such inclusions as muscovite, biotite, magnetite and liquid (?).

In contrast with the quartz, microcline and orthoclase are poorly present. The same tendency is also to be seen in the case of plagioclase, as is indicated in the specimen from near Ichinono.

Biotite and muscovite are abundant in all thin sections, both being intricately intermixed in a parallel arrangement. The former is strongly pleochroic from light brown (X) to reddish brown (Y or Z) and includes magnetite and zircon, whereas the latter is found as a flaky aggregate and contains magnetite.

Magnetite takes an irregular form and is mostly associated closely with biotite or muscovite in which it occurs as inclusions.

The occurrence of zircon is generally restricted to small quantities. When its rounded crystal is contained in biotite, it is characterized by the formation of a pleochroic halo.

(4) Crystalline limestone: This type of limestone has a greyish white or white color and is a fine to coarse-grained rock with a saccharoid appearance due to recrystallization. It is generally composed of calcite and several other kinds of minerals. One of its characteristic features can be seen in the specimens obtained from the old limestone quarry near Sekine where the rock contains such minerals as diopside, epidote, garnet, green hornblende, plagioclase, pyrrhotite, sericite, titanite, tremolite and vesuvianite.

Under the microscope, diopside is not as abundant as garnet, being commonly associated with epidote, garnet and vesuvianite and giving a light or dark green color to the mother rock. In this case, the crystal is subhedral or anhedral. The largest is 2.39 mm. long and 1.53 mm. across. When the mineral is found together with garnet, the interstices of the latter are sometimes filled by the former. The extinction angle, $Z \wedge c$, is 39°. Twinned crystals are unknown in the writer's specimens.

Epidote is contained in low frequency when compared with garnet and vesuvianite. It is occasionally found in an aggregate of elongated crystals in which the largest one is estimated to be about 30 cm. in

length. The mineral has a dark yellowish green color in fresh specimens, but obtains a brownish shade when decomposed, being slightly pleochroic from colorless (X) to light yellow (Z). The crystal has a perfect cleavage parallel to (001) and twins on (100). The extinction angle $X \wedge c$, is 4°.

Garnet (grossularite) is the most predominant mineral except calcite which constructs the main part of the mother rock. This mineral has a light brown or yellowish green color and a greasy luster. The crystal is represented by a combination of (110) and (211). The largest one is about 2 cm. in diameter. It occurs usually as irregular masses or bands, but occasionally forms dots in the mosaic aggregate of calcite.

Pyrrhotite is, however, a mineral of low frequency. It has an irregular form and is always associated with calcite and garnet.

A similar frequency is also indicated by titanite, the crystal taking an irregular or rounded form. In the latter case, it has mostly an imperfect rhombic section. The mineral is characterized by high refringence and relief.

So far as is known at present, the occurrence of tremolite is restricted to a small quantity. The mineral has a white color and forms a radial aggregate on the surface of the massive garnet where its fiber is about 3 cm. in the maximum length. It twins on (100), and the extinction angle, $Z \wedge c$, is 15° or thereabouts.

In contrast with the three minerals mentioned above, a remarkable occurrence of vesuvianite is known to be present in many of the specimens from here. The mineral is easily distinguishable from other lime silicates by its brownish black color and greasy luster as well as by its poor cleavage. The crystal shows a high relief, but low in birefringence, being abnormally biaxial and negative.

Plagioclase, sericite and green hornblende are in negligible amounts.

(5) Quartz diorite: It is composed of biotite hornblende or hornblende biotite quartz diorite, hornblende quartz diorite and biotite quartz diorite. Among them, biotite hornblende quartz diorite is most predominant, consisting of quartz, plagioclase, hornblende, biotite, magnetite, apatite, titanite, zircon, sericite, chlorite and calcite (Figs. 8, 10).

In these cases, quartz has an irregular form and fills up the interstices of other mineral ingredients. This mineral is characterized by its remarkable strain shadow and abundance of liquid inclusions.

The most important mineral in quartz diorite is plagioclase whch ranges from acidic andesine to basic andesine. The crystal is subhedral

or anhedral and takes a tabular form. It has a zonal structure, and its inner part is frequently sericitized intensely. Apatite, zircon, magnetite and titanite are sometimes included.

Subhedral or anhedral hornblende is found in high frequency except in biotite quartz diorite. It is green hornblende and twins occasionally on (100). The crystal contains magnetite, zircon and apatite, some of it being altered to chlorite and calcite.

Next to hornblende, another noticeable forromagnesian mineral is biotite, although it is lacking in some specimens from the Kariyasu-gawa and Haguro-gawa near Ichinono. The frequency of biotite varies from place to place. This mineral is occasionally more abundant than hornblende. Such inclusions as zircon, magnetite, titanite and apatite are seen in some crystals which are partly chloritized.

The minute apatite crystal is present almost in all thin sections. Its crystal has a long or short prismatic habit, and the largest one is 0.35 mm. in length. Magnetite is more or less titaniferous and some skeletal crystal is surrounded by a narrow zone of titanite. Its largest crystal is 0.59 mm. in diameter. Titanite is also a common accessory ingredient. This mineral is present to a remarkable degree in a specimen obtained on the river-bed of the Kariyasu-gawa. It has an irregular form and is sometimes associated closely with magnetite. The largest one is 1.19 mm. in its longer diameter.

The occurrence of zircon is rare. Mostly, it takes a granular form, but is occasionally prismatic. In biotite, a pleochroic halo is formed around the crystal. Chlorite is usually derived from biotite or hornblende, whereas sericite is an alteration product of plagioclase. Calcite occurs rarely as the secondary mineral of hornblende.

Table III. Essential mineral ingredients of quartz diorite.

Quartz	Plagioclase	Biotite	Hornblende
Generally, low in frequency Diameter=0.3 mm.–1 mm.	1 mm. long and 0.7 mm. across in the largest crystal. α(min.)=1.547 γ(max.)=1.560 An_{36-45}	0.6 mm. in the maximum diameter (base). $\gamma=1.662-1.672$ X=light yellow. $Y=Z$=dark brown.	Mostly, 0.7mm. ± in length. $\alpha=1.648-1.660$ $\gamma=1.662-1.672$ $Z\wedge c=16°$ X=light yellow. Y=yellowsh green. Z=dark green. $Z>Y>X$

Chemical Composition

As to the chemical characters of granite and granodiorite, there are only two available data at present. They are shown in Table IV.

Table IV. Chemical composition (weight %),norm and Niggli value of granitic rocks.

Weight %	I	II
SiO_2	68.67	69.04
TiO_2	0.41	0.39
Al_2O_3	14.97	15.12
Fe_2O_3	1.41	1.28
FeO	2.63	2.43
MnO	0.11	0.08
MgO	2.04	1.78
CaO	3.83	4.11
Na_2O	2.68	2.74
K_2O	2.91	2.35
$H_2O(+)$	0.67	0.71
$H_2O(-)$	0.49	0.42
P_2O_5	0.09	0.13
Total	100.91	100.58

Niggli value	I	II
al	37.0	38.0
fm	27.0	25.0
c	17.5	19.0
alk	18.5	18.0
k	0.41	0.36
mg	0.48	0.47
qz	113.5	112.0
c/fm	0.46	0.76

Norm	I	II
Q	29.70	31.80
Or	17.23	13.90
Ab	22.53	23.06
An	18.07	19.46
C	0.92	1.08
Fs	3.30	2.90
En	5.10	4.50
Mt	2.09	1.85
Il	0.76	0.76
Ap	0.34	0.34

I=Biotite granite from the lowermost course of the Kariyasu-gawa.

II=Hornblende biotite granodiorite from the river-bed of the Hagurogawa near the limestone quarry.

Analyst, T. Tōkairin.

Among several kinds of xenolith, amphibolite and quartz diorite were

selected for chemical investigation, since they are more important than others and there are some geological problems concerning the original

Table V. Chemical composition (weight %), norm and Niggli value of amphibolite and quartz diorite from the Sekine-Azusayama district.

Wt. %

	I	II	III
SiO_2	62.41	51.43	52.08
TiO_2	0.78	0.35	0.31
Al_2O_3	15.01	17.92	17.65
Fe_2O_3	4.04	1.45	1.21
FeO	3.41	5.07	4.88
MnO	0.02	0.19	0.14
MgO	3.26	7.83	7.51
CaO	3.64	12.40	11.87
Na_2O	3.30	2.65	3.06
K_2O	2.75	0.39	0.53
$H_2O(+)$	0.81	0.45	0.39
$H_2O(-)$	0.22	0.12	0.21
P_2O_5	0.22	0.12	0.10
Total	99.86	100.37	99.94

Niggli value

	I	II	II
al	31.0	25.0	24.0
fm	38.0	39.0	38.5
c	13.5	30.0	29.5
alk	17.5	6.0	8.0
k	0.36	0.09	0.11
mg	0.46	0.68	0.69
qz	50.0	−7.0	−8.0
c/fm	0.36	0.77	0.77

Norm

	I	II	III
Q	20.16		
Or	16.12	2.22	3.34
Ab	27.77	22.53	25.68
An	16.30	35.20	32.80
C	0.61		
Fs	1.58	6.20	5.41
En	8.20	15.70	13.10
Wo		10.56	10.56
Fa		1.33	1.73
Fo		2.73	3.99
Ap	0.67	0.34	0.34
Mt	5.80	2.09	1.86
Il	1.52	0.61	0.61

I=Biotite hornblende quartz diorite from the lowermost course of the Kariyasu-gawa.

II=Biotite amphibolite from the lowermost course of the Kariyasu-gawa.

III=Amphibolite from near Misawa.

Analyst, T. Tōkairin

rocks. The results of chemical analyses thus obtained are shown in Table V.

In this table, No. I is the type-specimen of quartz diorite which is widely distributed together with amphibolite. It is rich in biotite and hornblende. No. II also contains biotite, whereas No. III is quite free of this mineral.

Chemically speaking, two such kinds of amphibolite are similar to some of the Formosan amphibolite investigated by the writer,[1] but are more acidic than that of the Takanuki district.

Origin of Quartz Diorite

One of the interesting geological features is the relationship between quartz diorite and amphibolite. It resembles partly that of the Takanuki district[2] where the Takanuki series[3] is extensively exposed. According to Ogura's investigations,[4] quartz diorite and amphibolite of the Takanuki district are closely associated and pass into one another with a gradual transition between them. In this case, quartz diorite has the same schistosity as amphibolite and changes its texture from fine to coarse as it departs from the amphibolite. Thus, he attributed the origin of quartz diorite exposed here to the result of the granitization of amphibolite.

In the Sekine-Azusayama district, quartz diorite is not only associated with amphibolite, but is frequently exposed in the areas of biotite schist or biotite gneiss and crystalline limestone. Besides these modes of occurrence, its xenoliths are independently contained in granodiorite.

When amphibolite is found together with quartz diorite, the former is complicatedly traversed by the latter (Fig. 2). Most of them are sharply bordered, but there are some exceptional instances of a gradual transition from one to another. Moreover, quartz diorite is always free of schistosity even near amphibolite, as is shown at the lowermost course of the Kariyasu-gawa.

In connection with the facts mentioned above, it is also noteworthy that the xenoliths composed of quartz diorite are abundantly contained in granodiorite in other areas of Yamagata Prefecture. For instance,

1) T. ICHIMURA, *Mem. Fac. Sc. Taihoku Imp. Univ.*, Ser. III, **1** (1944), 102–104.
2) Y. OGURA, *Jour. Geol. Soc. Japan*, **62** (1956), 616.
3) Geology and Mineral Resources of Japan, *Geol. Surv. Japan*, (1960), 124.
4) Y. OGURA, *op. cit.*, 610–614.

the writer observed them frequently along the Karasu-gawa (Gassan)[5] and Tachiya-gawa (Yamadera). They have a rounded or irregular form and are always represented by biotite hornblende quartz diorite with a mineral composition similar to the specimens from the Sekine-Azusayama district. There is, however, no evidence for determining the exact origion of this rock. The same mode of occurrence is to be seen along the upper course of the Haguro-gawa between Ichinono and Yunosawa, although it is restricted to a small extent. The xenoliths of the Sekine-Azusayama district are mostly characterized by the occurrence of various metamorphics closely associated. The origin of quartz diorite in the district under consideration is, therefore, much complicated as compared with the case of the Takanuki district, but it is impossible to overlook the effect of granitization.

Formation of Metamorphics

Various kinds of metamorphic rock are still preserved in granodiorite or granite exposed largely on the Backbone Range and in its vicinity including such prefectures as Yamagata, Miyagi and Fukushima. They are found as isolated formations or xenoliths composed mostly of biotite schist and biotite gneiss.

The occurrence of amphibolite and crystalline limestone is, however, restricted only to the Sekine-Azusayama district. In this area, these rocks are always associated with biotite schist or biotite gneiss. Among them, the most characteristic rock is amphibolite which crops out in high frequency as compared with others. The rock passes gradually into biotite schist or biotite gneiss and is sometimes intercalated with crystalline limestone. Such a mode of occurrence suggests that it was metamorphosed from some tuffaceous rock. There is also a possibility of its having an igneous origin, as has been noticed by Ogura[6] in the same type of rock distributed extensively in the Takanuki district. This may be assumed from the result of chemical analyses carried out on the type speciments of amphibolite which were collected from the Sekine-Azusayama district. According to this investigation, its original rock seems to have been gabbroic or diabasic.

Amphibolite is a metamorphosed product of granitic intrusions as is the case of biotite schist, biotite gneiss and crystalline limestone. Of

5) T. ICHIMURA, *Bull. Earthq. Res. Inst. Univ. Tokyo*, **33** (1955), 422.
6) Y. OGURA, *op, cit.*, 612.

these, biotite schist and biotite greiss were probably formed in the same way as those of the formation which is traceable northwards or north-northwestwards at the southern foot of Kuriko-san rising at the boundary between Yamagata Prefecture and Fukushima Prefecture where metamorphism took place at the time of granitic intrusion.[7] It is, however, uncertain how many times such intrusions were repeated. The same may be said of granitic intrusions in the Sekine-Azusayama district where there are different kinds of granodiorite and other granitic rocks.

During these granitic intrusions, various kinds of older sediments were successively metamorphosed, resulting in the formation of biotite schist, biotite gneiss and crystalline limestone. In the same connection, some of such metamorphics are supposed to have been subjected to granitization.

Sources of Xenoliths

As has already been stated, the granite and granodiorite of the Sekine-Azusuyama district contain many xenoliths, large or small, composed of several kinds of rock. They are largely distributed with a trend of *N* or *NNW* and intricate features varying from place to place. All of these xenoliths are represented by metamorphic or hybrid rocks. In this case, some of them are undoubtedly of sedimentary origion, whereas others are supposed to have been derived from the basic intrusive or tuff. Hence, it is inferable that there had once been a large exposure of older rocks prior to the granitic intrusions which took place in the district under consideration.

In Yamagata Prefecture, the occurrence of older rocks is restricted to several districts where granodiorite is widely exposed, being mostly distributed as isolated formations or xenoliths. There is, therefore, no connection between them, and the absence of fossils renders them very difficult to confirm their geological age. Among them, those of Iide-san and the Oguni district may be assigned to the Permian from some evidence indicated by the similar formations in the neighbouring district of Niigata Prefecture. It is also noteworthy that most of the formations exposed in Yamagata Prefecture consist of clay-slate and sandstone which pass into hornfels and schist or injection gneiss towards the granitic contact. In the case of the Sekine-Azusayama district, older

7) N. Jimbo, Yamagata-ken Kozanshi, (1955), 3. Geological Map of Yamagata Prefecture (compiled by N. Jimbo), (1960).

rocks are somewhat different from those mentioned above.

So far as is known at present, this district seems to have formerly been built up of limestone, clay-slate and sandstone as well as of the basic intrusive or tuff. These rocks were greatly disturbed subsequently by the intrusions of granodiorite and associated intrusives. During that time, the older rocks are supposed to have been subjected to an intense metamorphism. The xenoliths now exposed here are probably erosion relics of roof pendants which had fallen into the granitic mass at that time.

Summary

(i) The Sekine-Azusayama district is a well-known area of granitic rocks which include various kinds of xenoliths composed of amphibolite, biotite schist, biotite gneiss, crystalline limestone and quartz diorite. They are extensively exposed in this district. Of these, the predominant xenoliths are those of amphibolite, biotite schist quartz diorite.

(ii) Such xenoliths, larger or small, have a trend of north or north-northwest, some of them passing into one another. So far as is known at present, amphibolite is found to a larger extent than biotite schist and biotite gneiss in the northern half of the area, but is *vice versa* at its southern half. Besides them, quartz diorite is mostly associated closely with these metamorphics, and crystalline limestone forms some lenticular masses in amphibolite.

(iii) From the facts mentioned above, it can be inferred that there had once been some large exposures of older rocks prior to granitic intrusions. Thus, the district seems to have been built up of clay-slate, shale, sandstone, limestone and basic intrusive or tuff.

(iv) These rocks were highly altered by repeated granitic intrusions, resulting in the formation of several types of metamorphics subjected partly to granitization.

(v) During and after the granitization and metamorphism, such alteration products were included in the granitic bodies. The xenoliths exposed largely in the Sekine-Azusayama district may, therefore, be erosion remnants of roof pendants fallen into them at that time.

Acknowledgments

The writer wishes to express his appreciation to Professor H. Tsuya

Fig. 2. Amphibolite traversed intricately by quartz diorite (light color) which passes into a leucocratic rock along its contact. These rocks are well exposed at the lowermost course of the Kariyasu-gawa.

（震研彙報 第三十八号 図版 市村）

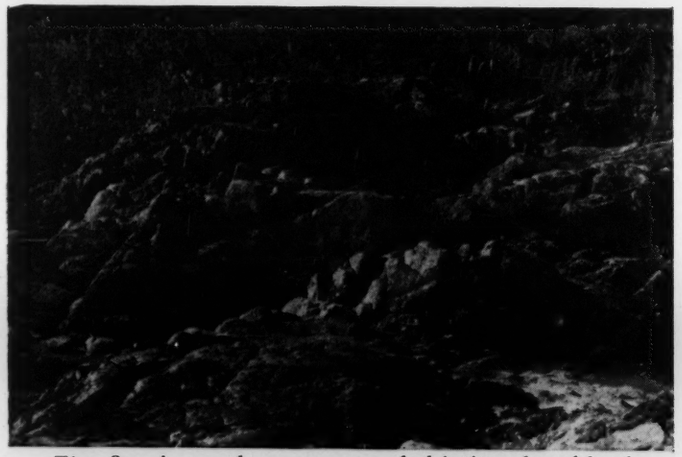

Fig. 3. A good exposure of biotite hornblende granodiorite along the Haguro-gawa.

Fig. 4. Biotite schist exposed near the junction of the Haguro-gawa and Kariyasu-gawa.

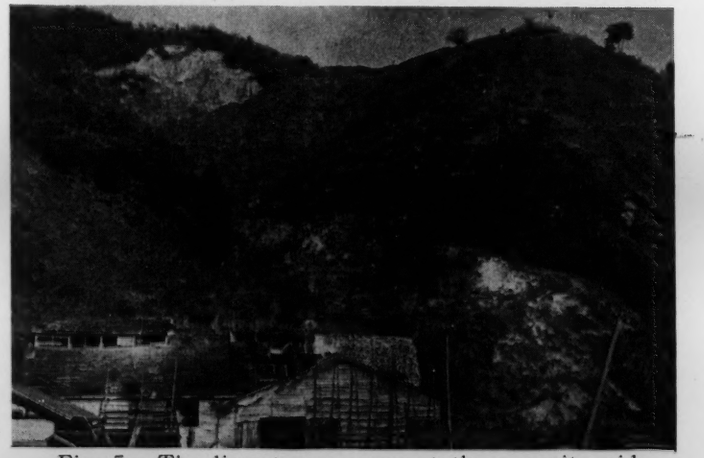

Fig. 5. The limestone quarry at the opposite side of Sekine.

Fig. 6. A xenolith of crystalline limestone in biotite granite exposed at the limestone quarry near Sekine. 1=Biotite granite, 2=Crystalline limestone.

(震研彙報 第三十八号 図版 市村)

Fig. 7. Granodiorite, 1=Apatite, 2=Biotite, 3=Plagioclase, 4=Quartz (The lowermost course of the Kariyasu-gawa). ×100.

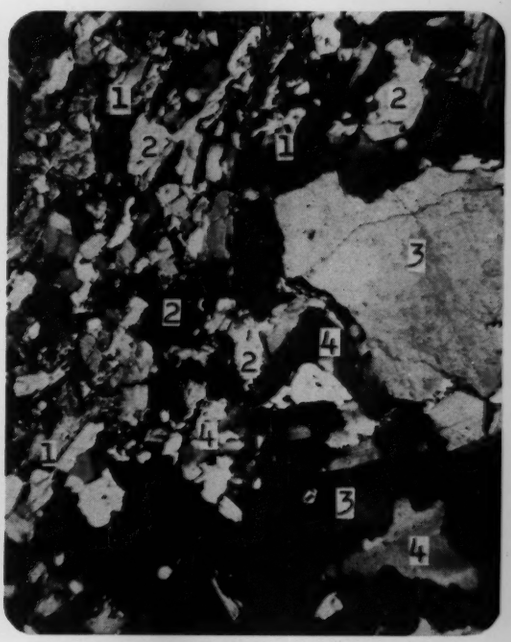

Fig. 8. Quartz diorite (right half, coarse) passing into amphibolite (left, half, fine). 1=Biotite, 2=Hornblende, 3=Plagioclase, 4=Quartz, 5=Titanite. (The Kariyasu-gawa). ×100.

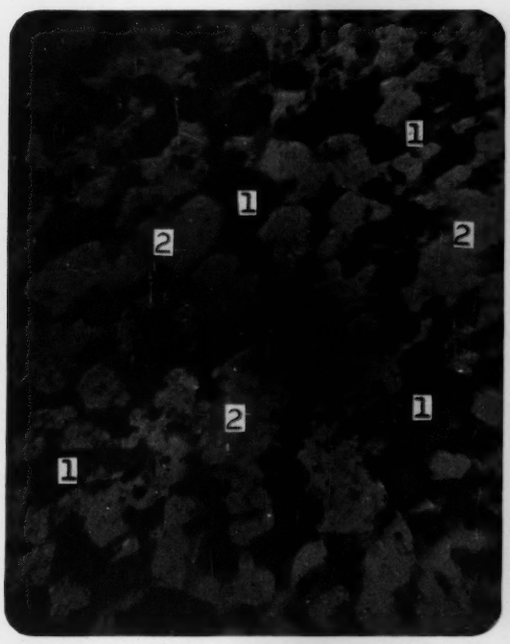

Fig. 9. Biotite schist. 1=Biotite, 2=Plagioclase and quartz. (The limestone quarry near Sekine). ×100.

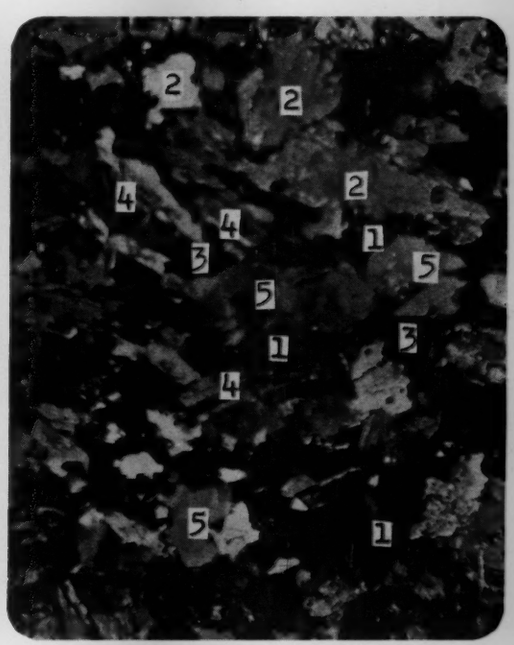

Fig. 10. Quartz diorite. 1=Biotite, 2=Hornblende, 3=Magnetite, 4=Plagiolcase, 5=Quartz. (The Kariysu-gawa). ×100.

and Mr. T. Watanabe as well as to Mr. T. Tōkairin who facilitated the writer's laboratory work.

Thanks are also due to Miss H. Kanauchi for her co-operation in the writer's petrographical investigations of igneous and metamorphic rocks collected from the Sekine-Azusayama district.

---

30. 山形県関根・梓山地方の花崗質岩に含まれる捕獲岩

市　村　　毅

関根·梓山地方に広く露出する花崗質岩には，いろいろな種類の捕獲岩が含まれている．これらは角閃岩，黒雲母片岩，黒雲母片麻岩，結晶石灰岩および石英閃緑岩よりなり，角閃岩，黒雲母片岩，石英閃緑岩などの捕獲岩が殊更多く認められる．その場合，結晶石灰岩は，角閃岩の間にレンズ状をなして挟在するか，直接黒雲母花崗岩中に不規則な塊をなし，時に柘榴石，透角閃石，ベスブ石，透輝石，緑簾石などを含むものも知られている．角閃岩，黒雲母片岩および石英閃緑岩は，しばしば相伴つて複雑な関係を示し，一方で角閃岩と黒雲母片岩とは，漸移する場合も少くない．また角閃岩と石英閃緑岩とは，一般に明瞭な境界を見せているが，まれに漸変的に移化して行くものもある．

以上の事実は，以前この地方に存在した粘板岩，頁岩，砂岩，石灰岩，凝灰岩あるいは塩基性化成岩が花崗質岩の大きな貫入によつて変成岩化し，他方では，花崗岩化作用のために，角閃岩その他が石英閃緑岩になつたことを物語つている．かくして生じた変成岩や石英閃緑岩の一部は，当時貫入を繰り返えした花崗岩体中に大小の岩塊または岩片として捕獲されるに至つたものと思われる．現在見られるのは，それらの侵触残骸である．

BULLETIN OF THE EARTHQUAKE
RESEARCH INSTITUTE
Vol. 38 (1960), pp. 497-544

31. *Fundamental Research for Predicting Volcanic Eruptions.* (*Part 1*)

Earthquakes and Crustal Deformations originating from Volcanic Activities.

By Takeshi MINAKAMI,

Earthquake Research Institute.

(Read* Sept. 19, 1944; May 18, 1948; Dec. 23, 1958; Feb. 23, 1960.—Received Sept. 30, 1960.)

Contents

1. Introduction.
2. On the depth at which earthquakes take place.
3. Characteristics of crustal deformations accompanying volcanic activity.
4. Crustal deformations that accompanied the development of Syowa-Sinzan, from the Usu volcano.
5. The nature of lava and volcanic eruption.
6. Pressure exerted on volcanic bodies at the time of lava extrusion and the viscosity of lavas.
7. Earthquakes originating from volcanoes.
8. Some examples of the hypocentral distribution of volcanic earthquakes.
9. The earthquake swarm in the Hakone volcano.
10. The relation between the B-type volcanic earthquakes and volcanic eruptions.
11. Vulnerability rates on the occurrence of eruptions viewed from the frequency of the B-type volcanic earthquakes.
12. On the magnitude and frequency of earthquakes originating from volcanoes.
13. General earthquakes and earthquakes originating from volcanoes.
14. Conclusion.

---

* This paper was read in its entire on twenty occasions at the monthly meetings E. R. I..

1. Introduction

Studies of volcanoes and volcanic phenomena are related to geophysics, geology, petrology, and geochemistry. Studies of volcanoes are now carried on from the standpoint of each of the associated sciences cited above and synthetic studies of volcanoes based on the above sciences are also being promoted. Even when a study is conducted from a purely geophysical point of view, considering the large physical quantities contained in volcanic phenomena, the study of volcanic phenomena may well have a special relation to seismology, geodesy, geomagnetism, and geothermy. In this paper which deals with earthquakes and crustal deformations, such problems as the difference between crustal deformations accompanying general earthquakes and those accompanying general major earthquakes, the relation between earthquakes and volcanic activity, and other problems will be discussed.

Volcanic activity, interpreted in a narrow sense, was formerly limited to the extrusion of magma in the form of molten lava and lava fragments on the ground surface, i. e. the phenomenon of volcanic eruption. At present, however, the series of phenomena including the production of magma at a depth of several tens of kilometers, the ascending of the magma, and its extrusion to the surface of the ground is regarded as volcanic activity and the series of subsequent phenomena has also become an object of study for volcanology.

Nowadays many volcanologists[1] hold the following view. Magma is produced at a depth of 50 km to 300 km under the earth's surface. The part in the earth melts or partially melts as a result of the excessive supply of heat as compared with other parts, and, on account of this the volume is increased. Consequently, because of the pressure exerted on the surroundings a strain is caused in the earth's crust. When the strain exceeds a certain limit, cracks are produced in the crust and the area is disintegrated, resulting in the occurrence of an earthquake. That is, the strain occurring in the crust is released in the form of seismic waves. On the other hand, magma intruding into the cracks formed in the crust sometimes ascends to the surface and is extruded. Considering the process of the production and ascent of magma, and in particular, the origin of magma, it is considered impossible to distinguish definitely general earthquake phenomena from volcanic phenomena. Probably the only difference may be that the

1) H. KUNO, *Bull. Volcanol.* [ii], **20** (1958), 37.

most important problem of earthquake phenomena is the propagation of seismic waves while that of volcanic phenomena is the rise and extrusion of magma, i. e., the motion of the substance itself.

If volcanic phenomena be regarded as phenomena in which magma ascends from a depth of several tens of kilometers and at last is extruded on the ground-surface, what are the phenomena caused in connexion with the above phenomena, in the earth's crust? Some-

Fig. 1. Geographical position of the volcanoes (closed circle) and the earthquakes (opened circle) cited in this report.

1. Tottori earthq.,	2. Tango earthq.,	3. Hukui earthq.,
4. Noobi earthq.,	5. Ito earthq.,	6. Imaiti earthq.,
7. Oga earthq.,	8. Suwanose-sima,	9. Sakura-zima,
10. Aso,	11. Hatizyo-sima,	12. Miyake-sima.,
13. Kozu-sima,	14. Nii-sima,	15. Sikine-sima,
16. Oo-sima,	17. Hakone,	18. Huzi,
19. Asama,	20. Kusatu-sirane,	21. Bandai,
22. Usu,	23. Tarumai.	

times magma will ascend to the surface and cause a volcanic eruption, while at other times it will fail to reach the surface and will remain in the interior of the crust. From earthquake phenomena associated with the above-mentioned various types of volcanic activity, may it not be possible to obtain an accurate knowledge of volcanic activity? May it not be possible to grasp some characteristics of crustal deformations? From such aspects the problem will be discussed in this paper.

2. On the depth at which earthquakes take place

First of all, in order to investigate the depth from which general earthquakes or the so-called tectonic earthquakes originate, the writer investigated the frequency distribution of the hypocenters of the major

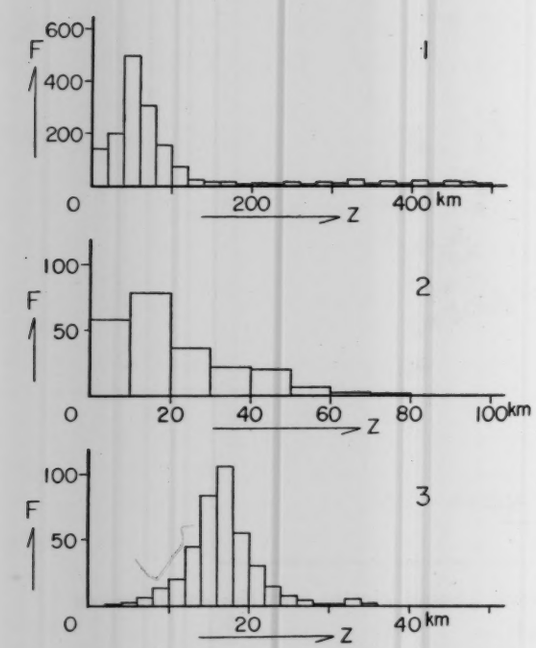

Fgi. 2. Frequency distribution (F) with respect to hypocentral depth (Z) for various earthquakes.
(1) General earthquakes in and near Japan.
(2) Earthquakes in Hawaii including Kilauea and Mauna-loa.
(3) Tango after-shock.

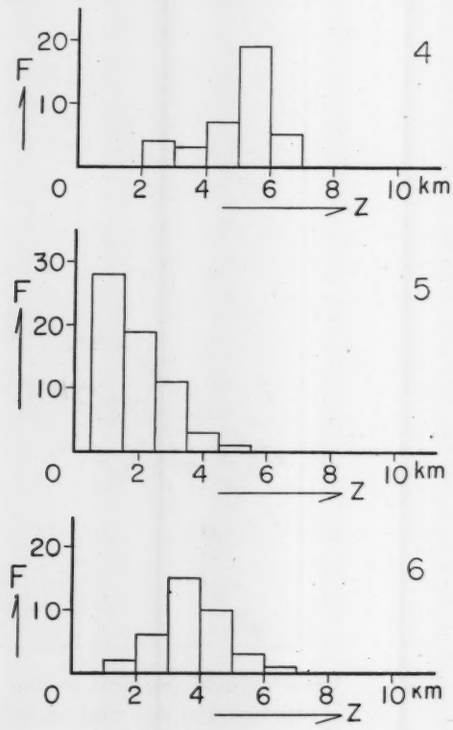

Fig. 3. Frequency distribution (F) with respect to hypocentral depth (Z) for various earthquakes.
(4) The 1930 Ito earthquakes.
(5) The 1959–1960 Hakone earthquake swarm.
(6) The A-type earthquakes which accompanied the 1944 Usu eruption.

earthquakes which have occurred in Japan and its vicinity. The major earthquakes mentioned in this paper are those over 5 in magnitude, and only those which took place from 1951 to 1958 are here considered. The hypocenters were determined by the Seismological Section, Japan Meteorological Agency[2].

The frequency distribution of the hypocenters of the above earthquakes is represented in Fig. 2 (1), which was prepared on the basis of the depths of the hypocenters disregarding the positions of the epicenters. This figure indicates the frequency of the hypocenters at depths of every 20 km, from 20 km to under 40 km, from 40 km to under 60 km and so on.

As seen in Fig. 2 (1), the maximum frequency is at depths of 40 km to 60 km. As the Mohorovičić discontinuity is supposed to lie at depths of 20 km–40 km in Japan and its vicinity, Fig. 1 shows that more than two-thirds of these earthquakes occurred under the surface of discontinuity. Moreover, it is noticeable that the hypocenters of destructive earthquakes were located in somewhat shallow parts as compared with the depths of maximum frequency (40 km–60 km).

It is rather common for destructive earthquakes to be followed by after-shocks. The frequency distribution of the focal depths of after-shocks will be here discussed. The hypocenters of the after-shocks which followed the Tango earthquake of 1927 were studied by N. Nasu[3]. In the course of his investigations unprecedentely numerous hypocenters of the after-shocks were determined. Fig. 2 (2) represents the frequency of the focal depths of after-shocks at every 2 km. According to this diagram, the maximum frequency is found at depths of under 16 km or 18 km, and shows the Gausian distribution at the same depth to be the centre. Consequently the depth of 17 km which is the maximum frequency is the mean depth of the after-shocks of the Tango earthquake and almost no after-shock originated from areas shallower than 3 km and deeper than 35 km. A characteristic of the after-shocks that followed the Tango earthquake is that in comparing the after-shocks of the several major earthquakes in Japan which have hitherto been investigated its hypocenters were the deepest.

Other examples of the frequency distribution of the focal depths of after-shocks will be given below. The after-shocks of the Oga earthquake[4] of 1939 show a distribution similar to a Gausian distribution with

2) *Japan Meteor. Agency, Seismol. Bull.*, 1951–1956.
3) N. NASU, *Bull. Earthq. Res. Inst.*, **6** (1929), 245; **7** (1929), 133.
4) T. HAGIWARA, *Bull. Earthq. Res. Inst.*, **17** (1939), 627.

13 km as the central point of evaluation, the Tottori earthquake[5] of 1943 9 km, the Hukui earthquake[6] of 1948 7 km, the Imaiti earthquake[7] of 1949 4 km respectively. The hypocenters of those after-shocks of which the depths were determined are fewer in number compared with the Tango earthquake, hence a Gausian distribution as seen in Fig. 2 is not clearly manifested.

Next, the frequency distribution of the focal depths of earthquakes originating from volcanoes will be discussed. As will be described later, earthquakes originating from volcanoes, according to the nature of the earthquake-motions and the relation of the earthquakes to volcanic eruptions, can be classified as follows: A-type earthquakes originating from somewhat greater depths in the volcano, or, from a depth of 1 km to 10 km (sometimes 20 km); B-type earthquakes originating in swarms from a shallow depth near the crater; explosion earthquakes accompanying explosive eruptions of the Vulcanian type; and volcanic microtremors accompanying Strombolian eruptions.

Of these four kinds of earthquakes originating from volcanoes the A-type earthquakes are almost similar in the nature of their earthquake-motions to the after-shocks of the great earthquake set down

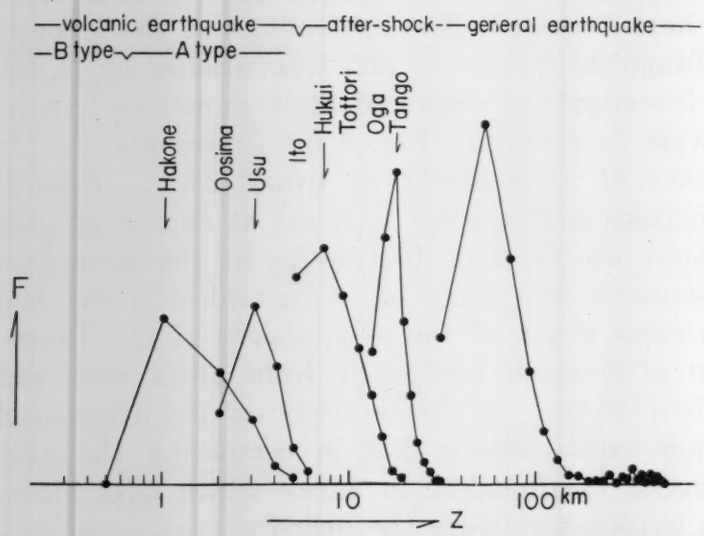

Fig. 4. Comparison of frequency distribution of hypocentral depth for general earthquake, after-shock and volcanic earthquake of the A and B types.

5) S. OMOTE, *Bull. Earthq. Res. Inst.*, **22** (1944), 223.
6) S. OMOTE, *The Hukui Earthquake of June* 28, 1948, (1950), 393.
7) T. HAGIWARA and K. KASAHARA, *Bull. Earthq. Res. Inst.*, **28** (1950), 393.

as the example in Fig. 28. Further examples are here given concerning the frequency distribution of the focal depths of A-type volcanic earthquakes. In the famous volcanic activity which gave birth to Syowa-Sinzan at the eastern foot of Usu-san[8], Hokkaido, from 1943 to 1945 the A-type earthquakes originated from depths of 1 km to 7 km with a maximum frequency of 3 km. The focal depths of the swarm earthquake which originated at Mihara-yama, Oo-sima[9], in 1938, indicate a distribution almost similar to that of the above-mentioned Usu-san.

The earthquake swarm that occurred in the Hakone volcano[10] quite recently (from September 1959 to March 1960) originated from Kami-yama, one of the central cones of the Hakone volcano, and its surroundings, and the earthquakes were very shallow, most of them being distributed at depths of 1 km to 2 km. Hence, these earthquakes should be regarded as A-type volcanic earthquakes.

Summarizing the above facts, the frequency distribution of the focal depths of tectonic earthquakes shallower than 100 km manifests a Gausian distribution with 60 km as the maximum frequency, and as to the frequency distribution of the focal depths of after-shocks, though differing with each major earthquake, the mean depth of 17 km for the Tango earthquake is the deepest, and the depth decreases in the order of the Oga, the Tottori, the Hukui, and the Imaiti earthquakes. The A-type volcanic earthquakes show a maximum frequency in still shallower parts. It is noteworthy that the focal depths of the Ito earthquake swarm[11] of 1930 were distributed with the centre at about 5 km. The focal depths were shallower than in general for the after-shocks of major earthquakes and deeper than volcanic earthquakes of the A-type, or in other words, the depths were between the above two cases. Many investigators incline to regard the Ito earthquake swarm as a kind of igneous activity in which magma under the ground intruded to a certain depth of the earth's crust. They regard the Ito earthquake swarm as an intermediate phenomena between general earthquake phenomena and volcanic phenomena. If the magma had ascended further, the magma would have been extruded and would have formed a volcano such as Syowa-Sinzan[12] or Parícutin[13].

8) T. MINAKAMI, *Bull. Earthq. Res., Inst.* **25** (1947), 71.
9) R. TAKAHASI and T. NAGATA, *Zisin*, **11** (1939), 161.
10) T. MINAKAMI, *Report on the 1959-1960 Earthquake Swarm of Volcano Hakone*, (1960), 1.
11) N. NASU, F. KISHINOUYE and T. KODAIRA, *Bull. Earthq. Res. Inst.*, **9** (1931), 22.
12) T. MINAKAMI, T. ISHIKAWA and K. YAGI, *Bull. Volcanol.* [ii], **11** (1951), 45.
13) J. GONZALEZ and W. F. FOSHAG, *Smithonian Report*, (1946), 223.

Volcanic earthquakes of the B-type[14)15)] originate in swarms from parts shallower than those of the A-type of active volcanoes. The focal depths of explosion earthquakes and volcanic microtremors are almost the same as those of volcanic earthquakes of the B-type. As far as is yet known, the focal depth of these earthquakes is shallower than 1 km from the floor of the craters, but the frequency distribution within 1 km in depth has not yet been clarified. This is a problem left to future study.

3. Characteristics of crustal deformations accompanying volcanic activity

Of the phenomena that accompany volcanic activity, crustal deformations are the most remarkable. Crustal deformations though only sometimes accompanying major earthquakes are also extremely remarkable.

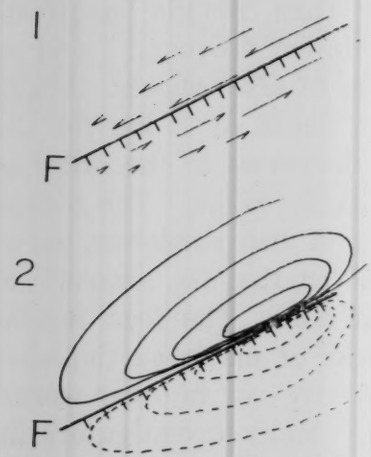

Fig. 5. Schematic illustration of the crustal deformation caused by major earthquake which produced earthquake fault (F).
1: horizontal displacement,
2: vertical displacement.

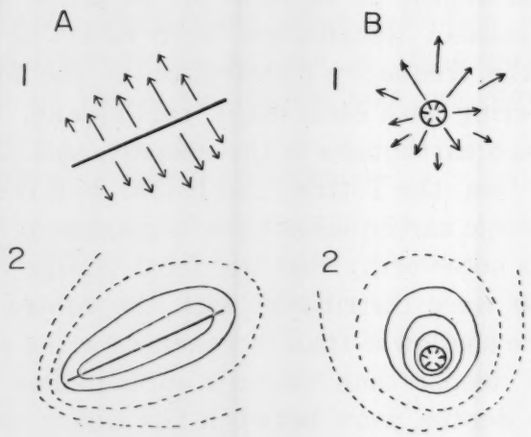

Fig. 6. Schematic illustration of the crustal deformations caused by volcanic eruption.
A: fissure eruption, B: central eruption,
1: horizontal displacement 2: vertical displacement
full line: upheaved area, dotted line: subsided area.

Now, in a comparison of the crustal deformations accompanying both phenomena, the characteristics of crustal deformations associated with volcanic activity will be mentioned.

14) T. MINAKAMI, S. SAKUMA, K. MOGI, and S. HIRAGA, *Bull. Volcanol. Soc. Japan*, [ii], **4** (1960), 133.
15) T. MINAKAMI, K. MOGI, S. HIRAGA and T. MIYAZAKI, *Bull. Volcanol. Soc. Japan*, [ii], **2** (1957), 77.

Resulting from major earthquakes, faults frequently appear on the earth's surface. The fault which appeared in the cases of the Californian[16], the Nōbi[17], The Tango[18], the North Izu[19], the Tottori[20], and the Hukui[21] earthquakes are well known. In each fault, the horizontal displacement is almost parallel with the fault plane, namely, with the fault line acting as the boundary and the directions of the displacement at the regions which are divided by the fault are reversed. As to the vertical displacement, in most cases the area is divided into two segments of upheaval and subsidence with the fault line as the boundary, but sometimes the area is divided into four quadrants by a straight line at right angles with the fault line. The first and the third quadrants represent upheaval, while the second and the fourth quadrants represent subsidence. Crustal deformations of such types are observed most commonly in the cases of major earthquakes.

Sometimes, accompanying volcanic activity, faultlike fissures are produced in the volcanic formation and lava is extruded from the fissures. This phenomenon was observed in the cases of the eruption of Sakurazima[22] in 1914 and that of Miyake-sima[23] in 1940. Crustal deformations in volcanoes in such cases are the same as in the case of earthquake faults with respect to reverse horizontal deformations with the faultlike fissures as the boundary, but the deformations differ remarkably from those associated with earthquake faults with respect to deformations in a right-angle direction to the faultlike fissure lines. That is to say, in the case of volcanoes, deformation manifests itself toward the horizontal direction so as to enlarge the faultlike fissures, while, on the contrary, in the case of tectonic earthquakes, deformation occurs so as to slip parallel to and toward the opposite direction along the fault plane. Hence, the direction of the former differs as much as 90° from that of the latter. Moreover, in the case where an eruption has a crater as the centre, namely, a central eruption, horizontal deformations radiate from the crater toward the outside. This was observed distinctly in the

16) A. C. LAWSON etc., *State. Earthq. Inv. Comm.*, (1909).

17) B. KOTO. *Jour. Coll. Sci., Tokyo Imp. Univ.*, **5** (1892). F. OMORI, *Bull. Imp. Inv. Comm.*, **1** (1907).

18) C. TSUBOI, *Bull. Earthq. Res. Inst.*, **8** (1930), 153.

19) Y. OTUKA, *Bull. Earthq. Res. Inst.*, **1** (1933) 530.

20) H. TSUYA, *Bull. Earthq. Res. Inst.*, **22** (1944), 1.

21) N. NASU, *Bull. Eatrhq. Res. Inst.*, **27** (1949), 27.

22) F. OMORI, *Bull. Imp. Earthq. Inv. Comm.*, **8** (1914-1922), 1. K. MOGI, *Bull. Earthq. Res. Inst.*, **36** (1957), 99.

23) S. OMOTE, *Bull. Earthq. Res. Inst.*, **20** (1942), 127.

course of the growth of Syowa-Sinzan, the Usu Volcano.

The most common vertical deformations accompanying volcanic activity are the dome-like upheavals having the crater as the centre and a subsidence of the surroundings of the upheaved area. Consequently, in volcanoes which display central eruptions, an almost circular area with the upheaved part as the centre is elevated (e. g., Usu-san[24] and Asama-yama[25]), and, in volcanoes which erupt from a faultlike fissure, and oval area having the fissure line as the longer axis is elevated (e. g., the eruption of Sakura-zima[26] in 1914). In both cases, subsidence occurs outside these upheaved areas. Hence, vertical deformations accompanying volcanic activity differ strikingly from those associated with major earthquakes accompanied by faults with respect to vertical crustal deformations as well.

As seen in the crustal deformations that accompanied the eruptions of Usu-san and Sakura-zima, sometimes the deformation is reversed after the eruption, and though the velocity is strikingly slow as compared with the deformation that directly accompanied the eruption, deformation in the reverse sense lasts. In most cases, however, the degree of recovery falls far short of the initial deformation. For example, after the great eruption of Sakura-zima of 1914 the Aira caldera (the inside) subsided to a great extent together with the skirt of Sakura-zima, and in the reverse process of deformation, i. e., continuous change lasted for more than 30 years after that. This is the most remarkable example of recovery by deformation, but still it fell short of a perfect recovery to the state of pre-eruption. Therefore it may be said that even now the deformation in recent eruptions is progressing toward a development of a subsidence topography in the caldera. Crustal deformations that accompanied major earthquakes somewhat resemble those of volcanic eruptions in that the process of deformations reversed after the outburst, but recovery in the former is not so conspicuous as in the latter.

It may be necessary to mention the magnitude of crustal deformations accompanying earthquakes and volcanic eruptions, i. e., the dimensions of an area which underwent changes and the velocity of those changes. The crustal deformations accompanying volcanic activity are generally limited to the vicinity of the volcano and the dimension is also smaller as compared with those accompanying major earthquakes.

24) T. MINAKAMI, T. ISHIKAWA and K. YAGI, *loc. cit.*, *15*).
25) T. MINAKAMI, *Bull. Volcanol.* [ii], **18** (1958), 39.
26) F. OMORI *loc. cit.*, 27).

As seen in the case of the eruption of Syowa-Sinzan, however, sometimes the local deformation with its centre at the crater manifests upheaval as far as more than 100 m. Therefore, crustal deformations accompanying volcanic activity sometimes are more remarkable in this respect than those accompanying earthquakes. In volcanic eruptions and earthquake swarms (for example, the Ito earthquake swarm[27]), the phenomena last long and crustal deformations accompanying these phenomena are also prolonged. On the contrary, in the case of crustal deformations accompanying major earthquakes, the crustal deformations come to an end within a short time, namely, from several to ten minutes, before the earthquake vibrations of the principal shock are over. Consequently, with regard to crustal deformations accompanying volcanic activities and earthquake swarms, surveys can be carried out over again, and the development of volcanic activity and earthquake swarms and the progress of crustal deformations with respect to these phenomena can be studied in detail. Some examples will be given in the following paragraph.

4. Crustal deformations that accompanied the development of Syowa-Sinzan, from the Usu volcano

The activity of Syowa-Sinzan which began in December 1943 was really conspicuous, and, in the course of about two years ending in October 1945, earthquakes, the upheaval of the ground, the formation of new craters, the extrusion of lava and the birth of a new volcano at the eastern foot of Usu-san occurred in succession. In the course of this period precise levelling was carried out along a route crossing the rising area. This was really an epochmaking investigation, and, as a result, crustal deformations were observed in detail from the beginning of the volcanic activity to the end. Above all, it is noteworthy that the rising area was confined with the approach of lava to the level of the earth's surface. That is, the rising area that was about 2 km in radius at first gradually diminished, and it was about 1 km in radius at the time when the lava began to appear on the earth's surface. The process of diminution of the rising area is represented in Fig. 8, in which the upheaval in the three stages, i. e., the beginning of volcanic activity, the stage in which phreatic explosion occurred frequently and the stage in which a lava dome developed on the ground surface, is represented with the upheaval velocity (cm/day). By this diagram it may be understood

27) C. TSUBOI, *Jap. Jour., Astr. and Geoph.* **10** (1932-1933), 93.

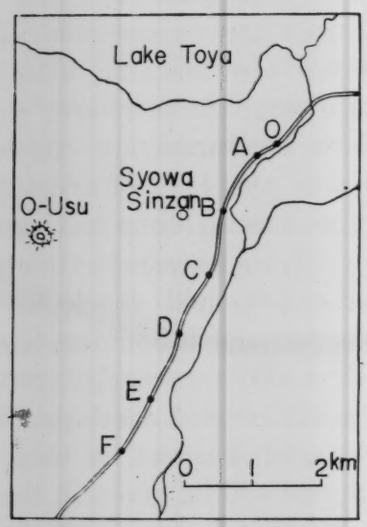

Fig. 7. Locality of levelling route near the newly formed mountain, Syowa-sinzan.

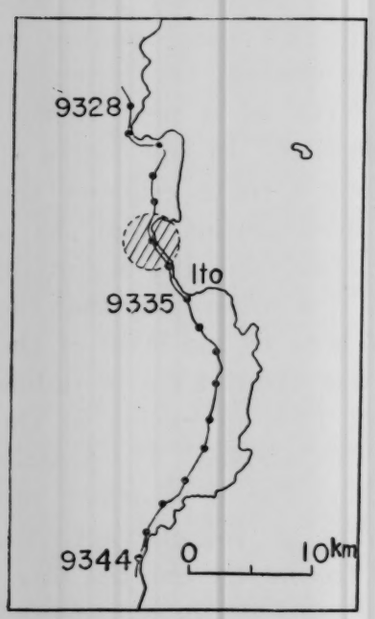

Fig. 9. Locality of the bench marks in the vicinity of Ito. hatched circle; central part of rising area.

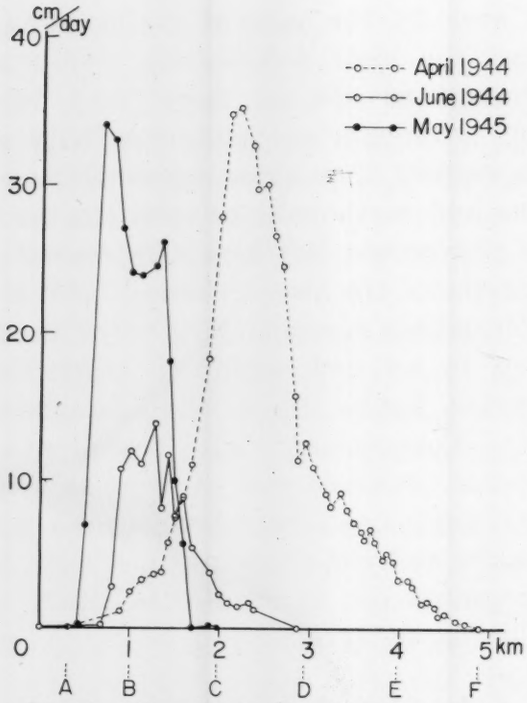

Fig. 8. Changes in the rising area in accordance with development of intrusion of viscous lava (Syowa-sinzan, Usu).

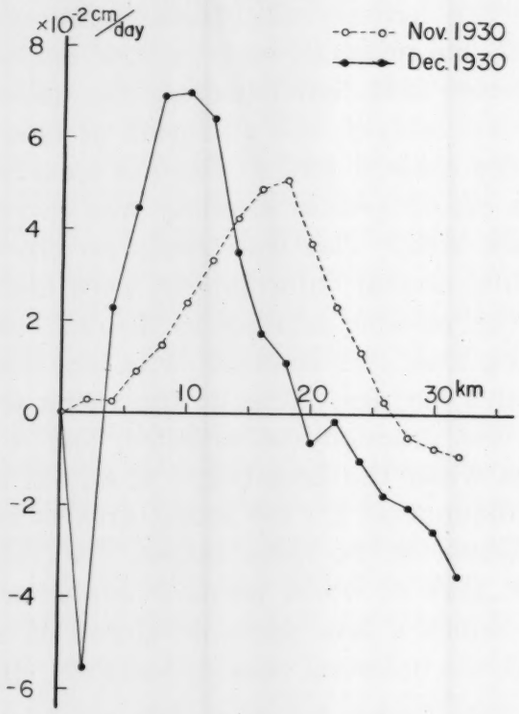

Fig. 10. Changes in the rising area with development of the Ito earthquake swarm.

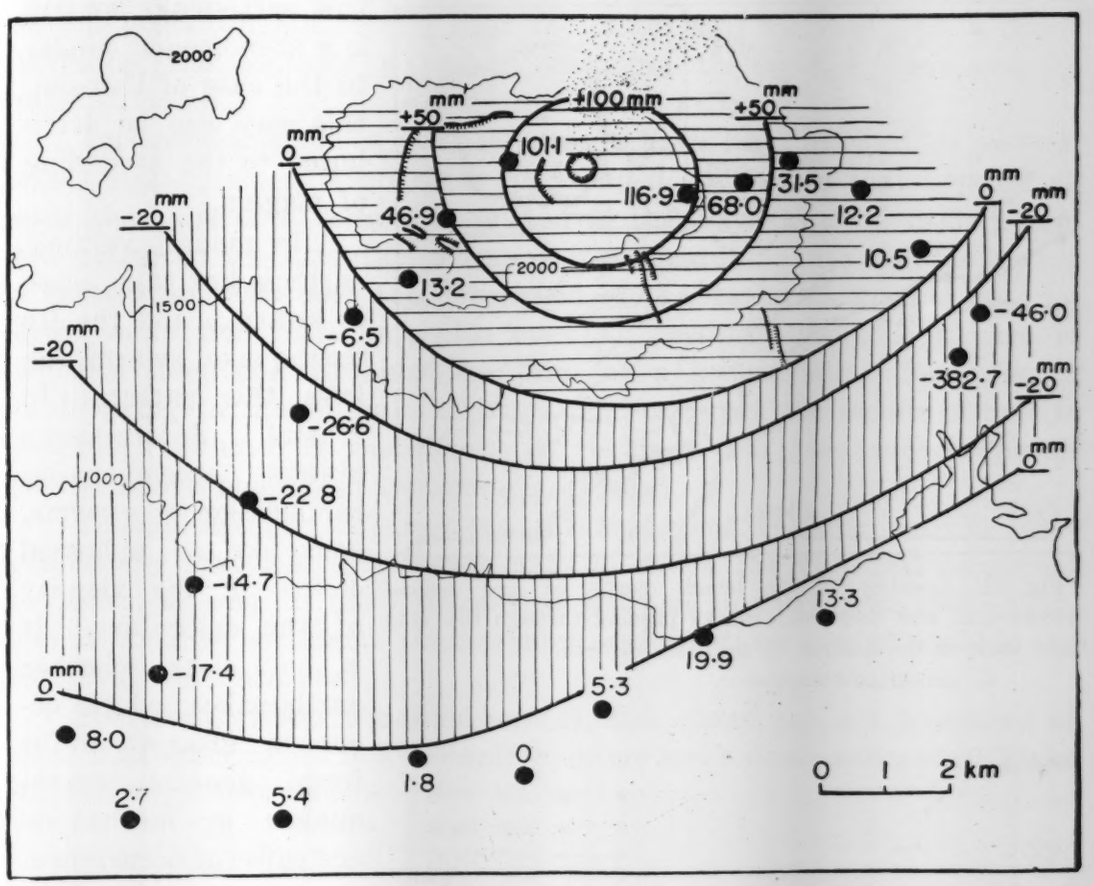

Fig. 11. Topographical deformation on and around Mt. Asama.

that the diminution in diameter of the rising area with the development of volcanic activity is an upheaval phenomenon resulting from the ascending of nearly solidified lava, namely, viscous dacitic lava, to the earth's surface.

Also in the course of the Ito earthquake swarm precise levelling was carried out three times. Through these levellings it has become possible to compare the crustal deformations in the first half of the earthquake swarm with those in the latter half. Assuming that the bench mark (No. 9328) is stable, the deformation in each stage is shown with the daily velocity (cm/day) in Fig. 10. As is shown clearly by this diagram, the crustal deformations that accompanied the Ito earthquake swarm also manifest a domelike upheaval, though it is not as conspicuous as that of Usu-san. Moreover, in the latter half of the earthquake swarm it is noticed that the rising area diminishes slightly. If it be assumed that

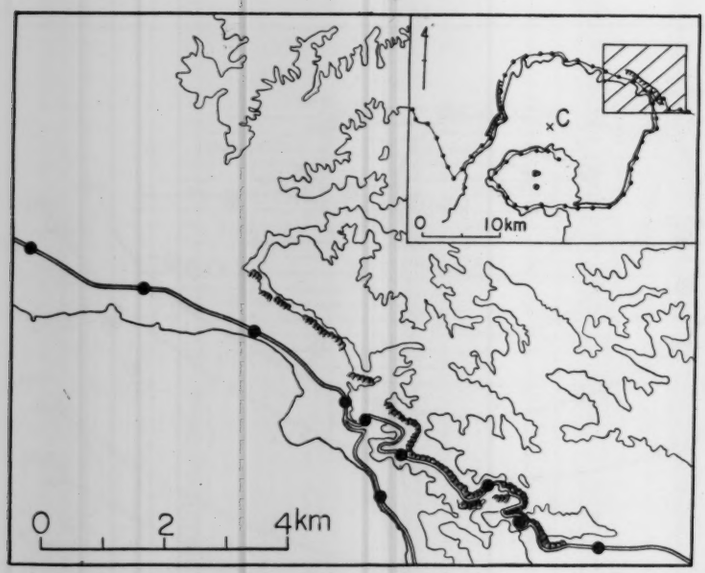

Fig. 12. Locality of the bench marks on and around Sakura-zima and the bench marks passing through the ring form fault at the margin of the Aira caldera.
C: center of subsidence.

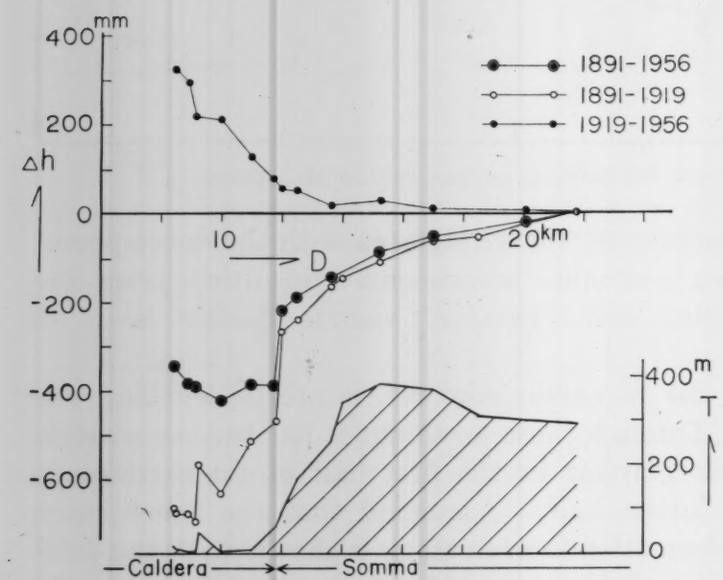

Fig. 13. Topographical deformations at the margin of the Aira caldera.
Δh, change in height of bench marks,
T, topography (height above sea-level of bench marks),
D, distance from the center of subsidence.

this earthquake swarm is a phenomenon similar to the case of Usu-san, this may also be attributed to the ascending of magma.

In general, volcanic earthquakes take place in swarms, and the Ito earthquake swarm follows this pattern. In crustal deformations always accompanying earthquake swarms, dome-like upheaval occurs in the vicinity of the epicenters. It is not clear whether earthquakes which occur in swarms differ from general earthquakes in mechanism and cause of occurrence, or whether this phenomenon is attributable to the difference in the nature of the earth's crust caused by the different depths of the source of the phenomenon, at any rate it seems to be a problem of some magnitude.

Asama-yama is famous for the fact that lava is explosively extruded in the form of lava fragments of various sizes from the

summit crater. Fig. 11 represents the conditions during eruptions in recent years when a section near the crater was uplifted like a dome, while on the contrary a section including the middle flank and the skirt subsided.

Topographic changes in such a mode have been noticed in several other volcanoes. Particularly a ring-shaped subsidence that appears all over the skirt of a volcano is related to the formation of caldera and has attracted the attention of many investigators. In a volcano having a caldera not only does the depression of the caldera continue to progress more and more but also even at present* there is a case in which a steep cliff forming the brim of a somma slips down like a fault owing to the volcanic activity. For example, the results of precise levelling conducted in the vicinity of Sikine in the Aira caldera revealed the above mentioned topographic change.

Though crustal deformations accompanying volcanic activity geographically localized, there were cases in which the upheaval amounted to 100 m, as seen in the eruptions of Usu-san in 1911 and 1943～1945, and as regards horizontal displacement, deformations almost equal to the upheaval were observed.

Therefore, when the dilation (Δ) and shear (σ) are compared at their maximum values in a volcanic eruption and a destructive earthquake respectively, they become

$$\Delta=\frac{\partial u}{\partial x}+\frac{\partial v}{\partial y}, \quad \sigma=\frac{\partial u}{\partial y}-\frac{\partial v}{\partial x}$$

$\Delta=10^{-1}$, $\sigma=10^{-1}$: Volcano (Syowa-Sinzan[28])
$\Delta=10^{-4}$, $\sigma=10^{-4}$: Earthquake (Tango earthquake[29])

As shown above, the crustal deformations in Syowa-Sinzan are strikingly larger than those caused by a major earthquake.

5. The nature of lava and volcanic eruption

Volcanic eruption is the phenomenon of subterranean magma being extruded as lava. However, each volcano manifests very different characteristics, at least apparently, in its mode of eruption. For example, in one volcano, lava is extruded as flowing lava; in another volcano, highly viscous lava is hurled out from the crater as pyroclastic ejecta; in another, minor eruptions are repeated continuously, and, in

* 1891–1956.

28) T. MINAKAMI, *Bull. Earthq. Res. Inst.*, **28** (1950), 143.

29) C. TSUBOI, *loc. cit.*, 27).

another, without forewarning great quantities of eruptives are extruded explosively. In accordance with the difference in the modes of eruption, there are differences in earthquakes, the crustal deformations and electromagnetic phenomena originating from volcanoes. That is, each volcano is characterized by a different mode of eruption.

The characteristics of volcanic phenomena are classified in several groups, and in many cases each characteristic is related to the chemical and petrological characteristics of the erupted lava. That is, the character of the eruptions, the intensity of the magnetization of the volcanoes, and earthquake phenomena accompanying the volcanic eruptions are characterized by the nature of the lava, i.e., basaltic, andestic, dacitic, or intermediate. The viscosity and temperature of the lava at the time of eruption also differs, and these have correlation with the nature of the eruptive phenomena.

First of all, the results of the analyses of representative lava, namely, basalt[30] (Kilauea), andestitic basalt[31] (Oo-sima and Miyake-sima), andesite[32] (Asama-yama and Sakura-zima), dacite[33] (Syowa-Sinzan) and liparite[34] (Katmai) are shown in Table 1.

Table 1. Chemical composition of various volcanic rocks.
(After G. A. Macdonald, H. Tsuya, R. Morimoto, J. Ossaka, K. Yagi and R. E. Wilcox.)

	Basalt (Kilauea)	Andesitic basalt (Oo-sima)	Andesite (Asama)	Dacite (Usu)	Liparite (Katmai)
SiO_2	49.80	52.44	60.00	69.17	76.53
Al_2O_3	12.42	15.44	16.67	15.68	12.31
Fe_2O_2	1.53	3.16	1.64	1.72	0.46
FeO	9.91	10.11	5.36	2.37	0.96
Mg O	10.31	4.66	4.14	0.92	0.00
Ca O	10.32	9.74	7.87	4.00	1.01
Na_2O	1.96	1.66	2.03	3.63	4.15
K_2O	0.45	0.33	0.88	1.32	3.05
TiO_2	2.68	1.59	0.97	0.41	0.17
P_2O_5	0.29	0.12	0.07	0.20	0.05
MnO	0.13	0.10	0.25	0.20	0.04
H_2O	—	0.76	0.18	0.70	1.12
Total	99.80	100.11	100.06	100.32	99.85

30) G. A. MACDONALD, *Bull. Geol. Soc. Amer.*, **60** (1949), 1541.
31) H. TSUYA, *Bull. Earthq. Res. Inst.*, **15** (1937), 215. H. TSUYA, R. MORIMOTO and J. OSSAKA, *Bull. Earthq. Res. Inst.*, **30** (1952), 231.
32) H. TSUYA, *Bull. Earthq. Res. Inst.*, **11**(1933), 575.
33) K. YAGI, *Trans. Amer. Geoph. Union*, **34** (1953), 449.
34) R. E. WILCOX, *Geol. Sur. Bull.*, **1028** (1959), 1.

In many volcanoes, the temperature and viscosity of the lava at the time of eruption was measured and reported, though fragmentarily. Summarizing these results, we may consider that the temperature and viscosity of the lavas during eruption were near the values shown in Table 2.

Table 2. Temperature and viscosity of fresh lavas at the times of eruption.

	Temperature	Viscosity	Volcano
Basalt	1200°C	10 —10^3 poises	Kilauea
Andesitic basalt	1150°C	10^3—10^4 poises	Oo-sima
Andesite	1050—1100°C	10^5—10^7 poises	Sakura-zima
Dacite	1000—1500°C	$>10^{10}$ poises	Usu (Syowa-Sinzan)

As shown in Table 2, viscosity differs greatly according to the kinds of lava, and the difference is closely related to the nature of eruption and the forerunning and subsequent phenomena associated with volcanic eruptions. For example, highly fluid lavas such as those of Kilauea and Mauna Loa in Hawaii Is., flow rapidly down the mountain-side. On the contrary, the dacitic lava which built up Syowa-Sinzan failed to flow after it was erupted on the ground surface and formed a lava dome at the position of the crater.

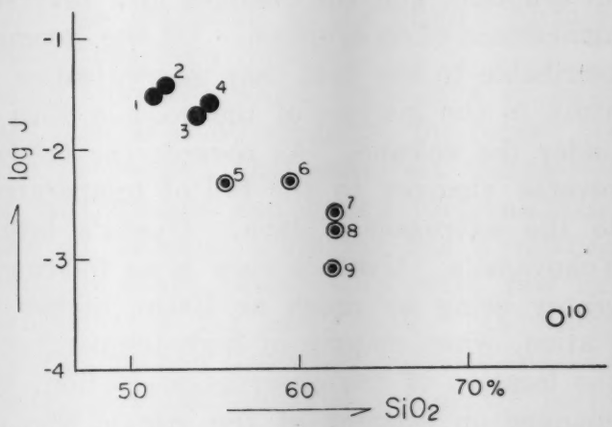

Fig. 14. The intensity of magnetization of volcanoes and the nature of volcanic rocks forming the respective volcanoes.
closed circle: andesitic basalt,
double circle: andesite,
opened circle: liparite.
1: Huzi, 2: Oo-sima, 3: Miyake-sima,
4: Hatizyo-sima, 5: Oomuro, 6: Tarumai,
7: Asama, 8: Sakura-zima, 9: Kusatu-sirane,
10: Koozu-sima.

Quaternary volcanoes[35)–39)] are magnetized in the direction $N-S$. Assuming that the lavas constituting these volcanoes retain the direction of magnetization at the time when the lavas were erupted and cooled on

35) T. NAGATA, *Bull. Earthq. Res Inst.*, **21** (1943), 1.
36) T. MINAKAMI and S. SAKUMA, *Bull. Volcanol.*, [ii], **18** (1956), 77.
37) T. MINAKAMI, *Bull. Earthq. Res. Inst.*, **19** (1941), 356.
38) T. RIKITAKE, *Bull. Earthq. Res. Inst.*, **29** (1951), 499.
39) S. SAKUMA, *Jap. Jour. Geoph.*, **1** (1957), 1.

the ground-surface, it indicates that the direction of the earth's magnetic field in the Quaternary period was not very different from that of the present time. On the other hand, the intensity of magnetization differs markedly according to the kinds of lava constituting the volcanoes. That is, the intensity of magnetization of volcano consisting of basalt contains a large quantity of FeO and Fe_2O_3. Some examples of the intensity of magnetization of volcanoes will be shown in Fig. 14.

T. Rikitake, I. Yokoyama, and S. Uyeda[40)41)] have conducted continuous observations on the geomagnetic changes at the foot of Mihara-yama, O-sima, since 1950. In the course of these observations Mihara-yama repeatedly erupted and extruded basaltic lava. The relationship between the changes of geomagnetism, especially the changes in the declination and the occurrence of volcanic eruptions were studied, and it was disclosed that the decreasing of the intensity of magnetization appears in the central part of the volcano a month or two before an eruption, and the changes in a reverse sense, appear after the commencement of an eruption. Of the geomagnetic changes, the former is ascribable to the fact that magentization is lost by the rise of temperature in the interior of the volcano with the ascending of magma lying under the volcano. As regards the latter, Yokoyama[42)] attributes the reverse changes to the fall of temperature in the volcanic body owing to the extrusion of lava. Uyeda's interpretation[43)] is different from Yokoyama's. Uyeda's view is as follows: The locality of the summit crater being as much as 700 m, higher than the magnetic observation station, when magma of high temperature ascends beyond the level of the location of the observation station, the intensity of magnetization changes on account of the rise of the geothermal temperature in the upper part of the mountain body. This change of magnetization is reversed in magnetic declination at the observation station. In either case, it is considered that the ascending of subterranean magma causes the changes in the geothermal temperature of the volcanic body and thereby the changes in the earth's magnetic field. That is, it has become possible to observe the ascending of magma in the interior of a volcano by the changes in the earth's magnetic field. Since basaltic volcanoes such as Mihara-yama are strongly magnetized as compared

40) T. RIKITAKE, I. YOKOYAMA, A. OKADA and Y. HISHIYAMA, *Bull. Earthq. Res. Inst.*, **29** (1951), 583.

41) T. RIKITAKE, *Bull. Earthq. Res. Inst.*, **30** (1952), 71.

42) I. YOKOYAMA, *Bull. Earthq. Res. Inst.*, **32** (1954), 17.

43) S. UYEDA, *read at the general meeting of Vol., Soc. Japan*, May, 1960.

with andesitic and dacitic volcanoes, and the changes of temperature in the interior are observable as changes of the earth's magnetic field on the ground surface, there arises the possibility of discerning the inner condition of such volcanoes by a different method from the method used for andesitic volcanoes.

6. Pressure exerted on volcanic bodies at the time of lava extrusion and the viscosity of lavas.

Magma which ascends and is extruded on the ground surface, is produced in depths between several tens of kilometers and 300 km. The course which magma follows from the interior of the earth to the earth's surface and the force by which magma is extruded have not yet been confirmed. With regard to various phenomena, however, observable in volcanoes in the course of the ascending of magma from the shallow depth of several kilometers and its extrusion to the ground surface, some information on measurements has been reported.

Generally speaking, comparing volcanoes which erupt lava of large viscosity with those which erupt lava of small viscosity, the former are more remarkable in the dynamic phenomena that manifest themselves before eruption, i. e., volcanic earthquakes and crustal deformations. Needless to say, the magnitude of volcanic eruptions has a relation with the above phenomena, but the above relationship, with few exceptions is noticed also in eruptions of the same scale. As stated above, in volcanoes such as Sakura-zima and Usu which extrude andesite and dacite lavas of large viscosity, local earthquakes frequently occur for several months or several days before eruptions and marked crustal deformations such as upheavals of the ground take place. On the contrary, in the case of the eruption of Mihara-yama of 1950–1951 which erupted lava of small viscosity, such phenomena were not observed. This is considered to be significant. One reason that occurs to us is that the degree of viscosity of the lava is related to the increase of the subterranean pressure needed for volcanic eruption. Now the pressure exerted in the depths of a volcano at the time of lava eruption will be considered by using a simple example.

At the time when lava of viscosity (η) ascends toward the ground surface and erupts from the lava-reservoir under the volcano through a tubelike conduit of radius (a) with mean velocity (v), the increase of pressure (Δp_1) in the reservoir is represented by

$$\Delta p_1 = \rho g \Delta l + \frac{1}{2}\rho v^2 + \frac{8\eta v l}{a^2} ,$$

where ρ, l, Δl are the density of lava, the length of the conduit and the ascending of the lava head respectively.

Consequently, taking into consideration the fact that the stress exerted on a volcanic body is related to the viscosity of the lava and, as shown in Table 2,[44)-50)] the degree of viscosity differs in accordance with the kind of lava, it may be expected that the increase of stress needed for the ascending of the lava differs markedly according to the nature of the lava.

In some volcanoes, there is a case where lava is extruded in the manner of dike along a long fissure. In such a case, the relation between the viscosity and the increase (Δp_2) of pressure in the lava-reservoir, assuming the width of the dike to be 2b, is represented by

$$\Delta p_2 = \rho g \Delta l + \frac{1}{2}\rho v^2 + \frac{3\eta v l}{b^2} .$$

That is, the relation is almost similar to the case where lava is extruded through a tube-like conduit.

The foregoing explanation is based on the most simple model of the relationship among the pressure which forces magma to ascend, the viscosity of the magma, and the structure of the volcano (namely, the length, diameter, etc. of the conduit).

In the case of lave eruption in a long-dormant volcano in which lava in the conduit has solidified and in the case of lava eruption which occurs in a locality where no crater existed like Syowa-Sinzan and Parícutin, a new fissure or crack forms first, and then eruption takes place. In order to open a passage for the lava to ascend through the structure of volcano, strong pressure must be exerted on the subterranean formation.

This corresponds with the case where a and b in the above formulae are extremely small. Hence, in cases where the viscosity of the lava is

44) G. A. MACDONALD, *Amer. Jour. Sci.*, **241** (1943), 241.
45) P. E. SCHULZ, *Bull. Geol. Soc. Amer.*. **54** (1943), No. 6.
46) R. H. FINCH, *Vol. Let.*, **480** (1943), 2.
47) T. HAGIWARA, *Bull. Earthq. Res. Inst.*, **19** (1941), 299.
48) T. MINAKAMI, *Bull. Earthq. Res. Inst.*, **31** (1951), 487.
49) S. SAKUMA, *Bull. Earthq. Res, Inst.*, **31**(1953), 291.
50) T. HAGIWARA and others, *Bull, Earthq. Res Inst.*, **24** (1946), 143.

large or where a volcano lacks a vent or where the vent is very small, innumerable earthquakes or conspicuous crustal deformations ought to take place previous to eruption. That is, in many cases, at first premonitory phenomena manifest themselves and then eruption occurs. There are some examples of this mode of eruption.

Even in the case where similar lava is erupted from the same crater of the same volcano, a slight difference in the temperature of the lava will give rise to a marked difference in the viscosity of the lava. Thus, the relation between the pressure exerted on a volcanic body and the eruption, or the relation between premonitory phenomena, namely, earthquakes and crustal deformations, and the eruption, is not a constant one but must be considered as a relation which holds only within a certain range. In other words, the relation between both phenomena is established as a relation made valid by the process of probability.

7. Earthquakes originating from volcanoes

As stated above, volcanic eruptions and earthquakes originating from volcanoes are closely related to each other in various aspects. In this paragraph, the relationship between the kinds of earthquakes which originate from volcanoes and volcanic phenomena will be classified and summarized.

In respect to the relation between general earthquakes originating from depths of 20 km–100 km and volcanic activity, no definite answer has been given, but it cannot be concluded that the general earthquakes have no connection with the production of magma. However, taking the eruptions of volcanoes and earthquakes in the world as the object of consideration, there are not many actual examples of the particular time relation between great earthquakes and great volcanic eruptions.

As mentioned briefly in the paragraph on the distribution of focal depths, earthquakes originating from volcanoes can be classified in the following four groups. Definitions of these four types of volcanic earthquakes will be given here.

1. A-type volcanic earthquakes

These are earthquakes originating from the bases of volcanoes or from the depths of about 1 km to 10 km. These earthquakes occur in every volcano and particularly in many cases these earthquakes take place markedly previous to and in the first stage of eruptive activity. The nature of earthquake-motions cannot be distinguished from those of general

shallow earthquakes (tectonic earthquakes). The P-phase and the S-phase of seismic waves also make themselves clearly manifest.

2. B-type volcanic earthquakes

The hypocenters are limited to an area of about 1 km in radius around the active crater. The hypocenters of these earthquakes are shallower than those of the A-type volcanic earthquakes. These earthquakes take place in swarms in the shallow part ranging from the earth's surface to depths of several hundred meters. Consequently, the surface waves predominate and the S-phase cannot be discerned distinctly. These earthquakes are frequently observed in volcanoes in which the eruptions are of the Vulcanian type, such as Asama-yama and Sakura-zima.

3. Explosion earthquakes

These are earthquakes which accompany individual explosive eruptions. The amplitude of these earthquakes is related to the magnitude of the explosive eruptions. As far the results hitherto ascertained are concerned, the initial motion is 'push' in every direction. The hypocenters are situated in the part not deep from the active crater floor. The nature of the earthquake-vibrations of these earthquakes resembles that of the B-type volcanic earthquakes, but the magnitude are larger than that of the B-type volcanic earthquakes.

4. Volcanic pulsation or continuous volcanic microtremors

In cases such as the Strombolian or Hawaiian type where eruptions are prolonged, explosion earthquakes accompanying the eruption become continuous vibrations. In volcanoes displaying Strombolian or Hawaiian type eruptions, no B-type volcanic earthquakes take place, and in many cases continuous vibrations originate from the shallow part in the vicinity of the craters. In volcanoes in which the eruptions are of the Vulcanian type, sometimes such vibrations are caused by continuous shocks in the vicinity of the bottom of the active crater. Needless to say, the main part of such vibrations consists of the surface waves.

Seismograms of the above four types recorded with seismographs which are 1 sec. in proper period and of the same type are represented in Figs. 28–31.

For convenience in description, the writer classified volcanic earthquakes into these four groups. Here the writer must refer to Omori's classification[51] of volcanic earthquakes. Omori established a volcanological observatory at Yunotaira about 2 km southwest of the crater of the

51) F. OMORI, *Bull. Imp. Earthq. Inv. Comm.*, **6** (1912), 1; **7** (1914), 1.

Asama volcano in 1910, and he made observations with seismographs and other instruments. He also studied the nature of volcanic earthquakes associated with marked volcanic activities displayed in the period 1910–1913, and, in addition, he investigated the relation between volcanic

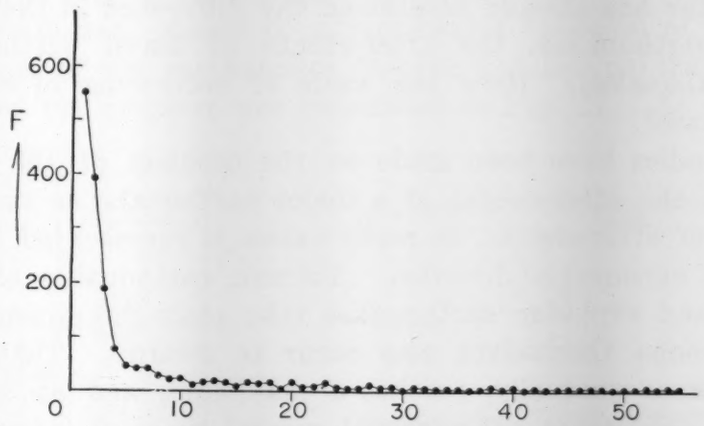

Fig. 15. Daily frequency of the after-shock of the Imaiti earthquake.

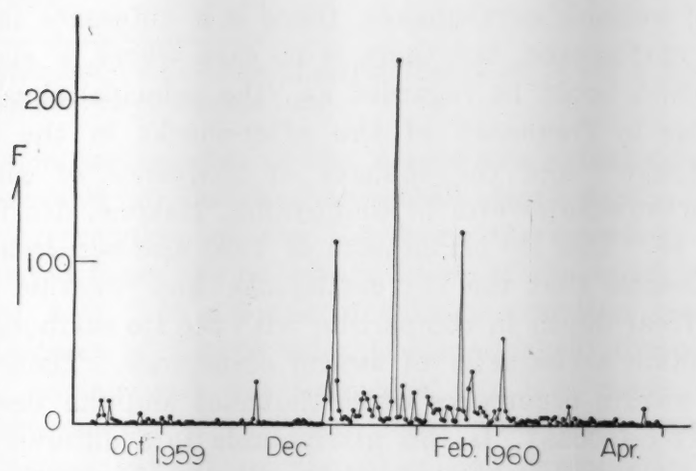

Fig. 16. Daily frequency of the Hakone earthquake swarm.

earthquakes and volcanic phenomena. This was an epoch-making study for that time. In this case, Omori classified the earthquakes originating from Asama-yama in two groups, namely, A-type and B-type. Omori defined the B-type earthquakes as earthquakes that accompany explosive eruptions or earthquakes accompanied by explosive eruptions. Omori's B-type earthquakes corrospond to the above mentioned explosion earthquakes as defined by the writer, and the former is different from

the B-type earthquakes as defined by the writer. On the other hand, Omori's A-type earthquakes correspond to both the A-type and B-type earthquakes as defined by the writer. The writer must mention that Omori's A-type and B-type earthquakes are different from those as defined by the writer.

The writer has already mentioned the difference in the focal depths of general earthquakes, the after-shocks of major earthquakes, and volcanic earthquakes. Here the mode of occurrence of each of them will be discussed.

Many studies have been made on the problem of the decrease in frequency of the after-shocks of a major earthquake as time advances. The decline of after-shocks, in many cases, is represented by a hyperbola and an exponential function. Volcanic earthquakes of the A-type and B-type and explosion earthquakes take place in swarms, and volcanic phenomena themselves also occur in swarms. That is, the frequency increases gradually, reaches a maximum, and at last declines. Such swarm occurrence are repeated several times at intervals. In the case of a major earthquake, the first shock (that is, the principal shock) is strikingly different in magnitude from the after-shocks which follow. In the case of volcanic earthquakes, there is a difference in the magnitude of each earthquake, but there is no case where a specially large earthquake which could be regarded as "the principal shock" occurrs.

The decline in frequency of the after-shocks in the case of the Imaiti earthquake[52] and the changes in frequency of earthquakes in the recent earthquake swarm in Kami-yama, Hakone, are illustrated in Figs. 15 and 16. The Ito earthquake of 1930 also occurred in swarms, and it is noticeable that the Ito earthquake and volcanic earthquakes shallower in focal depth in comparison with the Ito earthquake manifest without exception a character of swarm occurrence. Then what is the cause of the swarm occurrence of earthquakes and the decline in frequency of after-shocks? Is this attributable to a difference of occurrence mechanism between volcanic earthquakes and general earthquakes? Or is it a consequence of the character of the earth's crust which differs with the depths of the hypocentres? One or two examples have been quoted by way of solving this problem, but actually it may be a problem which will be solved only in the future. However, by clarifying the geographic distribution of the initial motions of seismic waves in volcanic earthquakes the solution to this problem may be hastened.

52) *Japan Meteor. Agency, Kisho-yoran* (*Geoph. Rev.*), No. 604, (1949), 605 (1950).

8. Some examples of the hypocentral distribution of volcanic earthquakes.

1) Usu-san[53)–55)]

The eruption of this volcano in 1943–45 was characteristic. This activity will live long in the history of volcanology by reason of the birth of Syowa-Sinzan, caused by a remarkable upheaval of the ground. The hypocenters of the earthquakes (A-type and B-type) that took place in the course of the eruption are illustrated in Fig. 17. As seen in the

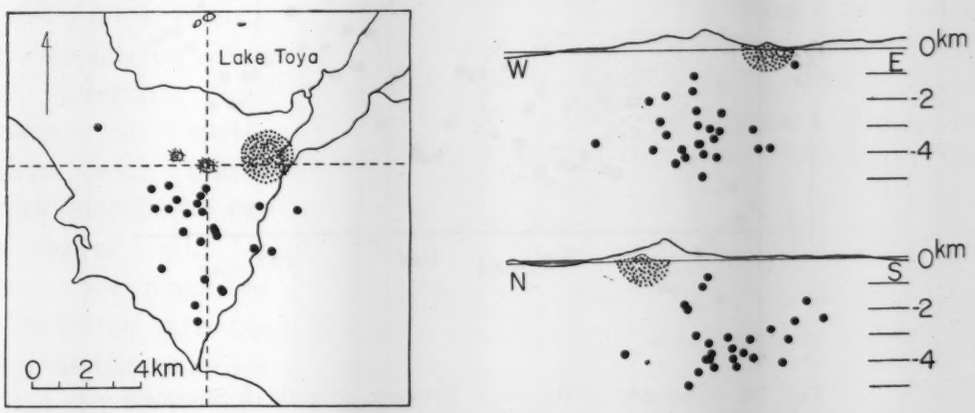

Fig. 17. Hypocentral distribution of earthquakes of the *A* and *B* types which took place in the 1944 activity of Volcano Usu.

diagram, volcanic earthquakes of the A-type are extensively distributed on the southern side of Usu-san, and their focal depths are 1–6 km. The volcanic earthquakes of the B-type on the contrary, were shown to have originated from depths within 1 km. of the earth's surface in a very limited area. In a series of volcanic activities beginning with frequent occurrences of A-type volcanic earthquakes, through upheaval and eruption, ending with the formation of a lava dome consisting of dacitic lava, the manner of the earthquake occurrence, particularly of A-type and B-type volcanic earthquakes was characteristic. That is, remarkable changes in the frequency of earthquakes of both type were manifested in the period from 1943 to 1945. All volcanic earthquakes that occurred in the early stage of activity towards the end of December 1943 were of the A-type, and there were no B-type earthquakes. At the time when the upheaval in the area at the eastern foot of Usu-san

53) T. MINAKAMI, *Bull. Earthq. Res. Inst.*, **25** (1947), 71.
54) T. MINAKAMI, T. ISHIKAWA and K. YAGI, *loc. cit.* 15).
55) T. KIZAWA, *Pap. Meteor. Geoph.*, **8** (1957), 150.

was noticed by the local inhabitants, B-type earthquakes also began to occur, while at the same time the occurrence of A-type earthquakes decreased, and before long phreatic eruption began. During the period when the lava dome was forming, most of the volcanic earthquakes were of the B-type, and the occurrence of A-type earthquakes decreased considerably. The variations in the frequency of A-type and B-type earthquakes are represented in Fig. 18. This is the frequency variation

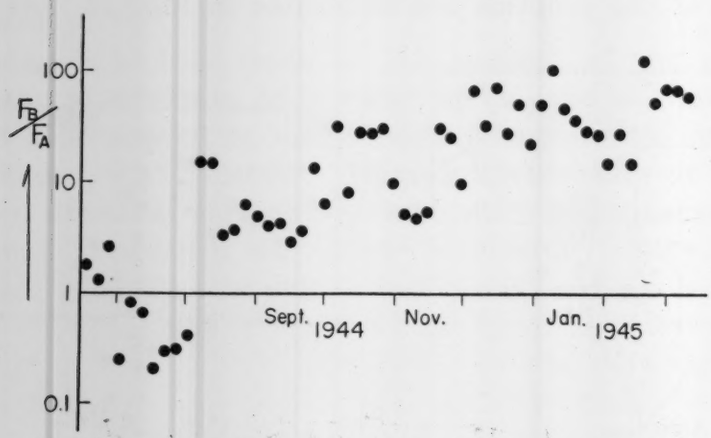

Fig. 18. Changes of the ratio between seismic frequencies (F_A and F_B) of the A and B types, which took place in the 1944 activity of Volcano Usu.

of the both types of earthquakes in the middle stage of this volcanic activity, i.e., from the beginning of the phreatic eruption to the time when the lava dome began to form. By this frequency variation, it is evident that the activity of A-type earthquakes originating from the somewhat deep part of this volcano migrated to a limited area near the earth's surface with the development of the volcanic activity, and B-type earthquakes took the place of A-type earthquakes. That is, this variation in frequency indicates that the rising area was reduced with the rise of magma from the deep part of this volcano (Fig. 8), and at the same time the hypocentres migrated near to the earth's surface, resulting in swarm occurrences of earthquakes from this area.

2) Asama-yama[56)–58)]

Asama-yama is representative of volcanoes that give off Vulcanian eruptions from the summit crater. The eruptions from the summit

56) T. MINAKAMI, *Bull. Vol. Soc. Japan*, [ii], **4** (1959), 104.
57) T. MINAKAMI and others, *Bull. Vol. Soc. Jap*, [ii], **4** (1959), 115.
58) T. MINAKAMI and others, *Bull. Vol. Soc. Jap*, [ii], **4** (1960), 113.

crater of Minami-dake, Sakura-zima, since 1955 have been activities of similar character.

Earthquakes originating from Asama-yama have been studied in relative detail since Omori's investigation which includes the remarkable eruptions extending over several years from 1910. Recently a tele recording apparatus has been adopted, and records of earthquakes, with transducers installed near the crater and in many other places of the volcano, are received at the recorder station. By this means it has been possible to detect occurrences of micro-earthquakes all over the volcano. Moreover, the hypocentre of these earthquakes can be accurately determined, and it has become possible to clarify the relationship between volcanic earthquakes and volcanic eruptions. As represented in Fig. 19, the greater part of the hypocentres swarm in an area 1 km in radius with the bottom of the summit crater as the centre (the hatched part in Fig. 19). One of the characteristics of earthquakes originating from Asama-yama is that the occurrence of A-type volcanic earthquakes originating from a

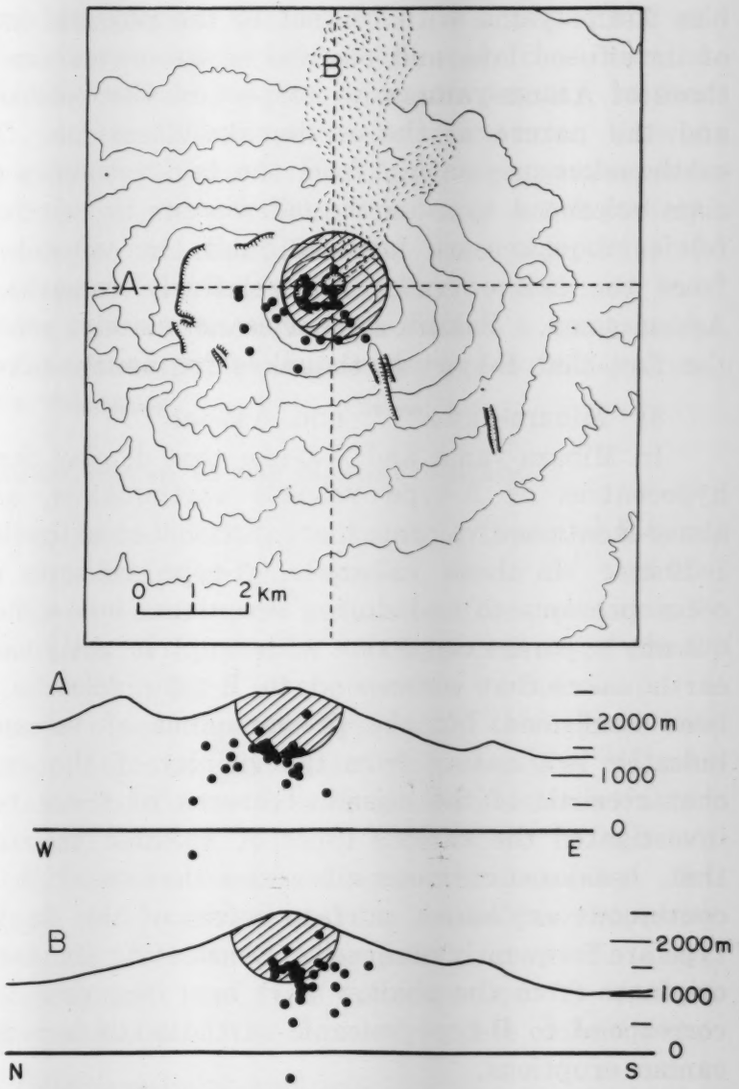

Fig. 19. Hypocentral distribution of earthquakes originating from Volcano Asama. Hatched area indicates hypocentral domain of the B-type earthquake.

somewhat deep part is very slight. Moreover, it is noteworthy also that almost no felt earthquake has occurred from Asama in the last 25 years.

The various types of earthquakes that have taken place in association with the recent activity of Minami-dake, Sakura-zima,[59] that resembles Asama-yama with respect to the physical and chemical properties of its effused lava and position of its crater are also closely related to those of Asama-yama with respect to the positions of the hypocentres and the nature of the earthquake-vibrations. The difference between earthquakes originating from the two volcanoes is that in the Sakura-zima volcano A-type earthquakes occur in relative abundance, in which felt earthquakes are involved, and the volcanic pulsations originating from the active crater are relatively remarkable as compared with Asama-yama. Sakura-zima volcano closely resembles Asama-yama in the fact that B-type earthquakes frequently take place.

3) Mihara-yama[60)–61)] and Aso-san[62)–63)]

In Mihara-yama and Aso-san that display Strombolian eruptions, the hypocentres of A-type volcanic earthquakes, as in the cases of the above-mentioned volcanoes, are distributed extensively in depths of about 1–10 km. In these volcanoes, A-type volcanic earthquakes sometimes occur previous to and during eruptions, but sometimes take place without any apparent connexion with eruptive activities. In these volcanoes, earthquakes that correspond to B-type volcanic earthquakes have not been confirmed, but the predominance of volcanic tremors or volcanic pulsation originating from the vicinity of the crater bottom may be a characteristic of the seismic features of these volcanoes. K. Sassa who investigated the various types of volcanic tremors in Aso-san reported that, besides continuous vibrations that occur in association with minor continuous explosions, surface waves of the Rayleigh type and the Love type are frequently observed. Considering the fact that these vibrations originate from the shallow part near the crater, the vibrations should correspond to B-type volcanic earthquakes in volcanoes displaying Vulcanian eruptions.

---

59) T. MINAKAMI, K. MOGI, S. HIRAGA and T. MIYAZAKI, *Bull. Volcan. Soc. Japan.* [ii], **2** (1957), 77.

60) R. TAKAHASI and T. NAGATA, *loc. cit* 9).

61) T. MINAKAMI, T. MIYAZAKI and T. TAKAHASHI, *Bull. Earthq. Res. Inst.*, **29** (1951), 359.

62) K. SASSA, *Mem. Coll. Sci. Kyoto Univ.*, [A], **18** (1935), 255, **19** (1936), 11, 171.

63) T. MINAKAMI and S. SAKUMA, *Bull. Volcan.*, [ii], **14** (1953), 79.

4) Hawaiian volcanoes[64)–71)]

In Hawaii I. there are the volcanoes, Kilauea and Mauna Loa that extrude basaltic lavas, and the Hawaiian Volcano Observatory has been striving to disclose the relation between earthquakes originating from the volcanoes and volcanic eruptions. Earthquakes that take place on the island, as seen in Fig. 2, are extensively distributed from near the earth's surface to depths of 70–80 km. When volcanic activity begins, the eruption is prolonged with resulting continuous vibrations. Viewed from the hypocentral distribution shown in Fig. 2, volcanic earthquakes including volcanic tremor (exclusive of B-type volcanic earthquakes), originate from every depth in the island. It has been reported that sometimes earthquakes occur in depths of 50–70 km a month or two before the eruptions of the above two volcanoes. This is a remarkable characteristic of the Hawaiian earthquakes that originate frequently from great depths under active volcanoes.

9. The earthquake swarm in the Hakone volcano[72)]

Earthquakes originating from volcanoes, not only A-type and B-type volcanic earthquakes but also explosion earthquakes, occur in swarms as already mentioned. These earthquakes originate from parts shallower than 10 km, and the greater number of the hypocentres of these earthquakes are distributed within 5 km of the earth's surface.

Sometimes such a swarm of earthquakes frequently takes place not only in volcanoes in eruption but also in dormant volcanoes and in volcanoes from which expectation of future lava eruptions is inconceivable. Earthquake swarms that occur at the rate of once or so in several years inside the somma of Hakone volcano belong to this category. In the recent earthquake swarm that extended over the period from September 1959 to April 1960 strongly felt earthquakes were involved. The earthquake activity was prolonged and was accompanied by rather remarkable subterranean rumblings. Consequently some inhabitants

64) *Univ. Hawaii, Volcano Letter.* **489** (1945)—**530** (1955).
65) R. H. FINCH and G. A. MACDONALD, *Rep. Hawaiian Vol. Obs.* (1951)–(1953)
66) G. A. MACDONALD and J. P. EATON, *Rep. Hawaiian Vol. Obs.* (1955)–(1957)
67) G. A. MACDONALD and I. B. ORR, *Rep. Hawaiian Vol. Obs.* (1949).
68) G. A. MACDONALD and C. K. WENTWORTH, *Rep. Hawaiian Vol. Obs.* (1954).
69) G. A. MACDONALD and J. P. EATON, *Hawaiian Vol. Obs.* Summary 1–2 (1956)
70) J. P. EATON and G. D. FRASER, *Hawaiian Vol. Obs.* Summary 3–7 (1956–1957).
71) A. E. JONES, *Jour, Washing. Acad. Sci.* **24** (1934), 413, **25** (1935), 429.
72) T. MINAKAMI, *Rep. on the 1957–1960 earthquake-swarm of Mt. Hakone,* (1960) 1.

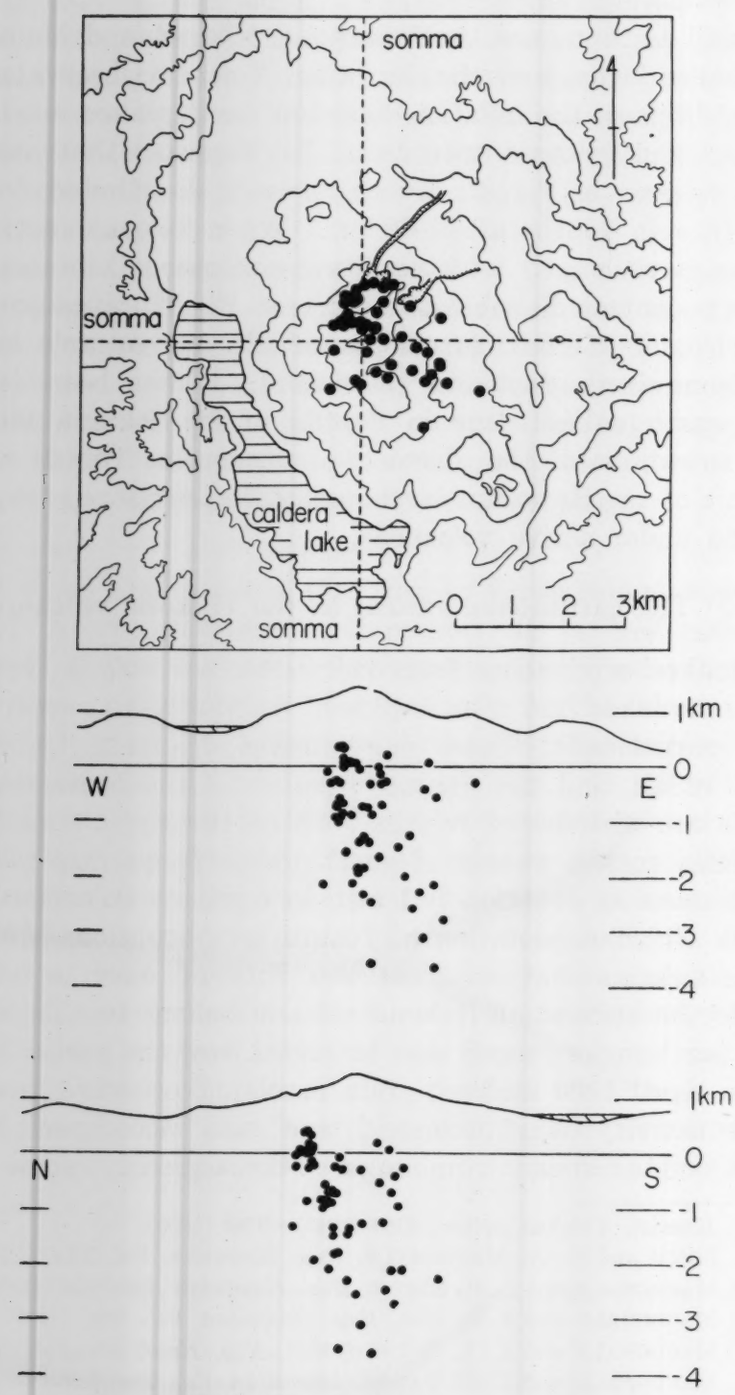

Fig. 20. Hypocentral distribution of the 1960 Hakone earthquake swarm.

felt uneasy about the possibility of impending eruption. Taking the historical activity of the Hakone volcano into account, however, the eruption of lava is almost inconceivable, but eruptive activity having a character of phreatic explosion, i. e., activity that destroys a mountain body as a result of an increase of steam pressure in the interior of the mountain as was seen in the explosion of Bandai-san of 1888 is not always improbable. Thereupon, in order to confirm whether or not the earthquake swarm will develop into such a disaster, the writer attempted to determine the hypocentres, and in particular the depths of hypocentres, as accurately as possible, and the possibility of the hypocentre migrating from the deep to a shallow part.

As a result of the seismometrical observations, as represented in Fig. 20, it was disclosed that all the epicentres of the earthquakes are distributed in a narrow area 1.5 km in radius having the summit of Kami-yama as the centre, and, as far as the focal depths are concerned the shallowest are 0.8 km. in depth, the deepest 5 km. and mostly 1–2 km. In view of the character of the earthquake-motions, these are A-type volcanic earthquakes manifesting distincty the P-phase and the S-phase, and no B-type volcanic earthquake has been recorded at all.

As mentioned above, eruption begins after the occurrence of A-type volcanic earthquakes, B-type volcanic earthquakes, or volcanic tremors corresponding to B-type volcanic earthquakes; or sometimes eruptive activities commence without the occurrence of A-type volcanic earthquakes but after the occurrence of B-type volcanic earthquakes or volcanic tremors. In the earthquake swarm in the Hakone volcano, A-type volcanic earthquakes alone occurred and no B-type volcanic earthquakes or volcanic tremors took place. This probably indicates that seismic activity did not migrate to a depths within 1 km from the earth's surface.

10. The relation between B-type volcanic earthquakes and volcanic eruptions

Physical volcanology aims at disclosing volcanic phenomena by representing quantitatively the physical quantities of volcanic phenomena and by studying the mutual relations among the physical quantities. Hence, it is required to represent numerically the magnitude and intensity of eruptive phenomena.

Volcanic eruptions or eruptive phenomena are the phenomena of

extruding solids including viscous fluids to the earth's surface. Therefore, the most available method is to represent the magnitude of the eruptions with the total mass of the extruded solids. One method is to represent the calories of the extruded materials with the total calories of volcanic ejecta mainly consisting of solids and vapour emitted to the ground-surface. The measurement, however, of the emitted gas, such as the vapour, being extremely difficult, reliable results have not been obtained from any volcano. Another method is to represent the magnitude of explosive eruptions of the Vulcanian type with the kinetic energy ($E=\frac{1}{2}MV^2$) of the eruption determined by the initial velocity (V) of ejecta at the time of eruption and the amount (M) of lava blocks, volcanic bombs, volcanic ash, etc., which was ejected by an individual eruption. On the other hand, as there is simple relationship between the maximum amplitudes of the explosion earthquake that accompanied the eruption and the kinetic energy, if the relationship between both is determined, the energy of the eruption can be ascertained from the results of seismometrical observation.

The largest explosive eruption of Asama-yama in the last 25 years was the explosion of June 7, 1938. On that occasion the extruded amount was 3.8×10^8 kg, the initial velocity 212.5 m/sec. and the kinetic energy 1.7×10^{20} ergs respectively. Moreover, in volcanic eruptions from 5×10^{17} ergs to 5×10^{19} ergs in kinetic energy, as reported before, there exists the following relationship between the maximum amplitude of the horizontal motion ($A=\sqrt{A_{E-W}^2+A_{N-S}^2}$) of explosion earthquake and the eruptive energy (E).

$$E=[0.03+4.5A+0.75A^2\pm0.08]\times10^{19}\text{ ergs},$$

or $$E=[0.06+5.9A_{E-W}\pm0.11]\times10^{19}\text{ ergs},$$

or $$E=[-0.01+7.5A_{N-S}\pm0.19]\times10^{19}\text{ ergs},$$

(where the unit of A is mm)

Representing eruptive activity by energy and earthquakes originating from volcanoes by their respective frequencies, the relationship between the above two phenomena in Mt. Asama was investigated. As mentioned above, the greater part of earthquakes originating from Asama-yama are classed into B-type volcanic earthquakes. Based on the results of observations over the period 1934–1951, the energy of the eruptions is represented with the monthly sum and the frequency of the earthquakes with the ten-days sum in Fig. 21. The frequency of earthquakes in this figure was recorded with a seismograph of low

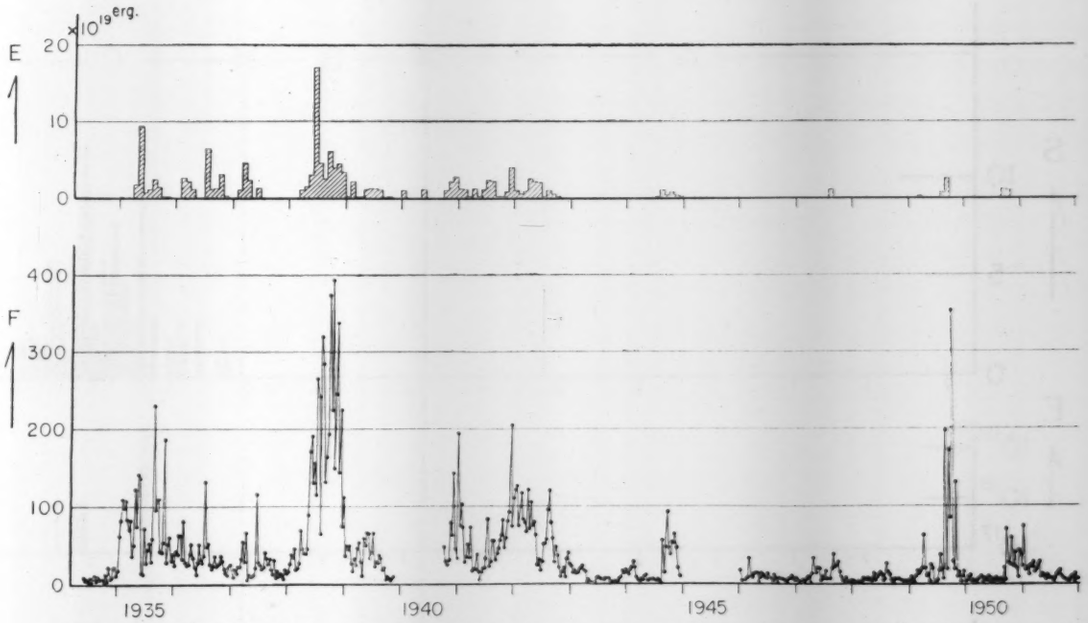

Fig. 21. Relation between the explosive eruption of Mt. Asama and the frequency of the B-type earthquake originating from the volcano.

E: Monthly kinetic energy of eruption.

F: Ten days frequency of earthquakes which were observed by seismograph of low magnification at Asama Volcano Observatory.

magnification (350 times) at a position 4.2 km distant from the crater. That is, these earthquakes are B-type volcanic earthquakes that originated from a shallow part very near the crater. As the earthquakes were recorded at a position about 4 km distant from area where they occurred, however, only some of the B-type earthquakes were recorded. The subsequent observations with seismographs of high magnification installed near the epicentres will be described later. It is noted that the energy of eruption and the frequency of B-type volcanic earthquakes represented in Fig. 21, vary somewhat in parallel. In other words, when eruptive activity is remarkable, B-type volcanic earthquakes occur frequently. On careful examination it is found, however, that in many cases the frequency of earthquakes increases a month or two before a swarm occurrence of eruptions. This fact has been confirmed also by statistical investigations.

The above-mentioned relation that has been clearly defined from the results of observations with a seismograph of high magnification tele-recording apparatus connected with transducers installed in many places on the volcano in recent years. The number of earthquakes recorded with seismographs of 4,000 times at positions 0.9 km., 2.5 km.,

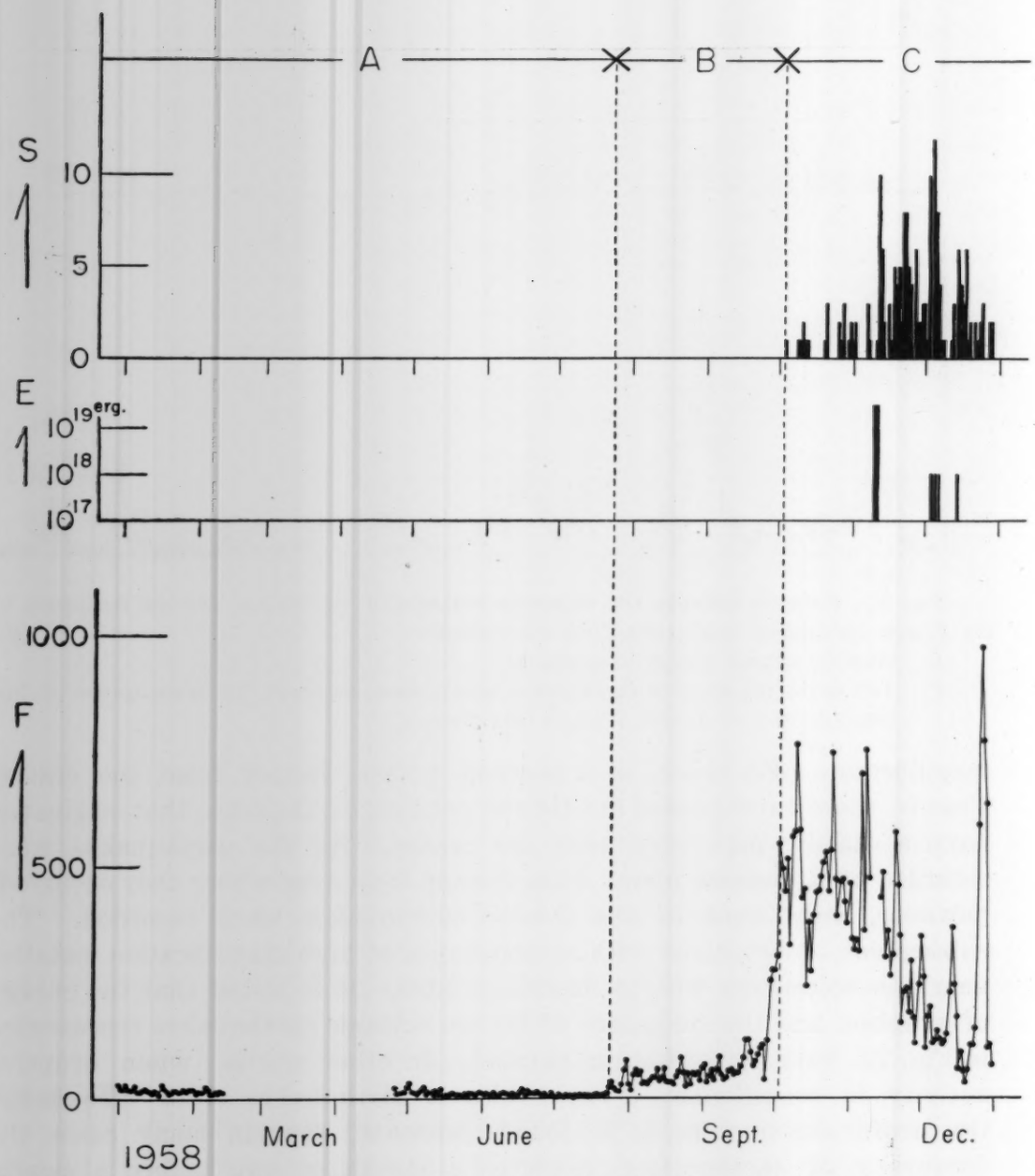

Fig. 22. Relation between eruptions and shallow earthquakes (B-type) of Asama.
A: Calm stage of the volcano, *B*: Pre-volcanic or pre-eruptive stage,
C: Stage of explosive eruption, *S*: Daily frequency of eruption,
E: Kinetic energy of strong eruption, *F*: Daily frequency of shallow earthquake.

and 4.0 km distant from the crater of the Asama volcano is on a daily average, 20, 16, and 6 respectively during calm periods. An increase of several times over is indicated from about two months before the

commencement of eruptive activity, and as much as twenty times several days before an eruption. In Fig. 22 the daily frequency of B-type volcanic earthquakes associated with the remarkable eruptions from October to December, 1958, is represented. This is an example in which premonitory phenomena preparatory to eruption were clearly represented in the remarkable increase in the frequency of B-type volcanic earthquakes.

11. Vulnerability rates on the occurrence of eruptions viewed from the frequency of B-type volcanic earthquakes

As mentioned above, it has been known that the occurrence of B-type volcanic earthquakes increases, preceding volcanic outbursts. Therefore, it becomes possible to forecast outbursts of volcanoes by calculating the frequency of B-type volcanic earthquakes, i. e., by the following method, which is the most simple method conceivable to us.

The method is to infer, on the basis of a five day calculation (N) of the daily frequency (n) of B-type volcanic earthquakes, the probability, or in other words, the vulnerability rates of eruption for the next five days.

$$n_1+n_2+n_3+n_4+n_5=N_5$$
$$n_2+n_3+n_4+n_5+n_6=N_6$$
$$n_3+n_4+n_5+n_6+n_7=N_7$$
$$\cdots\cdots\cdots\cdots$$

First, taking all values of N under observation the values are divided into the following groups: 0–100, 101–200, 201–300, ……, and the frequency distribution (F) of each group is examined. Next, taking N from the day before the eruption to five days before (this is called by N'), the distribution of frequency (F') is examined. If both distributions are clarified, the distribution of F'/F for N gives grounds to infer the vulnerability rates of eruption. Table 3 which represents the vulnerability rates based on the eruptions of 1954–55 and 1958 indicates that there is no remarkable difference in the general tendency of both rates. It is considered that this method can be applied effectively to future outbursts of the Asama volcano.

In the above description restricting the problem to the frequency of B-type volcanic earthquakes, shallow earthquakes originating from the vicinity of the crater were treated uniformly under the name of

Table 3. Vulnerability rates for an explosive eruption of Asama based on the frequency of the B-type earthquakes.
F_0, F_0'; observed value, F_c, F_c'; calculated value from Polyà-Eggenberger's function.

N	F_0'/F_0	F_c'/F_c
0— 50	0	0.013
50—100	0.018	0.044
100—150	0.139	0.092
150—200	0.216	0.154
200—250	0.264	0.226
250—300	0.243	0.305
300—350	0.489	0.388
350—400	0.542	0.468
400—450	0.389	0.549
450—500	0.722	0.622
500—550	0.800	0.691
550—600	0.500	0.752
600—650	0.900	0.811
650—700	0.500	0.843
700—750	1.000	0.874

B-type volcanic earthquakes. However, judging from the nature of the earthquake-motions, B-type volcanic earthquakes are not always of the same character. Some of them originate nearer the crater bottom as compared with others and the surface waves more clearly predominate. Some of them are of the shock type. It seems that there are also some difference in the depth of the hypocentres. From the above fact, it is understood that the relationship between B-type volcanic earthquakes and outbursts is not the same for every B-type volcanic earthquake. The relationship seems to be direct in some B-type earthquakes and indirect in other B-type earthquakes. As an example, in B-type volcanic earthquakes observed simultaneously with seismographs of the same type and the same magnification, the writer examined the difference in the amplitude of the earthquakes at different epicentral distance.

Comparing the maximum amplitude of each B-type volcanic earthquake observed at the two points (Fig. 23), the maximum amplitude of earthquakes observed at the point near the crater was always found to be the greater. This fact indicates that the epicentres of B-type volcanic earthquakes are centered at the crater. In this respect B-type earthquakes are always the same. On comparing the maximum amplitude of each B-type earthquake, however, it has been revealed that the ratio

of the maximum amplitudes at different epicentral distance differs with the periods of volcanic activity. Moreover, it seems that the amplitude ratio differs according to the conditions of volcanic activity at different times, i. e., in the early stage of eruptive activity, the later stage, and the calm period. In Fig. 23, of numerous earthquakes observed on the day before a great eruption, the maximum amplitude of earthquakes observed at the two points was plotted in the ordinates and abscissa according to the respective points, and the maximum amplitude of earthquakes that occurred after the eruption was also plotted in the graph with other symbol. Thereby it is evident that the ratio of the maximum amplitude observed in the periods is different, i.e., immediately before a great eruption, earthquake-motion are attenuated remarkably and the mean ratio of the amplitudes is 1:0.1, while the mean amplitude ratio after the eruption is 1:0.5. In short, such a remarkable difference in the attenuation of earthquake-motions is considered to be a result of the fact that immediately before an eruption the hypocentres of B-type volcanic earthquakes are extremely shallow, the vibrations are of the shock type, and are of short period while the hypocentres of earthquakes that took place after the eruption are rather deep and the periods of vibrations are lengthy. As described above, there are B-type volcanic earthquakes different in character and focal depth, and, on the other hand, there are also different volcanic phenomena with relation to the difference in B-type volcanic earthquakes. Therefore, by classifying B-type volcanic earthquakes into types according to their characteristics and by studying the relation between each type and eruption, it is expected

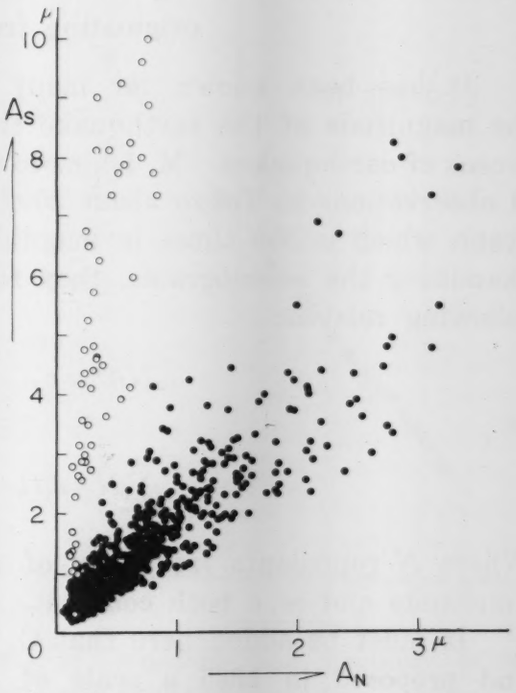

Fig. 23. Comparison of the maximum amplitude of the B-type earthquake-motions at the stations, Sannotorii and Nakanosawa, before and after the strong explosive eruption.
opened circle: earthquakes before the strong explosion on Nov. 10, 1958.
closed circle: earthquake after the strong explosions from Nov. to Dec., 1958.

that the relationship between the above two phenomena will be revealed more distinctly.

12. On the magnitude and frequency of earthquakes originating from volcanoes

It has been known for many years that, in general, the smaller the magnitude of the earthquake the more frequent become the occurrences of earthquakes. M. Ishimoto and K. Iida[73] conducted seismological observations in Tokyo about 20 years ago, making use of a seismograph which is 350 times in magnification and 1 sec. in period, and, on examining the seismograms, they found in 1939 that there exists the following relation:

$$NA^m = c,$$

or

$$\sum_{A=\infty}^{A} N = c[(1-m)A^{1-m}]_{\infty}^{A}.$$

Where N represents frequency of earthquake, A the maximum trace amplitude and m, c both constant. The value of m at this time was 1.8.

It must be added here that C. Richter[74] studied the same problem and proposed in 1935 a scale of magnitude of earthquakes based on their maximum amplitude.

Subsequently, this problem was studied by numerous investigators[75)-83)], and, as a result, it has been confirmed that Ishimoto-Iida's formula has been established almost irrespective of the place of observation, the magnification of the seismographs, etc., and the value of m is 1.8 to 2.2 in general earthquakes and after-shocks. From the fact that the relation between the magnitude and frequency of earthquakes in various places is always the same, it is concluded that the magnitude and fre-

73) M. ISHIMOTO and K. IIDA, *Bull. Earthq. Res. Inst.*, **17** (1939), 443.
74) C. F. RICHTER, *Bull Seism. Soc. Amer.*, **25** (1935), 1.
75) K. IIDA, *Bull. Earthq. Res. Inst.*, **18** (1940), 575.
76) T. MATSUZAWA, *Bull. Earthq. Res. Inst.*, **19** (1941), 411.
77) H. KAWASUMI, *Bull. Earthq. Res. Inst.*, **30** (1952), 319.
78) C. TSUBOI, *Jour. Phy. Earth.*, **1** (1952), 47.
79) Z. SUZUKI and T. ASADA, *Geophys.* Notes 1, 2, (1947, 1949).
80) T. ASADA, Z. SUZUKI and Y. TOMODA, *Bull. Earthq. Res. Inst.*, **29** (1951), 289.
81) Z. SUZUKI, *Sci. Rep. Tohoku Univ.*, [V], Geophys., **5** (1953), 177.
82) S. SAKUMA, *Geophys. Bull Hokkaido Univ.*, **6** (1958), 1.
83) Y. TOMODA, *Zisin*, [ii], **7** (1954), 155. etc.

quency of earthquake at the hypocentres are also in the same relation.

Here, the above relation in respect to earthquakes originating from volcanoes will be outlined. To make clear the problem it is necessary to investigate each kind of earthquake, i. e., the A-type, the B-type, and the explosion earthquakes.

A-type volcanic earthquakes originating from Hawaii Is. and Aso-san have been investigated, and the results obtained in each case indicate that the A-type volcanic earthquakes are not different from general earthquakes. The hypocentres of these A-type volcanic earthquakes in Hawaii Is. are 2 km, to several tens of kilometers in depth, those in Aso-san are 1–8 km, in depth, and the value of m is 1.8–1.9 in both cases. However, observation data on A-type volcanic earthquakes is not always sufficient. Therefore, it seems necessary to investigate this problem again in the future together with an accurate determination of the hypocentres.

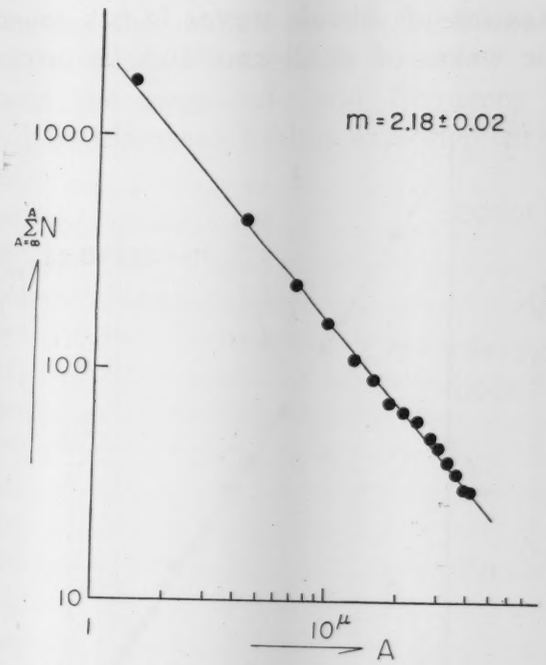

Fig. 24. Magnitude and frequency of the Hukui after-shocks.

As to B-type volcanic earthquakes, the results of investigation based on a great deal of observation data in Asama-yama indicate large values of m, 2.8–4.5, which are vastly different from the values in general earthquakes. As regards B-type volcanic earthquakes associated with the activities of Minami-dake in Sakura-zima and Usu-san, the value of m is 4.0–4.1 in the former and 3.1–3.8 in the latter. These values are almost similar to those in Asama. In B-type volcanic earthquakes in Asama, sometimes there are cases where the value of m obtained from the observations conducted at points 2–3 km. distant from the crater appears as a function of the amplitude, and the relationship pointed out by Ishimoto and Iida is not established apparently. This phenomenon, however, is ascribable to the following reason: The vibration-period of

the maximum amplitude of earthquake-motions, is short, at least statistically, in the case of the lesser amplitude, and, in the case of the amplitude greater than a certain degree, the vibration-period is almost constant. Therefore, the attenuation associated with the propagation of seismic waves is not constant, and the attenuation of seismic waves of small amplitude is prominent. In such a case, if, taking

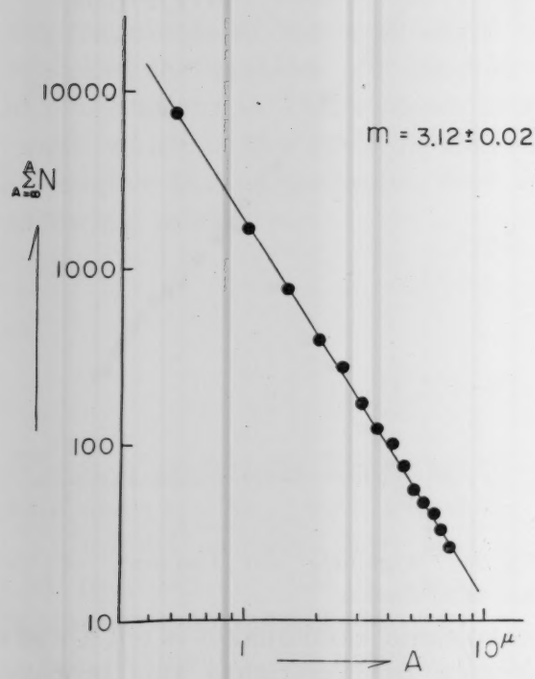

Fig. 25. Magnitude and frequency of B-type volcanic earthquakes originating from Asama.

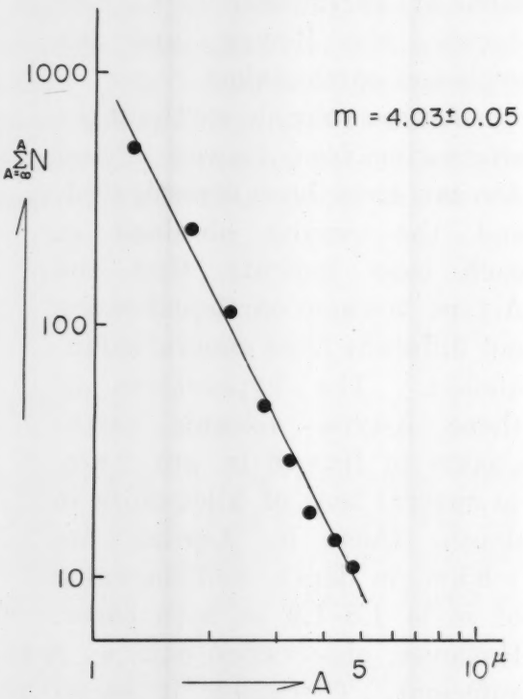

Fig. 26. Magnitude and frequency of the B-type earthquakes originating from Minami-dake, Sakura-zima.

the attenuation into account, the amplitude is reduced to that at the hypocentre (the crater in this case) and the relationship between the magnitude and frequency is reduced to that at the hypocentre, then the value of m becomes constant almost irrespective of the amplitude, and the values 2.8–4.5 are obtained.

In short, the attenuation associated with the propagation of seismic waves is represented by

$$A_{(\Delta)} = A_0 e^{-k\Delta} \Delta^{-n}$$

where $A_{(\Delta)}$ is the amplitude of earthquake-motion observed at distance (Δ) from the epicentre (crater), A_0 is the amplitude at the epicentre, n

1 or 1/2 in accordance with the body waves or surface waves, and k the attenuation coefficient. The value of k in this formula is a function of the amplitude and not constant, therefore, the relationship between the magnitude of amplitude A and the frequency observed at Δ does not represent the relationship between the magnitude of amplitude A and the frequency at the hypocentre unless a correction is made.

Next, the relationship between the magnitude and frequency in cases of explosion earthquakes will be discussed taking explosion earthquakes in Asama and Minami-dake in Sakura-zima as examples. As regards the magnitude and frequency of explosion earthquakes in the above two volcanoes, the relationship has been established to be that pointed out by Ishimoto and Iida and the value of coefficient m is 2.7–3.5 in the former and 3.9–4.0 in the latter, which is extremely large when compared with that of general earthquakes and is of almost the same value as those in B-type volcanic earthquakes.

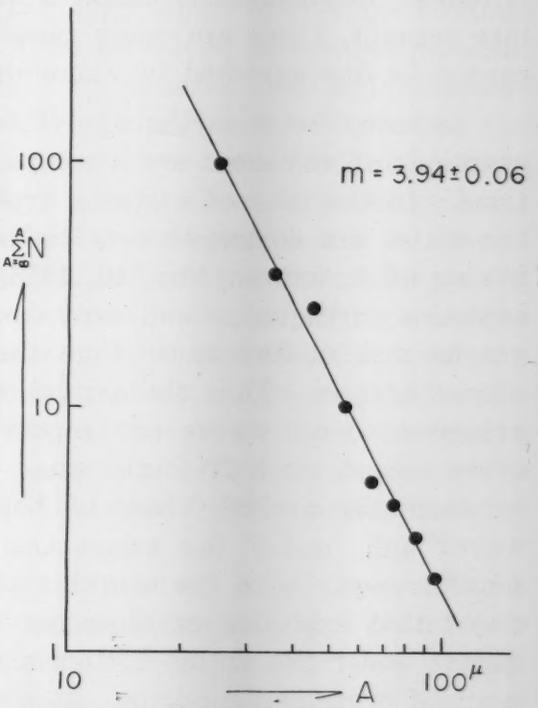

Fig. 27. Magnitude and frequency of the explosion earthquakes originating from Minami-dake, Sakura-zima.

It is noticeable that the relationship between the magnitude and frequency of explosion earthquakes in Mt. Asama and Sakura-zima, i. e., the value of Ishimoto-Iida's coefficient (m), coincides with the value of m in B-type volcanic earthquakes originating from each of the above volcanoes.

On the other hand, the magnitude of explosion earthquakes and B-type volcanic earthquakes was compared. The upper limit of the magnitude of B-type volcanic earthquake in Asama-yama is about 5μ at a distance of 4 km from the crater (or the epicentre), and about 20μ at a distance of 2.5 km from the crater, where few earthquakes of larger magnitude occur. It has also been discovered that the lower limit of the magnitude of explosion earthquakes is about 5μ at the former point and 20μ at the latter point. Thus the upper and lower limits

of the maximum amplitude of earthquake-motions of both kinds almost agree with each other.

As described before, the hypocentres of these two types of earthquakes are distributed over an area of several hundred metres under the bottom of an active crater, that is to say, these two kinds of earthquakes agree also with each other in the positions of the hypocentres. They resemble each other in the nature of the earthquake motions and no remarkable difference can be found except in their amplitudes. Consequently, unless a magnification of seismograph is taken into account, there are many cases where the two kinds of earthquakes cannot be distinguished by examining the seismograms alone.

In many cases earthquake-vibrations associated with the explosive eruptions of volcanoes are accompanied by explosion sounds or detonations. In the case of a strong explosion sometimes window-panes facing the crater are destroyed over the whole foot of the volcano. The explosion of Asama on Nov. 10, 1958, is a remarkable example. At Asama explosion earthquakes and explosion sounds are recorded with seismographs and at the same time the explosion sounds are recorded on a magnetic tape. Thus the arrival times of explosion earthquakes and explosion sound waves are accurately measured by the recording of every second mark from the same clock. Making use of the difference between the arrival times of both earthquake-vibrations and sound waves and, under the assumption that the explosion sound occurred simultaneously with the eruption at the crater bottom, it has been disclosed that explosion earthquakes took place in area several hundred meters under the crater bottom a second or two before the commencement of eruption.

Previously the writer defined explosion earthquake as earthquake accompanying explosive eruption. From the above observation, however, explosion earthquake should be defined as earthquake accompanied by explosive eruptions. That is, from the occurrence times of both phenomena, it is reasonable to conclude that the earthquake is the cause, and the explosive eruption takes place as a result of the earthquake.

The geographic distribution of the initial motions of earthquake offers a key to the force that causes earthquake. The initial motions of explosion earthquakes indicate 'push' in every direction irrespective of which directions is taken from the epicentre and no initial motions of 'pull' appear. This has been disclosed as far as explosion earthquakes

of Asama are concerned. Earthquakes accompanied by explosive eruptions at Minami-dake in Sakura-zima are also considered similar, though the observations carried out there are not sufficient. Whether or not the initial motions of B-type volcanic earthquakes are the same as those of explosion earthquakes is an important clue for clarifying the mechanism not only of B-type earthquake but also of the explosion earthquake and volcanic eruption. This has not yet been confirmed however, owing mainly to the insufficiency of observation. It is also one reason why, as described above, the magnitude of B-type volcanic earthquakes is small. This problem must be solved as soon as possible.

In the previous paragraph, based on observations and measurements of explosion earthquakes and B-type volcanic earthquakes, the characteristic and the relationship between these two kinds of earthquake hitherto revealed, were described. From these facts the problem naturally arises whether or not explosion earthquakes are a special type of B-type volcanic earthquake, i. e., whether or not, though the cause of both earthquakes is the same, when a B-type volcanic earthquake larger than a certain degree takes place, the solidified lava surface of the crater bottom is destroyed causing eruptions. As to the cause of why of B-type volcanic earthquakes occur, it is conceivable that magma rises near the crater bottom and the strain is newly produced by the separation of the gas contained in the magma and its expansion in volume.

Thus the remarkable increase in the frequency of B-type volcanic earthquakes previous to and during eruptions indicates a high probability that when numerous earthquakes occur, as seen in the relationship expressed by Ishimoto and Iida's formula, earthquakes larger than a certain degree are also liable to occur, or in other words, the remarkable increase in the occurrence of B-type volcanic earthquakes indicates a highly probable occurrence of B-type volcanic earthquakes strong enough to cause an explosive eruption. Herein lies the reason why the relationship between the frequency of B-type volcanic earthquakes and the occurrenc of eruptions is represented in the form of the above-mentioned relationship based on probability.

13. General earthquakes and earthquakes originating from volcanoes

It was described that general earthquakes and earthquakes originating from volcanoes differ in the area where the earthquakes take place,

and that this difference is particularly apparent in the depths of the hypocentre.

As to the cause of the earthquake-generating force by which these earthquakes of different hypocentral depths are caused, there is no confirmed elucidation. Some consider that, with regard to general earthquakes originating from depths of several tens of kilometers and earthquakes originating from greater depths, strain is produced by the change in volume brought forth by the partial solution of solid substance crystallized in the interior of the earth's crust, or in other words the change from a solid phase to a liquid phase. Some are of the opinion that magma produced by melting rises to the upper part because of a local increase in the pressure through the separation of the gas in the magma together with the decrease in outside pressure, resulting in the production of strain which causes earthquakes before the magma reaches the ground surface.

In shallow earthquakes originating from dormant or extinct volcanoes like the Hakone volcano in or directly under which the existence of magma is inconceivable, the earthquake-generating force might be the stress in the volcanic bodies resulting from gas of a high temperature separated from the magma, or in other words breaking of an unstable equilibrium accompanying the changes in pressure and temperature of liquid phases and gaseous phases.

The relation between the magnitude and frequency of general earthquakes, i. e., Ishimoto-Iida's coefficient m ranges from 1.8 to 2.2 for general earthquakes and from 2.7 to 4.0 for B-type volcanic earthquakes and explosion earthquakes. This value differs greatly from the former value. Is this difference ascribable to the mechanism of earthquake occurrence or the complex and heterogeneous structure of volcanoes or should it simply be attributed to the difference in the depth of the hypocentre?—this is a vital problem that must be solved.

The effective method by which the difference in the mechanism of earthquake occurrence can be investigated is by clarifying the geographic distribution of the initial motions of earthquake-vibrations. In the cases of general earthquakes, the 'push' and 'pull' of the initial motions are always apparent and the push region and the pull region are sometimes set out in a quadrant formation and sometimes both regions are separated by a conical curve.

However, as far as explosion earthquakes are concerned, 'push' alone appears and 'pull' does not appear in the distribution of initial

motions. This problem has not yet been confirmed for B-type volcanic earthquakes, but, judging from the distribution of the initial motions in the case of explosion earthquakes and general earthquakes, both earthquakes are considered to be different in the mechanism of their occurrence. Hence one may suspect that the difference in the relationship between the magnitude and the frequency of earthquakes is caused by the difference in the mechanism of their occurrence. Therefore, it becomes impossible to conclude that the above difference is attributable to the depths of the hypocentre alone. The only way to solve this problem is by determining accurately the distribution of the initial motions, the Ishimoto-Iida coefficient m, and the depths of the hypocentre of A-type volcanic earthquakes originating from volcanoes and having intermediate characteristics between general earthquakes and B-type volcanic earthquakes including explosion earthquakes.

Fortunately, from observations of the earthquake swarms carried out on the Hakone volcano from September 1959 to April 1960, useful data concerning the problem was obtained. Needless to say, the earthquakes that originated in swarms from the Hakone volcano belong to A-type volcanic earthquakes and the hypocentre was determined within a probable error of 200 m–300 m. On the other hand, the value of Ishimoto-Iida's coefficient m as the acceleration amplitude and the displacement amplitude observed with an acceleration seismograph and a displacement seismograph respectively is as follows:

Acceleration amplitude	$m_A = 2.64 \pm 0.02$
Displacement amplitude	$m_D = 2.60 \pm 0.02$

That is, both amplitudes show the value 2.6. The value is larger than that of general earthquakes and somewhat smaller than that of B-type and explosion earthquakes which is 2.7–4.0.

As described above, the depths of the swarm earthquakes in Hakone were situated between 0.8 km and 5.0 km under the ground surface, and most of them were between 1.0 km and 2.0 km in depth. Consequently the depths of the hypocentres also are shallower than those of general earthquakes and deeper than those of B-type and explosive earthquakes.

Next, the distribution of the initial motions will be mentioned. As a result of an investigation of about 100 earthquakes belonging to the earthquake swarm in Hakone, it was confirmed that in most earthquakes both 'push' and 'pull' appeared and were formed in quadrants. That is, in spite of being different from explosion earthquakes in the mechanism of occurrence as viewed from the distribution of the initial motions, the

coefficient m shows a value close to that of explosion earthquakes and B-type volcanic earthquakes and, the value is larger than m of general earthquakes which have the same distribution of initial motion. In short, it may be concluded that the difference in the value of the coefficient m is not a result of the difference in the mechanism concerning the production of seismic waves but of the difference in the depth of the hypocentre alone. Needless to say, for a solution to this problem, further study is necessary, on A-type volcanic earthquakes of other volcanoes.

The shallower the hypocentre, the larger is the value of coefficient m. This means that, in the case of a shallow hypocentre, major earthquakes are not apt to occur, minor earthquakes taking the place of major ones. Based on this fact one can consider an example with an upper limit on the magnitude of earthquakes originating from a certain depth (h). Earthquakes exceeding the limit cannot take place. That is, in the shallow section, the volume of the hypocentral domain is more controlled than in the deep part, and the uppermost limit for the accumulation of the strain that causes earthquake-vibrations is low. Accordingly, the upper limit (A) of earthquakes that originate from a certain depth (h) is, for example, represented by

$$A = ch^x ,$$

where x is, for example, 2–3 and c is a constant related to the destructive strength and the elasticity of materials constituting the earth's crust. Therefore, c also has a relationship with the depths of the hypocentre.

Therefore, the above formula will be written as follows:

$$A = c'h^y h^x = c'h^{x+y}$$

where c' is a constant relating to material only and y is generally positive.

Thus, major earthquakes are not apt to occur in the area near the earth's surface, and on the other hand, when a strain is produced in the earth's crust with the rise of magma or gas of a high temperature near the earth's surface, numerous minor earthquakes take place accompanied by numerous small destructions through which the strain is released.

Besides the reasons mentioned above, it must be added that the large value of the coefficient (m) for the extremely shallow earthquakes from volcanoes depends on the complex and heterogeneous structure of volcanoes and on the manner of the concentration of stress in volcanoes, which is given by the heat from the magma.

14. Conclusion

In this paper, the various characteristics of earthquakes originating from volcanoes and crustal deformations associated with eruptive phenomena were discussed in comparison with general (or tectonic) earthquakes and crustal deformations associated with general earthquakes.

First, general earthquakes and volcanic eathquakes are compared with respect to their hypocentral depths, and volcanic earthquakes are classified in four types according to the position of the hypocentre and the relationships with the volcanic eruption.

With respect to crustal deformations, remarkable differences between those relating to the phenomena are shown as represented in several examples.

It is the writer's main purpose to elucidate how earthquakes and crustal deformations from volcanoes are connected with the rising movements of the magma from the earth's interior to the earth's surface and what are their special features compared with those not originating from volcanoes.

Besides the differencees in depth of the hypocentral position, there is a remarkable difference in the relationship between the magnitude and the frequency of the volcanic and the general earthquakes.

After investigating the relationship between the magnitude and the frequency of various kinds of volcanic earthquakes, the writer arrived at the conclusion that the explosion earthquake is a special type of the B-type earthquake. In other words, B-type earthquakes exceeding a certain degree in magnitude are followed by an explosive eruption.

In general, explosive eruptions in andesite and dacite volcanoes are preceded by a marked increase in B-type earthquakes. It is reasonable to say that the relationship between explosive eruptions and the frequency of B-type earthquakes, or the relation between explosive eruptions and the frequency of B-type earthquakes, or the relationship available for predicting volcanic eruptions of the Vulcanian type, based on the frequency of B-type earthquakes, is provided by a relationship of probability as infered from the Ishimoto-Iida formula. The reason is that the more frequently B-type earthquakes occur, the stronger is the probability that B-type earthquakes of big magnitude will occur.

31. 噴火予知に関する基礎的研究 (I)
火山活動に関連する地震と地殻変動

地震研究所 水 上 武

地下数十粁以上の深さに岩漿が生成し，上昇して，やがて地表に噴出する現象が火山の噴火であるが，岩漿の生成，上昇に伴つてどのような現象が現われるであろうか．

1) ここでは噴火現象に関係して現われる地震及び地殻変動を一般の地震並にそれに伴つた地殻変動と比較して，それぞれの著しい特徴を述べた．

特に岩漿の上昇に伴つて火山の地震及び地殻変動がいかなる性質を示すかに注目した．

2) 火山に発生する地震をその震源の位置及び噴火現象との関連によつて四種類に分類した．同時に 2, 3 の火山について，震源位置の分布の実例を示した．

3) 安山岩質火山（浅間山）に発生する B 型火山地震とヴォルカノ式噴火の発生との関係を調べ，B 型火山地震の頻度から噴火発生の危険率を推定することの可能なることを述べた．

4) 各種の火山地震について，その大きさと頻度との関係についての概略を記述した．

5) B 型火山地震と爆発地震について，次の諸点から爆発地震は B 型火山地震の特別な場合であることを結論した．

a) 震源の位置がほぼ一致すること．

b) 石本・飯田の係数 m の値が共に 3～4 を示すこと．

c) B 型火山地震の上限と爆発地震の下限とがほぼ一致すること．

d) 地震動の性質が類似すること．

以上の理由で，ある程度以上大きい B 型火山地震の発生によつて爆発的噴火が発生することが推定される．

6) 以上の事から，B 型火山地震の発生頻度が増大すれば．大きい B 型火山地震の発生する確率が増加し，従つて火山の爆発を伴う確率も増大する．

7) 最近の箱根火山の群発地震，つまり A 型火山地震についてその震源位置を精しく調査した結果，その深さの大部分は神山中央火口丘の下 1～2 *km* の間であること，石本・飯田の係数 m の値が 2.6 を示し，一般の地震と B 型ないし爆発地震との中間の値を示すことが判つた．

8) 石本・飯田の係数 m の値が一般の地震，A 型火山地震，B 型火山地震及び爆発地震について，それぞれ 1.8～2.2, 2.6, 3.0～4.0 の値を示す結果となつた．この事に関して，次のような事が考えられる．震源の深さによつて震源の大きさは制限を受けるが，震源が極端に浅い場合には，特にその影響が著しい．そのために地震の大きさの上限について制約される．また，地震の大きさと頻度は，そこを構成する物質の破壊強度，弾性，不均一性，地質構造等に関係すばかりでなく，火山地震の場合の如く，地表近くの狭い範囲に急激に，しかも過剰に与えられる stress の集中の仕方に関係するものと考えられる．

[本研究の一部は文部省科学研究費によつて行つた.]

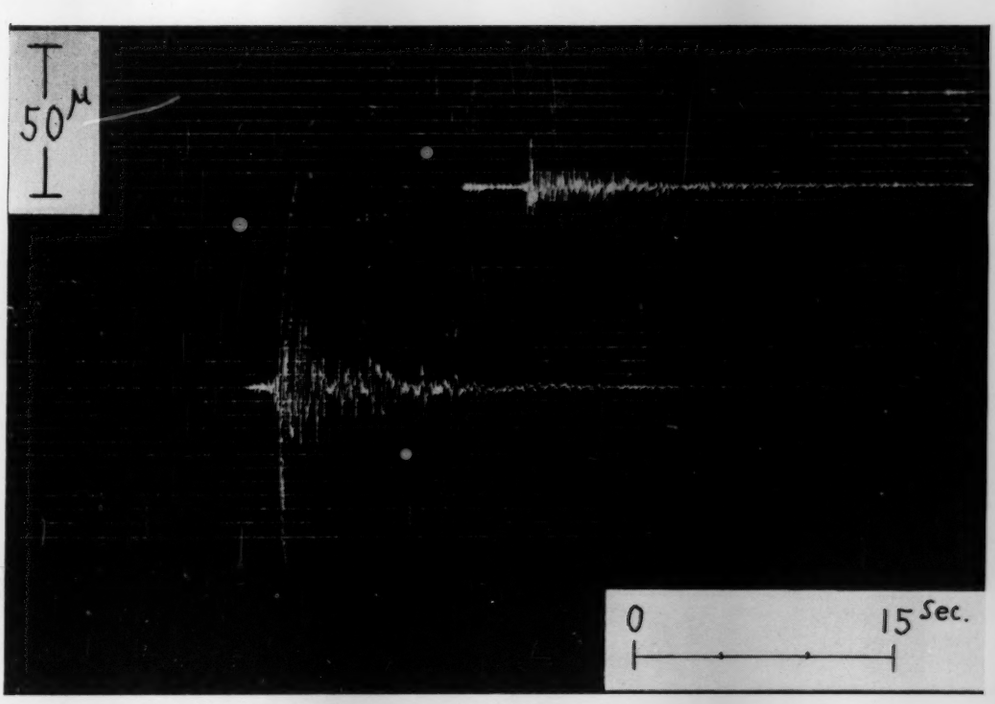

(a)

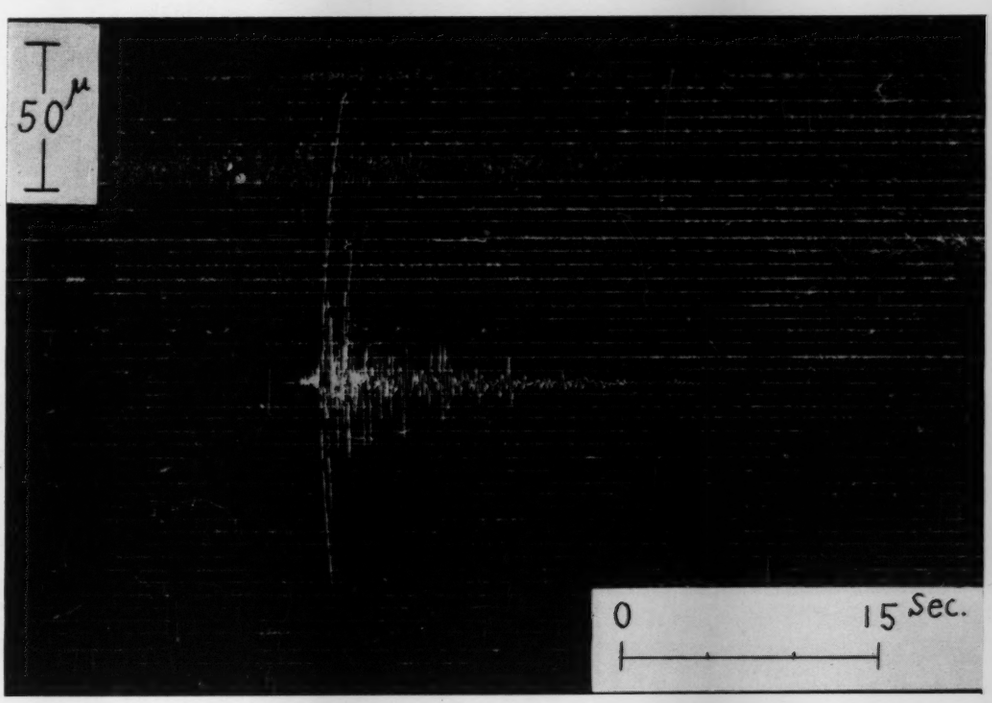

(b)

Fig. 28. The seismogram of the Hukui after-shock (a), and the seismogram of the A-type volcanic earthquake from Usu (b).

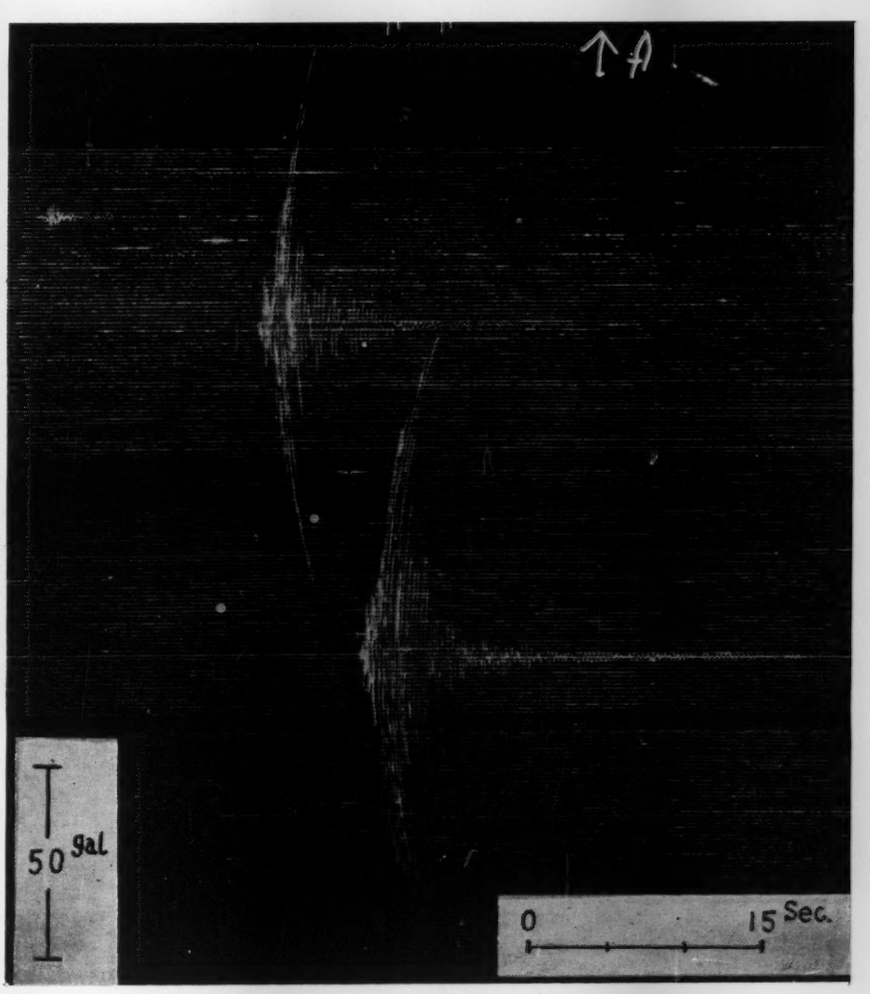

(a)

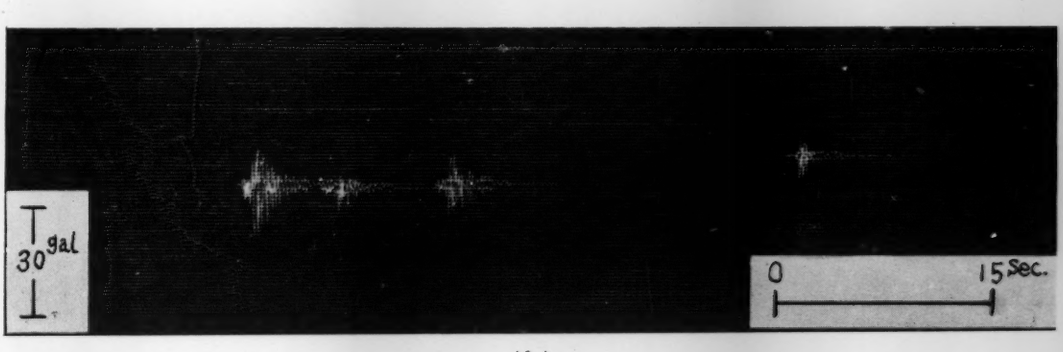

(b)

Fig. 29. The seismograms of the 1960 Hakone earthquake swarm.

(震研彙報 第三十八号 図版 水上)

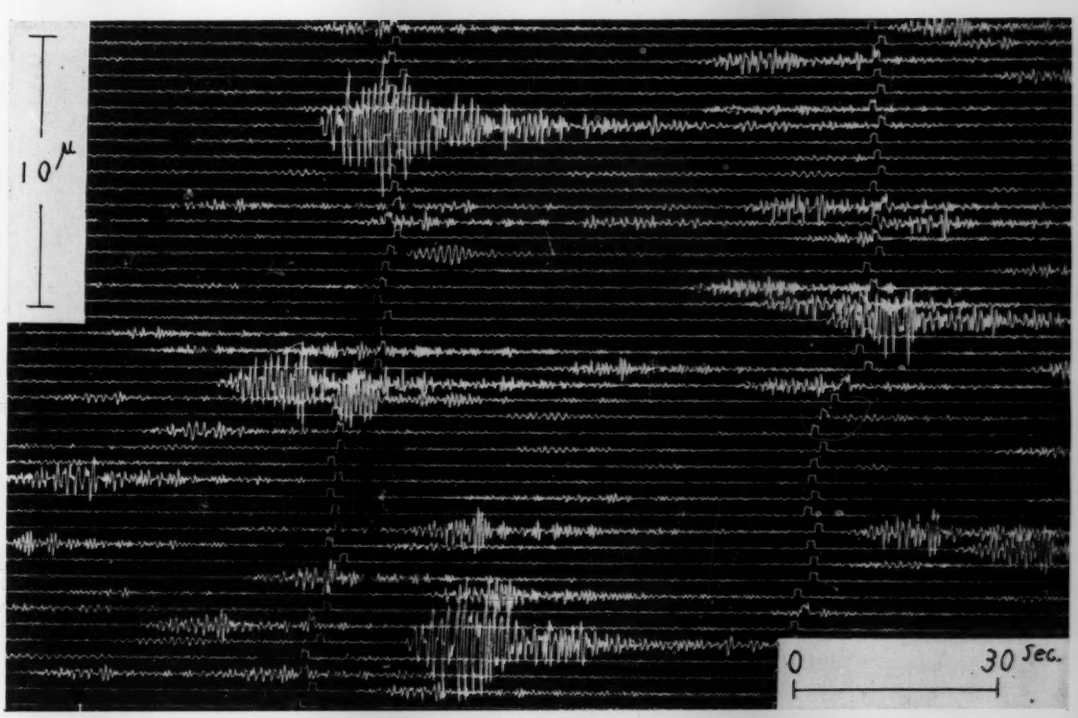

(a)

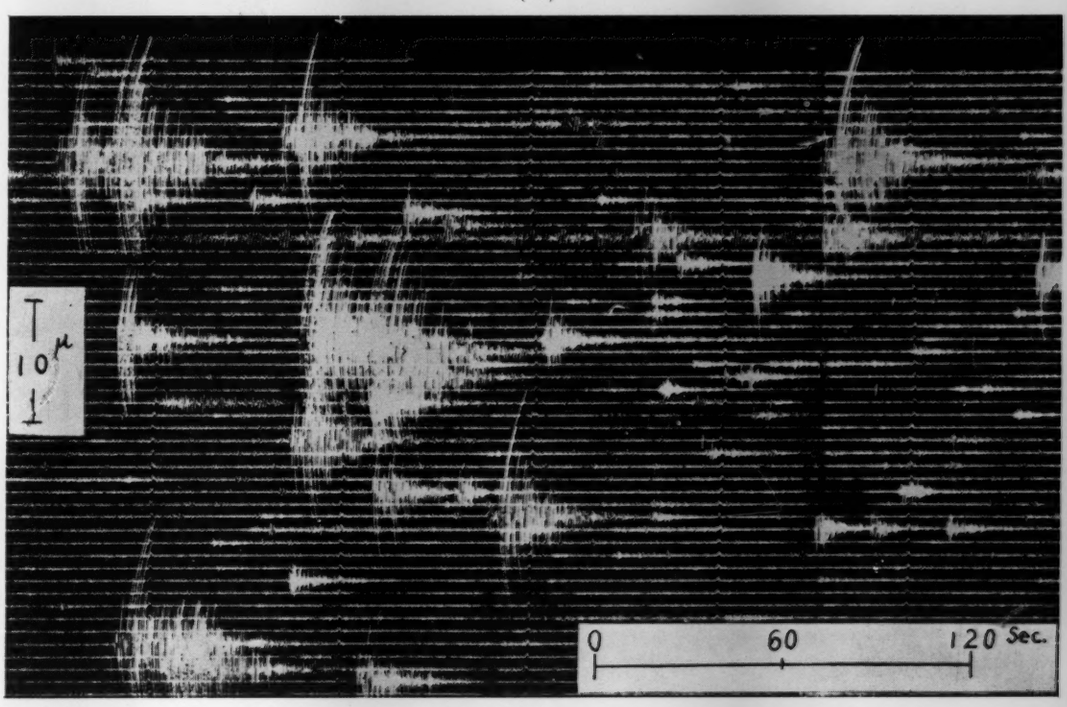

(b)

Fig. 30. The seismogram of the B-type earthquakes which appeared about one month before the 1958 activity of Asama (a).

The seismogram of the B-type earthquakes which appeared about 20 hours before the strong explosive eruption of Asama on Nov. 10, 1958 (b).

(震研彙報 第三十八号 図版 水上)

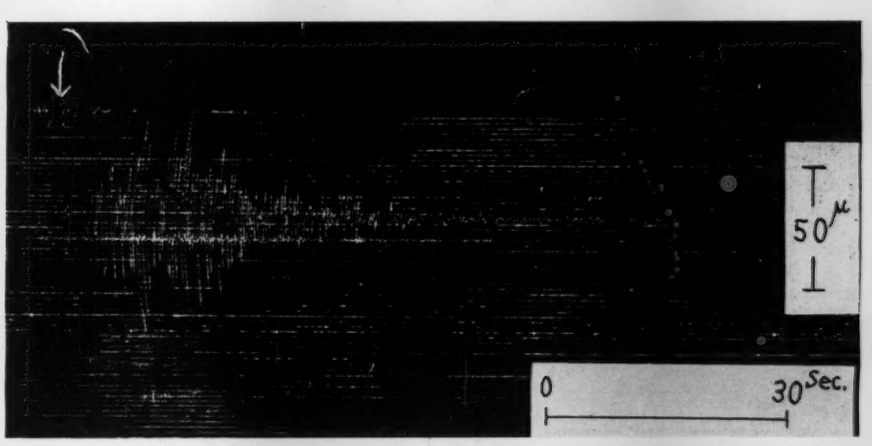

(a)

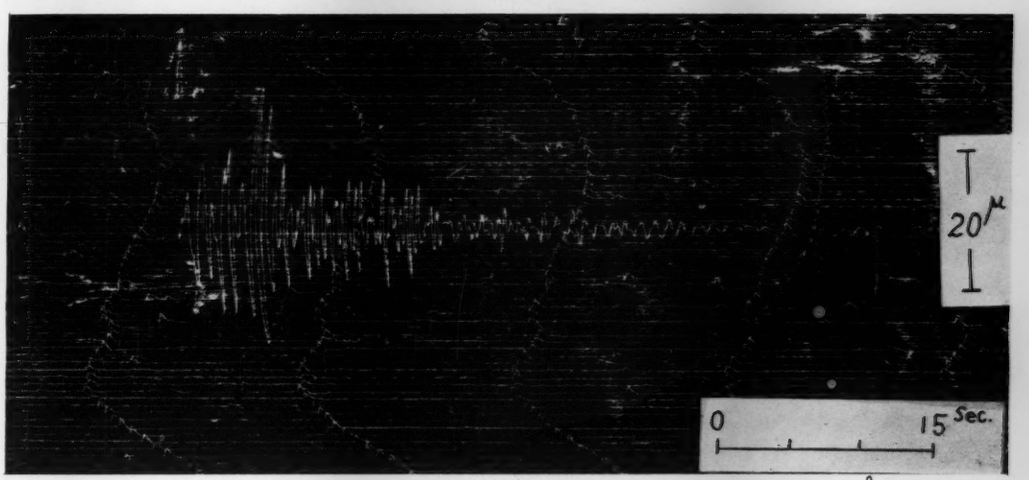

(b)

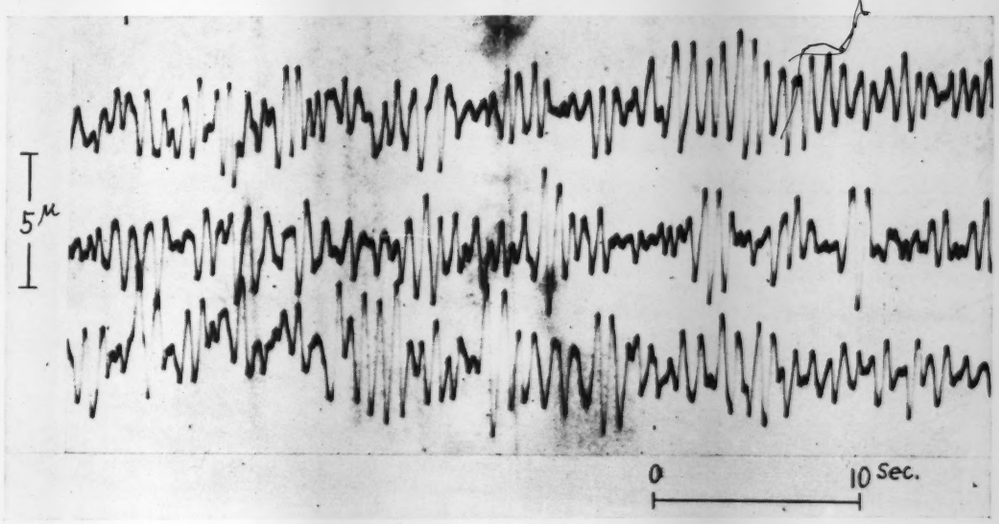

(c)

Fig. 31. The seismogram of the Asama explosion earthquake (a).
The seismogram of the Minami-dake (Sakura-zima) explosion earthquake (b).
The seismogram of the volcanic tremor of Oo-sima (c).

地震研究所彙報
第38号(1960)545-557頁

32. 電磁式地震計の磁気回路について

地震研究所　嶋　悦三

(昭和 35 年 6 月 28 日発表——昭和 35 年 9 月 30 日受理)

1. Introduction.

前報告[1]において著者は電磁式地震計の電圧感度を簡単に調べる方法を述べた．この報告のなかでわれわれは，地震計の四定数として，質量，ダンピングの係数，もどす力および電圧感度があり，もしこのなかの一つがわかつていれば，他の三つは電気的測定で決定できるということを述べた．このなかの電圧感度，つまり force factor A[2] は，力学系から電気系への変換に必要な量であり，この大きさは coil の導線部分の有効長を l，磁束密度を B とすれば，$A \equiv Bl$ で与えられる．従つて電圧感度を大にするためには，B または l を大きくすればよいことがわかるが，あるきまつた大きさの磁石が与えられた場合には，A を大きくするために，その磁束をもつとも有効に使い B を大きくするようにしなければならない．

このように電磁式地震計を設計するさいには，その磁気回路の設計が重要部分を占めることはよく知られている．ところで，磁気回路では電気回路の場合に対応して，電流を flux に，起電力を起磁力に置き換えて考えれば，電気回路の場合と全く同様に取り扱うことができるはずである．しかしながら，磁気回路の設計は電気回路と違つて簡単にはいかない．なぜならば，電気回路においては，導体と絶縁物との固有抵抗の差が非常に大きく，電流が電気回路外にもれることが殆んどないと見てよいのであるが，磁気回路にあつては，磁気抵抗体として，絶縁物と同じ非磁性体を用いるのであるから，導体と絶縁物との permeability の比は $10^3 \sim 10^4$ 程度であり，従つて leakage が相当に大きいと考えられる．このように磁気回路は leakage を考えに入れて設計せねばならないが，一般に正確な計算は非常に複雑であり，殆んど不可能であるといつても過言ではない．ゆえに，磁気回路設計の上手下手は，この leakage flux をいかにうまく近似計算するかによつてきまつてしまうのである．今まで，これらの困難のために，磁気回路の設計には，何度も設計して始めて得られる経験をもとにしなければ，よい地震計は設計できないとさえいわれていたのである．しかしながら，地震学者の立場から考えれば，地震計はあくまで研究するための一つの手段として用いられるものである以上，自分の研究に一番都合のよいものをつくらなければならないことはいうまでもない．従つて，さて設計しようというさいに，試作をいくつもするということは，時間的にも，また経済上からいつても無駄であるといわねばならない．

1) E. SHIMA, *Bull. Earthq. Res. Inst.*, **38** (1960), 29-39.
2) K. TAZIME, *Zisin*, **6** (1953), 43-44; **7** (1954), 96-115.

磁気回路の近似計算をする方法として有力なものは，現在のところ磁界描画法および仮定磁路法の二つが考えられる．ところで，磁気回路にあつては，その磁気抵抗を求めるよりもその逆数である permeance を求める方が便利なことが多い．よつて今後回路の計算をする場合には，permeance を主として用いることにする．さて磁界描画法というのは，pole piece 間の等磁位線および磁力線を，これらにより分割される各小区劃の permeance が等しいように画き，それらの直列，並列回路としての空間の全 permeance を求めるのである．ゆえに，正確に線を描けば，非常に正確な結果が得られる．しかしながら，この方法の最大の欠点は，線を描くこと自体が非常に面倒であるということである．それに較べると，仮定磁路法は，磁路を仮定して，その合成permeance を求めるやり方で，前者に較べればはるかに簡単である．工業用の電磁石には既にこの方法により設計されたものがあるが[3]，地震計用磁石にこの方法を応用して設計したという例は聞かない．従つてこの方法をわれわれの場合に適用して計算を行なつて見たものと，実測を較べ，適用性を調べて置くのは無駄ではないと考える．

2. 磁気回路設計に必要な理論[4]

磁気回路各部の permeance を P_i とすれば，各部の leakage flux は，全起磁力を U とすれば，UP_i できまる．われわれが使い得る磁束は，Fig. 1 の 1 の部分の per-

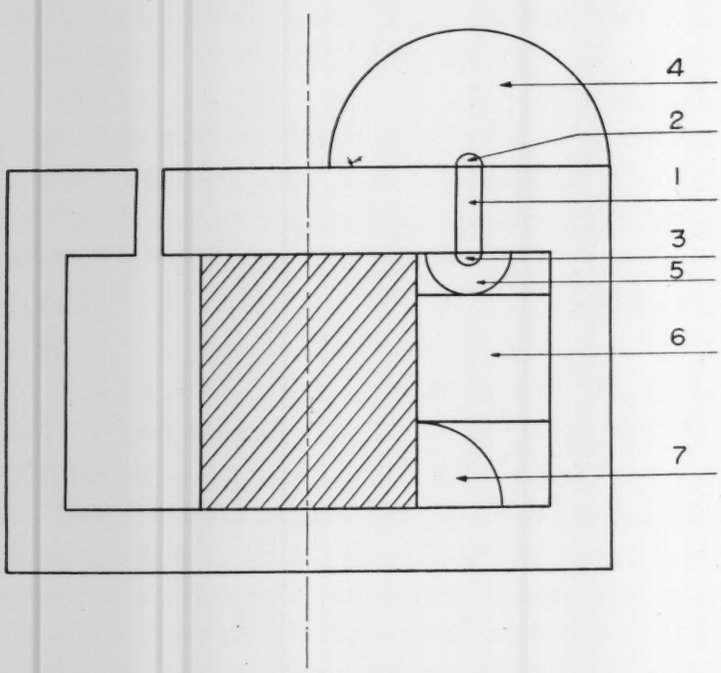

Fig. 1.

3) H. C. ROTERS, *Electromagnetic Device*. (John & Sons. Inc. N. Y., 1941.). M. I. T., 磁気回路と変圧器（上巻）（日本放送協会 昭和 25 年）

4) R. M. BOZORTH, *Ferromagnetism* (D. Van Nostrand Co. 1951.). T. ASADA, *Zisin*, **7** (1954), 116-135.

meance を P_1 とすれば，UP_1 である．磁石の出し得る total flux は $U\sum_{i=1}^{n}P_i$ であるから，漏洩係数を ν=total flux/useful flux$=U\sum_{i=1}^{n}P_i/UP_1$ と定義すれば，ν が小さいほどうまい設計であるといえる．

磁石の断面積を S，磁束密度を B，空隙部の断面積を S_g，磁束密度を B_g とすれば，

$$BS=\nu B_g S_g \tag{1}$$

が成立する．空隙に必要な起磁力は，$B_g l_g/\mu_0$ であり，この起磁力は磁石の消磁起磁力とつりあわなければならないから，

$$\frac{B_g}{\mu_0}l_g=HL \tag{2}$$

ここに μ_0 は空気中の permeability，l_g は空隙の長さ，L は磁石の有効長である．

勿論式 (2) は厳密には成立しない．なぜならば，空隙において出入する flux がどこでも pole face に直角とは限らないという事実があるからである．従つて実際には l_g は僅かばかり大きくなる．しかしここでは簡単のため，l_g に対する補正はいらないものとする．ゆえに磁石の容積 V は，(1) (2) 式より

$$V=SL=\frac{\nu B_g{}^2 S_g}{\mu_0 BH}l_g \tag{3}$$

従つてよく知られているように，磁石の容積は BH が最大になるような点で動作させれば，最も少なくてすむということがわかる．また，(3) 式は，磁石の供給し得る全エネルギー BHV が空隙部分に蓄えられる全磁気エルギーの ν 倍であることを示しているのである[5]．また，

$$\frac{B}{H}=\mu_0\frac{\nu S_g L}{S l_g}=\frac{\nu L}{S}P_1 \tag{4}$$

(4) 式の左辺は，与えられた磁石の消磁曲線から，BH_{max} の条件によつてきまつてしまう．また例えば，磁石として $MK5$ を，pole piece として純鉄を使用するとすれば，純鉄が飽和しないようにするためにその断面積が磁石のそれの半分より小さくすることはできない．また，BH_{max} の点では近似的に

$$\frac{B}{H}=\frac{B_r}{H_c} \tag{5}$$

が成立する．ただし B_r，H_c は，それぞれ消磁曲線において，消磁起磁力 0 の場合の残留磁気誘導，残留磁気誘導 0 の場合の消磁起磁力である．(1) (2) 式より

$$S=\nu\frac{B_g}{B}S_g,\quad L=\frac{B_g}{\mu_0 H}l_g \tag{6}$$

---

5) $\frac{B_g{}^2 S_g l_g}{\mu_0}=\frac{B_g{}^2}{\mu_0}V_g=B_g H_g V_g$．$V_g$ は空隙部の体積である．

となり，この式から逆に S をきめることができる．また，容積最小の条件で磁石を設計する場合には，(5) (6) 式より，

$$S=\nu B_g S_g\sqrt{\frac{H_c}{B_r(BH)_{\max}}},\quad L=\frac{B_g l_g}{\mu_0}\sqrt{\frac{B_r}{H_c(BH)_{\max}}} \tag{7}$$

となる[6]．これらの式には ν がはいつているので，地震計の磁気回路の場合 ν がどの位になるものかを，このさい調べて置く必要がある．

3. 磁気回路部分の Permeance

ここで，moving-coil type seismometer 用の磁気回路を設計することを考えよう．まず一番能率のよい円壔型にすることは当然として，内磁型にするか外磁型にするかをきめなければならない．磁石鋼は表面積が広ければ広いほど leakage flux の量も多いと考えられるから，同じ容積の磁石であれば，内磁型を採用した方が有効である．従つてわれわれの場合も，内磁型の磁石を作ることを考える．

内磁型の磁石を Fig. 1 に示すものとし，斜線をほどこした部分を磁鋼，何もないところを純鉄とすれば，円弧で等磁位線を近似することにより，磁界はおおよそ7ケの部分に分けられる．これらの各部について permeance を計算し，それらの直列，並列回路として permeance の合計をもとめれば，これと磁鋼の消磁曲線から，この磁石の特性が与えられる．われわれはまず磁界の7ケの部分について，それぞれ permeance を計算して行こう．

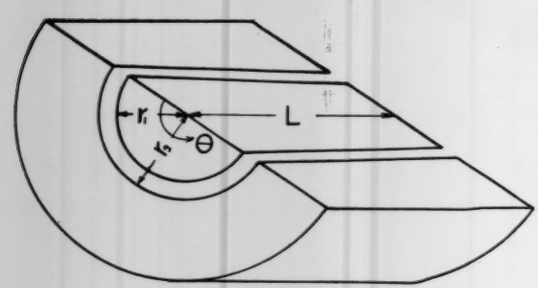

Fig. 2.

i) P_1

Permeance P_1 は，Fig. 2 の pole pieces の長さをここでは L_1，空気中の permeability を μ_0 とすれば，

$$P_1=\frac{\mu_0}{\int_{r_1}^{r_2}\frac{dr}{L_1 r\theta}}=\frac{2\pi L_1\mu_0}{\log\frac{r_2}{r_1}}\quad(\because\ \theta=2\pi) \tag{8}$$

で与えられる．gap の巾を l_g とすれば，(8) 式は書きなおせて，

$$P_1=\frac{2\pi L_1\mu_0}{\log\left(1+\frac{r_2-r_1}{r_1}\right)}=\frac{2\pi L_1\mu_0}{\log(1+l_g/r_1)} \tag{9}$$

となる．

6) A. J. HORNFECK and R. F. EDGAR, *Trans. Amer. Inst. Elec. Engrs.*, **59** (1940), 1017.

l_g が r_1 に較べて小さい時には，分母を展開し l_g/r_1 の二乗の項までをとることにすれば，

$$\frac{2\pi L_1\mu_0}{\log\left(1+\frac{l_g}{r_1}\right)} \fallingdotseq \frac{2\pi L_1\mu_0}{\frac{l_g}{r_1}-\left(\frac{l_g}{r_1}\right)^2\Big/2}$$

$$=\frac{2\pi\mu_0 L_1}{\frac{l_g}{r_1}\left(1-\frac{l_g}{2r_1}\right)}$$

$$\fallingdotseq\frac{2\pi\mu_0 L_1\left(1+\frac{l_g}{2r_1}\right)}{\frac{l_g}{r_1}}$$

$$=\pi\mu_0 L_1\left(\frac{r_2+r_1}{r_2-r_1}\right) \tag{10}$$

Table 1

$\frac{r_2}{r_1}$	1.05	1.10	1.15	1.20	1.25	1.30	1.35	1.40	1.45	1.50	1.55	1.60
$\log\frac{r_2}{r_1}$	0.0488	0.0953	0.1398	0.1823	0.2231	0.2624	0.3001	0.3365	0.3716	0.4055	0.4383	0.4700
$2\left(\frac{r_2-r_1}{r_2+r_1}\right)$	0.0488	0.0952	0.1395	0.1818	0.2222	0.2609	0.2979	0.3333	0.3674	0.4000	0.4314	0.4615
Diff.	0.0000	0.0001	0.0003	0.0005	0.0009	0.0015	0.0022	0.0032	0.0042	0.0055	0.0069	0.0085
Error %	0.00	0.10	0.21	0.27	0.40	0.57	0.73	0.95	1.30	1.36	1.57	1.85

となる．参考のために，r_2/r_1 が 1.05～1.60 の場合について $\log(r_2/r_1)$ と $2[(r_2-r_1)/(r_2+r_1)]$ がどのくらい違うかを計算したものが Table 1 に掲げてある．これによると，r_2/r_1 が 1.60 の時でも誤差は 2% にしかならないことがわかる．われわれの場合 r_2/r_1 が 1.30 をこえることは珍らしいと考えられるから，(10) の最後の式で計算すれば充分である．

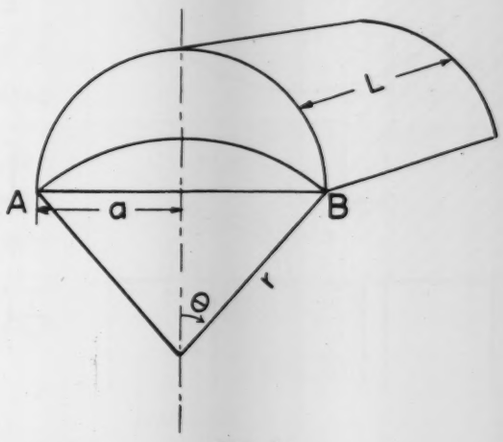

Fig. 3.

ii) P_2, P_3

Fig. 3 において，AB 間の permeance を求める問題に帰着する．AB 間の permeance は，全体積を AB 間の平均長で割つた平均断面積と，平均長を用いて近似的に求めることにする．AB 間の平均長は Fig. 3 を参照すれば，

$$\frac{4}{\pi}\int_0^{\pi/2}\frac{a\theta}{\sin\theta}d\theta=\frac{4a}{\pi}\left[\theta+\frac{\theta^3}{3\cdot 3!}+\frac{7\theta^5}{15\cdot 5!}+\frac{31\theta^7}{21\cdot 7!}+\cdots\right]_0^{\pi/2}\fallingdotseq 2.33a \tag{11}$$

全体積は $(\pi/2)a^2L_2$. ゆえに平均断面積はこれを (11) で割つた $(\pi/2)a^2L_2/2.33a \fallingdotseq 0.67aL_2$ となる. ゆえに permeance P_2, P_3 は,

$$\left.\begin{matrix}P_2\\P_3\end{matrix}\right\} \fallingdotseq \frac{0.67aL_2\mu_0}{2.33a} \fallingdotseq 0.288\mu_0 L_2 \tag{12}$$

となる. ここで面白いことは, (12) 式が gap の巾 $2a$ に無関係となることである. ここで L_2 を gap の中間にとれば, $L_2 \fallingdotseq \pi(r_1+r_2)$ となるから (12) 式は,

$$\left.\begin{matrix}P_2\\P_3\end{matrix}\right\} \fallingdotseq 0.904\mu_0(r_1+r_2) \tag{13}$$

と書くことができる. ただし r_1, r_2 は Fig. 2 に示すように, pole piece の内側および外側の半径である.

iii) P_4, P_5

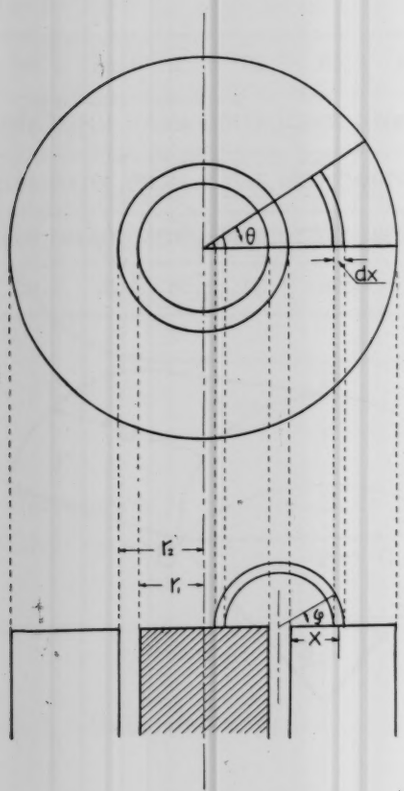

Fig. 4.

Fig. 4 において gap から半径方向に x だけはなれた内側の pole piece 上の小区劃

$$\left[\frac{r_1+r_2}{2}-\left(\frac{r_2-r_1}{2}+x\right)\right]d\theta dx \tag{14}$$

から出た flux は, 反対側の pole piece 上で gap から x だけ離れた,

$$\left[\frac{r_1+r_2}{2}+\left(\frac{r_2-r_1}{2}+x\right)\right]d\theta dx \tag{15}$$

なる面積の小区劃にはいり込む. 従つて, この path の任意の点における面積は,

$$\left[\frac{r_1+r_2}{2}+\left(\frac{r_2-r_1}{2}+x\right)\cos\varphi\right]d\theta dx \tag{16}$$

で与えられる. ゆえに平均断面積は,

$$\frac{1}{\pi}\int_0^{\pi}\left[\frac{r_1+r_2}{2}+\left(\frac{r_2-r_1}{2}+x\right)\cos\varphi\right]d\theta dx d\varphi = \frac{r_1+r_2}{2}d\theta dx \tag{17}$$

となるから, permeance P_4, P_5 は

$$\left.\begin{matrix}P_4\\P_5\end{matrix}\right\} = \frac{\mu_0}{\pi}\int_0^{2\pi}\int_0^{R}\frac{\frac{r_1+r_2}{2}}{x+\frac{r_2-r_1}{2}}d\theta dx$$

$$=\mu_0\frac{r_1+r_2}{2\pi}\left[\log\left(x+\frac{r_2-r_1}{2}\right)\right]_0^R\int_0^{2\pi}d\theta$$

$$=\mu_0(r_1+r_2)\log\left(1+\frac{2R}{r_2-r_1}\right) \tag{18}$$

となる．ここに R は磁石の形によつてきまる値である．P_4 に関しては，R として air gap の内側から centre pole piece の中心まで，または air gap の外側から，磁石枠外側までをとる．一般に，この二つの場合，R は等しくない場合が多いのではないかと考えられる．こういう場合は，その短かい方をとり，magnetic path が交わらないように注意する必要がある．その場合，われわれのように円弧による magnetic path の近似をすると，磁石の一部分からは，flux が出ないことになるが，この flux は実際上にはすくないと考えられるから無視しても大した問題は起らない．次に P_5 に関しては，

$$\pi\left(R+\frac{r_2-r_1}{2}\right)=D \tag{19}$$

によつてきめられるものである．ここに D は，永久磁石と磁石枠内側との距離である．つまり P_5 のような場合，magnetic path がこれによつてきまる R より大となれば，永久磁石表面からの leakage flux は，円弧の path をとらず直接磁石枠にはいり込むからである．

iv)　P_6

i) の場合と全く同様に考えればよい．ただし，この場合違つていることは，i) では flux の出て行く pole piece が等磁位であるから問題がないが，今度の場合は，永久磁石が場所によつて磁位が異なるためにその補正を入れなければならないということである，磁石全体の長さを L とするとき，x の点における起磁力は全体の起磁力の x/L 倍となる．ゆえにその点における permeance の効果は i) の場合と同様にして行なつた計算結果の x/L 倍となる．従つて，Fig. 5 のように ab 区間の永久磁石と磁石枠との間の permeance の効果は $(b+a)/2L$ 倍となる．ゆえに，

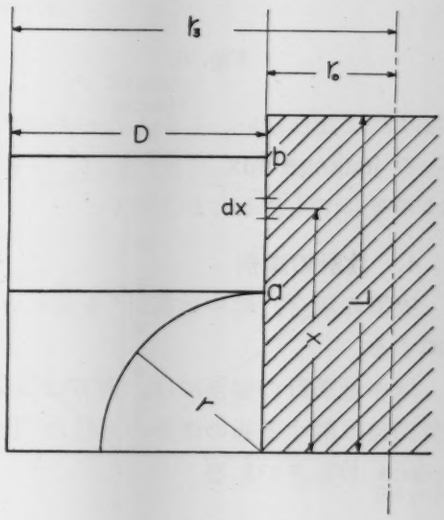

Fig. 5.

$$P_6=\frac{2\pi(b-a)}{\log\left(1+\frac{D}{r_0}\right)}\frac{(b+a)}{2L}\mu_0=\frac{\pi(b^2-a^2)}{L\log\left(1+\frac{D}{r_0}\right)}\mu_0 \tag{20}$$

となる．

v)　P_7

Fig. 5 において，b の点は，iii) において述べたようにしてきまるが，a の点は，

$D=\pi a/2$ を満足するように選らぶのである．Fig. 6 において，x の点で dx なる巾のところについて permeance を考えて見る．path 上の任意の点 P における断面積は，$2\pi(r_0+x\cos\theta)dx$ で与えられる．従つて平均断面積は，

$$2\pi(r_0+x\overline{\cos\theta})dx,\ \text{但し}\ \overline{\cos\theta}=\frac{2}{\pi}\int_0^{\pi/2}\cos\theta\,d\theta=\frac{2}{\pi} \tag{21}$$

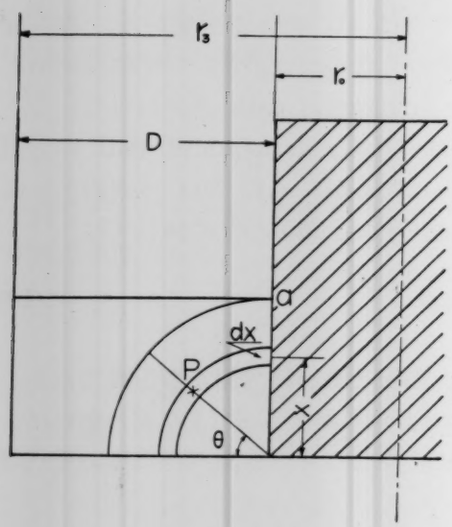

Fig. 6.

となる．ゆえに x の点における磁位は全体の x/L になることを考えに入れると，

$$dP_7=\frac{2\pi\mu_0\left(r_0+\frac{2}{\pi}x\right)}{\frac{\pi}{2}x}\cdot\frac{x}{L}dx \tag{22}$$

$$\therefore\ P_7=4\mu_0\int_0^a\frac{r_0+\frac{2}{\pi}x}{L}dx$$

$$=\frac{4\mu_0}{L}\left(r_0a+\frac{a^2}{\pi}\right) \tag{23}$$

となる．

以上考えてきた他に，例えば pole piece に使う純鉄それ自体がそのすべての点で等磁位では有り得ないから，ここにも leakage flux を考えなければならない．しかしながらこれらの leakage flux は，前に調べた 7 つの部分からの leakage flux に較べれば，一般に小さいものであるから，この程度の議論の場合には無視しても差しつかえない．

4. 設計の実例

実際の場合，地中地震計[7]を例にとつて，計算と実測がどの位合うかを調べてみることにする．

地中地震計の場合には，磁石は $MK5$[8]($\phi=2.0$ cm, $L=1.5$ cm) を使用した．なお，磁気回路に関する他の部分の寸法は Table 2 に掲げてある．(Fig. 1 参照) 表中 h は pole piece の長さである．

Table 2.

r_0	r_1	r_2	r_3	h	a	b
cm	cm	cm	cm	cm	cm	cm
1.0	1.2	1.4	1.6	0.4	0.38	1.31

7) H. KAWASUMI, E. SHIMA and M. SIBANO, *Annual Meeting of the Seismological Society of Japan* (April, 1955).

8) *MK* 磁石は三菱鋼材から売り出されている．*MK*5 は三島博士の発明品 (1931 年) を研究改良したものであり，その化学成分は，*Ni*: 13.5%, *Co*: 24%, *Al*: 9%, *Cu*: 3%, *Fe*: 50.5% である．

よつて，P_i は，cgs-emu では $\mu_0=1$ であるから，μ_0 をとれば，(10) 式より

$$P_1=\pi h\frac{r_2+r_1}{r_2-r_1}=16.33,$$

(13) 式より

$$P_2=P_3=0.904(r_1+r_2)=2.35,$$

(18) 式より

$$P_4=(r_1+r_2)\log\left(1+\frac{2R}{r_2-r_1}\right)=4.67,\ (R=0.5\,\mathrm{cm})$$

$$P_5=(r_1+r_2)\log\left(1+\frac{2R'}{r_2-r_1}\right)=1.67,\ (R'=0.09\,\mathrm{cm})$$

(20) 式より

$$P_6=\frac{\pi(b^2-a^2)}{L\log\dfrac{r_3}{r_0}}=7.00,$$

(23) 式より

$$P_7=\frac{4}{L}\left(r_0a+\frac{a^2}{\pi}\right)=1.14,$$

となる．

$$\therefore\ \nu=\frac{\sum P_i}{P_1}=2.17$$

(4) 式より

$$\frac{B}{H}=\frac{\nu S_g L}{Sl_g}=\frac{\nu S_g L}{S(r_2-r_1)}\fallingdotseq 17.0$$

$MK5$ の demagnetization curve で $B/H=17.0$ の点をさがすと，$B=10100$ gausses, $H=595$ oersteds であることがわかる．$MK5$ の demagnetization curve および，BH-curve は Fig. 7 に示してある．ただし製品には±数%のばらつきがあるので[9]，平均のものを掲げてある．ゆえに平均的に見て useful flux$=B_gS_g=BS/\nu\fallingdotseq 14{,}500$ (maxwells)

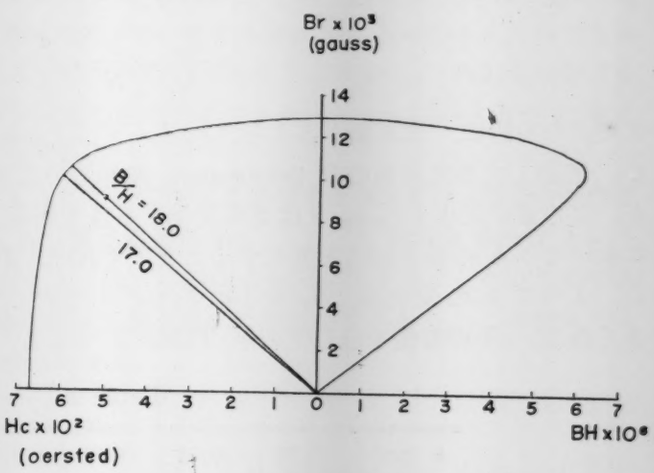

Fig. 7. (三菱鋼材のパンフレットに依る)

9) 例えば三菱鋼材のパンフレットによれば，$MK5$ についての仕様は，$B_r=12{,}000\sim13{,}5000$ gausses, $H_c=620\sim720$ oersteds となつている．

$$\therefore\quad B_g=\frac{BS}{\nu S_g}=\frac{\text{useful flux}}{S_g}\fallingdotseq 4400\ (\text{gausses})$$

となる．地中地震計 8 コの磁石について，flux meter による実測例では，useful flux が，14,500～16,500 maxwells になつた．この結果は前にものべたように製品のばらつきを考に入れれば，計算例と非常によくあつて居る．ところで flux meter で磁束をはかる場合，今までのように bobbin の一カ所だけに線を捲いた search coil を使うと，空隙部以外の leakage flux を一緒にはかつてしまうおそれがある．これをさけるため bobbin の 2 カ所におのおの反対向きに同じ回数だけ捲いた search coil を使つた．これによれば，不要の flux による meter の振れは meter 上では打ち消されてしまうから，空隙部のみの磁束をはかるのには便利である．すなわち search coil が，最初には，それぞれ Fig. 1 で permeance の区分をした時の 1 と 2 の部分の最下点にあり，これから search coil を動かすように工夫すればよいわけである．

5. Discussions

Fig. 7 で見ると，BH_{max} の点では $B/H\fallingdotseq 18$ であるから，この場合に磁石の容積が最小になる．言い換えれば，与えられた容積の磁石鋼で最高の能率をあげるためには，BH_{max} の点で使用するように磁気回路を設計せねばならないということである．この意味では，磁気回路に関する限り，本例の設計は必らずしもよいとはいえない．ここで，もう一度 (4) 式を見直してみよう．(4) 式から，

$$\nu\frac{S_g}{l_g}=\frac{B}{H}\cdot\frac{S}{L}\qquad(4')$$

この式の右辺は，磁石鋼が与えられれば，すべてわかつてしまう．そしてこの式は右辺が，設計した磁気回路の全 permeance に等しいことを示している．$S_g/l_g=P_1$ であるが，この値が変化すれば，ν は当然変化する量である．これをすこし調べて見る．Fig. 1 において，h の長さだけを変化することにすれば，P_2～P_7 の permeances は変化しない．よつて ν の変化は，S_g を小にすれば ν は大となる．また S_g を大にすれば ν は小さくなる．その有様を示したのが Table 3 である．これを見るとわかるように，

Table 3

h (cm)	0.30	0.35	0.40	0.45	0.50	0.55
P_1	12.24	14.28	16.33	18.37	20.40	22.44
ΣP	31.42	33.46	35.51	37.55	39.58	41.62
ν	2.57	2.34	2.17	2.04	1.94	1.86
B/H	15.0	16.0	17.0	17.9	18.9	19.9

$h=0.45$ cm の附近で $B/H=18$ となる．この点では，Fig. 7 から，$B=10{,}400$ gausses,

H=580 oersteds となる．ゆえに非常にうまく設計すれば空隙を通る useful flux=$BS/\nu \fallingdotseq$16,000 maxwells にすることも可能であると考えられる．本例では，磁石そのものの重量および大きさに制限をうけていたために，すこしの損を承知の上で使用しているのである．

純鉄の磁路は，途中でくびれる，つまり断面積が小さくなる点があつては困る．むしろ磁路の途中ではふくらんでおり，pole piece のところで，磁束をあつめるようになつていることがのぞましい[10]．これは，磁性材料の形が回転楕円体に近くなると，内部は均一に磁化され，磁石各部の負担が一様になるが，そうでない形の時には，負担の重いところと軽いところができてしまうためと考えられる．更に主磁束に直角方向の磁石の各部の断面積を考えると，純鉄の部分は磁石鋼の部分の半分以下にすることはできない．これは純鉄の磁気飽和特性から考えても明白である．また純鉄の磁路の部分もなるべく短かくした方がよいことはいうまでもない．しかしさればといつて，磁石鋼と純鉄の磁石枠とをあまり近づけすぎても，ここでの leakage flux が多くなつて困ることになる．したがつてこのことは，前述の条件を考えに入れて適当なところで妥協するより仕方がない．この部分における permeance は，(9) 式を使つて大ざつぱにみつもれば，一般の場合 r_2/r_1=1.2 位，またはそれ以下であろうから，磁石鋼の有効長が，pole piece の厚さの 5 倍の時には，$r_3/r_0 \fallingdotseq$1.5，4 倍の時には，$r_3/r_0 \fallingdotseq$1.4 位にすれば，P_1 におけると同程度またはそれ以下の permeance におさえることができるということがわかる．

前節で述べたように．νは内磁型の場合には，割合簡単に 2 ぐらいにすることができる．しかしながら．外磁型の場合には．leakage flux のでる表面がもう一つふえるのであるから．上記の計算法で近似計算することはできないであろう．しかし．内磁型の磁石を設計する場合にも，もし容積に制限が加えられないのであれば，ν=2.5～3.0 だと考えて．多めの磁石鋼を使用する方が安全である．

特に強力な外部起磁力が作用するような場所で磁石を使用する場合には，磁石の動作点を安定化するために．knock down して置く必要がある．ここに knock down というのは，磁石にある程度の交流起磁力を与えて磁石の動作点を安定化することをいうのである．knock down をすると，する前に較べて磁束値は当然減少するから，この意味でも磁石鋼を多目にとつて置くことは必要といえる．

6. Summary

地震計用磁石を設計するにあたり，その磁気回路からの leakage flux を評価するために，円弧の leakage path を仮定して，近似計算を行つた．この方法を，地中地震計 8 コの磁石に適用した結果，良く合うことがたしかめられた．なお，一例ではあるが，ϕ=40 mm, L=30 mm の $MK5$ を使用した磁石についても計算結果は良く合つている．この計算において純鉄の部分は，たとえば電気回路でいえば，earth 線と同様に見做し，この部分はどこでも等磁位であり，純鉄同士の間には leakage はないものと仮定してい

10) 例えば，川口寅之輔　新磁石鋼　産業図書株式会社版　昭和 23 年.

る．このことは，永久磁石そのものが，現在それ程均一の特性の揃つたものが得られない現状からみれば，（メーカーのパンフレットによれば，個々の磁石については平均の demagnetization-curve から，数%以上のばらつきがみられる．）この程度のあらい議論でも差支えはないようである．また純鉄の磁路は，途中でくびれるようなこと，いい換えれば，断面積が磁路の途中で小さくなつているというようなことは，なるべくさけなければならない．このようなことをすると無益な leakage flux を生ずるおそれがあるからである．強磁性材料についていえば，むしろ真中あたりがふくらんでおり，pole piece の附近で，磁束をあつめるために断面積が小さくなつているものの方が能率は良いようである．更に，純鉄の部分は，いかなる場合においても，その断面積が永久磁石のそれの半分以下にはならないようにしなければならない．このことは，純鉄の磁気飽和特性から考えても明白である．

本報告においては，内磁型の磁石のみを取り扱い，外磁型のものについては，触れなかつた．しかし磁性材料というものは，その表面における不均一性その他の理由により，その表面積に正比例して leakage flux がふえるのであるから，なるべくならば，内磁型の磁石を設計した方がとくである．本報告において述べた近似計算により，内磁型の磁石の場合には $\nu \fallingdotseq 2$ ぐらいにすることは可能であることがわかつた．しかし外磁型の磁石の場合には，上に述べた理由により，恐らくこの方法では取り扱かうことはできないであろう．

この報告が，将来地震計を設計する人に，少しでも役に立てば幸いである．

本研究にあたり，河角広教授には多大な御援助と御指導を賜わつた．ここに厚く御礼を申上げる．また，厄介な図表の作成を手伝われた松本憲明氏にも謝意を表したい．

32. Note on the Magnetic Circuit of the Moving-coil Type Seismometer.

By Etsuzo SHIMA,
Earthquake Research Institute.

It is aimed in this paper to contribute to the design of a highly sensitive seismometer. We know that the voltage sensitivity A is a product of B and l, where B is the flux density of the air gap of the magnet used and l is the effective length of the conductor. So we can easily obtain the desired aim by providing the seismometer with a powerful magnet of high flux density in its air gap. Thus the design of the magnetic circuit is one of the most important items at the present time.

It is well known that analyses of magnetic circuits and electrical circuits can be similarly reached, if we consider the analogous relations between them. Namely, magneto-motive forces, magnetic fluxes and magnetic resistances are analogous to electro-motive forces, electric currents and electric resistances respectively. In the case of the electrical circuit, the difference in the resistivity of the conductor and the insulator is so large that no current will leak out of the circuit. In the case of the magnetic circuit, on the con-

trary, the ratio of the permeability between the conductor and the insulator is found to be as low as 10^3-10^4, so we have to consider the effect of the leakage flux. This is, notably one of the reasons why the design of the magnetic circuit is somewhat complicated as compared with that of the electrical circuit. The behaviour of the leakage flux is, in fact, so complex that the accurate evaluation of the leakage flux is almost impossible. So we are compelled to estimate the leakage flux by assuming an approximate magnetic path. At present, two approximate methods are in a practical way used for this purpose. The first method is more accurate though it is rather involved. In this method, first we draw the lines of magnetic force and of equi-magnetic potential so that the permeances, *that is* the reciprocal of the magnetic resistances, of the part bound by these lines are equal; and second we evaluate the total permeance of whole space considering that these permeances of the elementary portions are each connected with the other three dimensionally. The weak point of this method is in the troublesome calculation of the permeances of the circuit. On the contrary, the second method is more practical and easier than the above mentioned method. In this method, we assume that the shape of the path of the magnetic flux can be approximated by a circular path. Then the total permeance of the circuit is evaluated easily bearing in mind that the each part of the circuit is connected in series or parallel with the others.

We have felt it necessary, in our study of the theoretical and experimental approach to the design of an electro-magnetic seismograph, to know whether the above-mentioned simplified assumption can be used in the analysis of the magnetic circuit of the actual seismometer or not, because, no relevant study of the magnetic circuit used in ordinary seismometers is known to the writer. And so the main purpose of this paper is to check this method, and to investigate how to achieve a large useful flux.

In section 2, is given a brief review of the theory pertinent to a design for a magnetic circuit. Special considerations were given to obtaining optimum working point of the magnet with a minimum volume of magnetic material.

In section 3, an example is set out taking a model circuit as shown in Fig. 1. For convenience we divide the magnetic circuit into seven parts. We could verify in some actual circuits, that the total permeances can be calculated by the combinations of the above-mentioned seven parts, while in others some slight modifications to the path are necessary.

In section 4, we examined the magnetic circuits of eight bore-hole-seismometers, and found strong agreement between the values calculated by the second method and the direct measurements of the useful fluxes.

We may therefore conclude that, the second approximate method can be used safely in analysing the magnetic circuits of the seismometers.

——所　　報——

◎談話会記事

第378回談話会（昭和35年6月28日）

1. チリ地震とそれに伴う日本の津浪　　河角　広

2. 1960年5月24日チリ地震津浪踏査速報

北海道	東京水産大学 三好　寿
下北半島西岸，青森間	気象庁 宮崎正衛 東大理学部 高野健三
尻屋崎，八木間	東大理学部 佐藤良輔 東大大学院 栗本　広
久慈，小本間	東京学芸大学 富永政英
田老，船越間，及び津軽半島	気象研究所 宇野木早苗 気象研修所 土屋瑞樹 （以上河角所員紹介）
大槌，吉浜間	表　俊一郎 小牧昭三
越喜来，間之浜間	桃井高夫 黒木義弘
大野，気仙沼間	笠原慶一 東大大学院 茅野一郎
志津川，御前間	平能金太郎 東大大学院 平沢朋郎
女川，石巻間	相田　勇 東大工学部研究生 影山正樹
松島，那珂湊間	羽鳥徳太郎 東大大学院 高　隆二
房総半島	山口林造 岡田惇

三浦半島，浜松間

東大大学院
寺本俊彦
上同
永田豊
上同
須藤英雄
上同
竹田厚
(河角所員紹介)

宮城，岩手，青森県下の土木災害について

東大工学部
堀川清司
東大大学院
鮮于澈
(河角所員紹介)

3. 地球のねじり振動
不均質な地球

竹内均
(佐藤所員紹介)

均質な地球

佐藤泰夫
松本利松

4. 電磁式地震計の理論的実験的研究
その 2. 地震計の磁気回路について

嶋悦三

5. 地球熱学 第5報 (続)
関東地方の地殻熱流量

上田誠也
宝来帰一

6. 非定常ダイナモ 第2報

行武毅

追加 筑波山で観測されたチリ地震について

萩原尊礼
松本利松

追加 1960年5月24日チリ地震津浪踏査速報
八丈島

羽鳥徳太郎

第379回談話会 (昭和35年7月26日)

1. 木造家屋の耐震性
浅草寺五重の塔における地震動の観測結果

西村源六郎
鈴木正治

2. 海洋底を伝わるレーリー波の分散 (第4報)
海洋の平均深度と分散の相関性

三東哲夫

3. 日本の広域変成作用の年代

坂野昇平
紫藤文子
John Miller
上田誠也
(森本所員紹介)

4. アメリカ合衆国における常時微動の測定 (序報)

金井清
田中貞二
U.C.L.A.
C. M. Duke
D. J. Leeds

5. アメリカ合衆国における地震動の周期特性

金井清

6. 強震動の周期特性に関する実験式
(アメリカ合衆国の強震記録との比較)

金井清

第380回談話会 (昭和35年9月27日)

1. 木造家屋の耐震性（第5報）
   浅草寺五重の塔における地震動の観測結果（補遺）
   — 西村源六郎・鈴木正治
2. 不均質な媒質を伝わる弾性波の安定性に就いて — 吉山良一
3. 海洋底を伝わるレーリー波の分散（第5報）
   海の深さと分散（続報） — 三東哲夫
4. 大島及び三宅島に於ける湧水，雨水の化学成分 — 野口喜三雄・後藤達夫
5. 南極昭和基地に於ける脈動観測 — 村内必典
6. 岩石の破壊に伴う Elastic Impulses（第2報） — 茂木清夫
7. 信貴山附近の水準測量 — 森本良平・岡田惇
8. 第三紀地球磁場の変動に関する研究 — 百瀬寛一

第381回談話会 (昭和35年10月18日)

1. 長周期表面波による発震機巧の研究 — 安芸敬一
2. レーリー波によるマントル上層の研究 — 安芸敬一・Frank Press
3. 海洋底をつたわるレーリー波の分散
   —西太平洋の地殻構造—（第6報） — 三東哲夫
4. 軽石のみかけの比重 — 村井勇
5. 明神礁昭和35年7月21日の新噴出岩石 — 森本良平・小坂丈予・福田知子

第382回談話会 (昭和35年11月22日)

1. 褶曲境界面における弾性波の反射・屈折
   その2 P波入射の場合 I — 浅野周三
2. 地球ののびちぢみ振動 — 竹内均（萩原所員紹介）
3. 電磁式地震計の理論的実験的研究
   その3 動特性について — 嶋悦三
4. 南極昭和基地に於ける脈動観測結果（続報） — 村内必典
5. 今市—鹿沼附近の堆積火山灰層の風化について
   今市地震地域の地質 第4報 — 森本良平・小坂丈予

Index to Vol. 38.

Page

ASANO, S., (10) Reflection and Refraction of Elastic Waves at a Corrugated Boundary Surface. Part I. The Case of Incidence of SH Wave. (in English) 177

HÔRAI, K. and UYEDA, S., (11) Studies of the Thermal State of the Earth. The Fifth Paper: Relation between Thermal Conductivity of Sedimentary Rocks and Water Content. (in English)... 199

HÔRAI, K. and RIKITAKE, T., (25) Studies of the Thermal State of the Earth. The Fourth Paper: Terrestrial Heat Flows related to Possible Geophysical Events. (in English) 403

HÔRAI, K. and UYEDA, S., (26) Studies of the Thermal State of the Earth. The Sixth Paper: Terrestrial Heat Flow at Innai Oil Field, Akita Prefecture and at Three Localities in Kanto-District, Japan. (in English) 421

ICHIMURA, T., (15) Geological Investigations on the Zaō Volcanoes. V Kumano Volcano. (in English) 255

ICHIMURA, T., (30) Xenoliths Included in Granitic Rocks of the Sekine-Azusayama District, Yamagata Prefecture. (in English) . 479

KASAHARA, K., (12) An Attempt to Detect Azimuth Effect on Spectral Structures of Seismic Waves (The Alaskan Earthquake of April 7, 1958). (in English) 207

MATSUI, Y. and MINAMI, E., (16) Composition of the Main Chemical Components in the Rocks from Hotoke-iwa Volcanic Body of Mt. Asama. (in English)..... 291

MATUMOTO, H., (20) A Transistor Amplifier for Seismographs. (in Japanese) 345

MATUMOTO, T., (2) On the Spectral Structure of Earthquake Waves. — The Relation between Magnitude and Predominant Period—(in English) 13

MINAKAMI, T., (31) Fundamental Research for Predicting Volcanic Eruptions. (Part 1) Earthquakes and Crustal Deformations originating from Volcanic Activities. (in English) 497

MINAMI, E. and MATSUI, Y., (16) Composition of the Main Chemical Components in the Rocks from Hotoke-iwa Volcanic Body of Mt. Asama. (in English) 291

MIYAMURA, S., (6) Local Earthquakes in Kii Peninsula, Central Japan. Part 4.—Location of Earthquakes by the Temporary Network of Stations near Wakayama—(in Japanese) 71

MIYAMURA, S. and OKADA, A., (21) Results of Levelling Resurvey between Wakayama and Gobō, Wakayama Prefecture. (in Japanese) 355
MURAI, I., (5) On the Mud-flows of the 1926 Eruption of Volcano Tokachi-daké, Central Hokkaido, Japan. (in English) 55
MURAI, I., (17) Pyroclastic Deposits distributed on the East Foot of Volcano Myôkô. (in English) 307
MURAI, I., (28) Pumice-flow Deposits of Komagatake Volcano, Southern Hokkaido. (in English) 451
NISHIMURA, G. and SUZUKI, M., (19) Aseismic Properties of a Wooden House (III). (in English) 329
OKADA, A., (7) Land Deformation of the Southern Part of the Kii Peninsula, Southwestern Japan. (in Japanese) 113
OKADA, A. and MIYAMURA, S., (21) Results of Levelling Resurvey between Wakayama and Gobō, Wakayama Prefecture. (in Japanese) 355
RIKITAKE, T. and TANAOKA, I., (18) A Differential Proton Magnetometer. (in English) 317
RIKITAKE, T. and HÔRAI, K., (25) Studies of the Thermal State of the Earth. The Fourth Paper: Terrestrial Heat Flows related to Possible Geophysical Events. (in English) 403
SANTÔ, T. A., (13) Observation of Surface Waves by Columbia-type Seismorgraph Installed at Tsukuba Station, Japan. (Part 1)—Rayleigh Wave Dispersions across the Oceanic Basin.—(in English) 219
SANTÔ, T. A., (14) The Observation of Microseisms at a Wave Gauge Station.—On the Origin of Microseisms (Part III).—(in English) 241
SANTÔ, T. A., (24) Rayleigh Wave Dispersions across the Oceanic Basin around Japan (Part II). (in English) 385
SATÔ, Y. and YAMAGUCHI, R., (23) Coupling Effect of Shear Vibrations of the Structure with Elastic Foundations, and the Maximum Response of Rocking Motion. (in English) 369
SHIMA, E., (3) Theoretical and Experimental Approach to the Designs and Calibrations of Electro-magnetic Seismograph: I. Voltage Sensitivity of the Moving-coil Type Seismometer. (in English) 29
SHIMA, E., (32) Note on the Magnetic Circuit of the Moving-coil Type Seismometer. (in Japanese) 545

SUZUKI, M. and NISHIMURA, G., (19) Aseismic Properties of a Wooden House (III). (in English) 329
TANAOKA, I. and YUKUTAKE, T., (4) Magnetic Survey on Hakone Volcano by Use of a Proton Magnetometer. (in English) 41
TANAOKA, I. and RIKITAKE, T., (18) A Differential Proton Magnetometer. (in English) 317
UYEDA, S. and HÔRAI, K., (11) Studies of the Thermal State of the Earth. The Fifth Paper: Relation between Thermal Conductivity of Sedimentary Rocks and Water Content. (in English) 199
UYEDA, S. and HÔRAI, K., (26) Studies of the Thermal State of the Earth. The Sixth Paper: Terrestrial Heat Flow at Innai Oil Field, Akita Prefecture and at Three Localities in Kanto-District, Japan. (in English) 421
YAMAGUTI, S., (6) On the Changes in the Heights of Mean Sea-levels, before and after the Great Earthquakes. (in English) .. 145
YAMAGUCHI, R. and SATÔ, Y., (23) Coupling Effect of Shear Vibrations of the Structure with Elastic Foundations, and the Maximum Response of Rocking Motion. (in English) 369
YOSHIYAMA, R., (22) Propagation of Surface Waves and Internal Friction. (in English) 361
YOSHIYAMA, R., (29) Stability of Waves through a Heterogeneous Medium and Apparent Internal Friction. (in English) 467
YUKUTAKE, T., (1) Stability and Non-Steady State of Self-Exciting Dynamos. I. (in English) 1
YUKUTAKE, T. and TANAOKA, I., (4) Magnetic Survey on Hakone Volcano by Use of a Proton Magnetometer. (in English) 41
YUKUTAKE, T., (27) Stability and Non-Steady State of Self-Exciting Dynamos. II. (in English) 437
Research Group for Proton Magnetometer, (8) Proton Magnetometers. (in Japanese) 125

索 引 第 38 号

頁

浅野周三 (10) 褶曲境界面における弾性波の反射，屈折 第1報 SH波入射の場合 (英文)..... 177

宝来帰一·上田誠也 (11) 地球熱学 (第5報) 堆積岩における熱伝導度と含水量の関係 (英文)..... 199

宝来帰一·力武常次 (25) 地球熱学 (第4報) マントル内熱対流その他に伴う熱流量 (英文)..... 403

宝来帰一·上田誠也 (26) 地球熱学 (第6報) 秋田県院内油田，および，関東地方三地点における地殻熱流量 (英文)..... 421

市村 毅 (15) 蔵王火山の地質学的研究 (第5報) (英文)..... 255

市村 毅 (30) 山形県関根·梓山地方の花崗質岩に含まれる捕獲岩 (英文)..... 479

笠原慶一 (12) 大地震発震スペクトルの方位特性に関する一つの試み (アラスカ地震の場合) (英文) 207

松井義人·南 英一 (16) 浅間山仏岩火山体岩石の主化学成文組成 (英文)..... 291

松本英照 (20) 地震計用トランジスター増幅器 (邦文) 345

松本利松 (2) 地震波のスペクトル構造 — マグニチュードと卓越周期の関係 —(英文) 13

水上 武 (31) 噴火予知に関する基礎的研究 (I) 火山活動に関連する地震と地殻変動 (英文)..... 497

南 英一·松井義人 (16) 浅間山仏岩火山体岩石の主化学成分組成 (英文)..... 291

宮村摂三 (6) 紀伊半島の局地地震 (第4報)— 臨時観測網による震源位置の決定—(邦文) 71

宮村摂三·岡田 惇 (21) 和歌山—御坊間水準測量結果 (邦文)..... 355

村井 勇 (5) 北海道，十勝岳火山の泥流について (英文)..... 55

村井 勇 (17) 妙高火山東麓に分布する火砕堆積物 (英文) 307

村井 勇 (28) 北海道，駒ケ岳火山の軽石流堆積物 (英文) 451

西村源六郎·鈴木正治 (19) 木造家屋の耐震性 (第3報) (英文) 329

岡田 惇 (7) 紀伊半島南端部附近の地殻変動について (邦文)..... 113

岡田 惇·宮村摂三 (21) 和歌山—御坊間水準測量結果 (邦文)..... 355

力武常次·棚岡 巌 (18) プロトン磁力計による地磁気傾度計 (英文)..... 317

力武常次·宝来帰一 (25) 地球熱学 (第4報) マントル内熱対流その他に伴なう熱流量 (英文)..... 403

三東哲夫 (13) コロンビア型地震計による表面波の観測 (第一報) —海洋底を伝わるレーリー波の分散— (英文)..... 219

三東哲夫 (14) 脈動源について (第三報) —波浪観測点における脈動観測— (英文) 241
三東哲夫 (24) 海洋底を伝わるレーリー波の分散 (第二報) (英文) 385
佐藤泰夫·山口林造 (23) 構造物の剪断振動と弾性地盤の相互作用 附: ロッキングの最大倍率 (英文) 369
嶋 悦三 (3) 電磁式地震計の理論的実験的研究 その1 電圧感度について (英文) 29
嶋 悦三 (32) 電磁式地震計の磁気回路について (邦文) 545
鈴木正治·西村源六郎 (19) 木造家屋の耐震性 (第3報) (英文) 329
棚岡 巌·行武 毅 (4) プロトン磁力計による箱根火山の磁気測量 (英文) 41
棚岡 巌·力武常次 (18) プロトン磁力計による地磁気傾度計 (英文) 317
上田誠也·宝来帰一 (11) 地球熱学 (第5報) 堆積岩における熱伝導度と含水量の関係 (英文) 199
上田誠也·宝来帰一 (26) 地球熱学 (第6報) 秋田県院内油田, および, 関東地方三地点における地殻熱流量 (英文) 421
山口生知 (9) 大地震前後の平均海水面変化について (英文) 145
山口林造·佐藤泰夫 (23) 構造物の剪断振動と弾性地盤の相互作用 附: ロッキングの最大倍率 (英文) 369
吉山良一 (22) 表面波と地球の内部摩擦 (英文) 361
吉山良一 (29) 不均質な媒質内を伝る弾性波の安定性について —見掛けの内部摩擦係数— (英文) 467
行武 毅 (1) 非定常ダイナモ (1) (英文) 1
行武 毅·棚岡 巌 (4) プロトン磁力計による箱根火山の磁気測量 (英文) 41
行武 毅 (27) 非定常ダイナモ (2) (英文) 437
文部省科学試験研究費研究班 (代表者 力武常次) (8) プロトン磁力計の試作研究 (続報) (邦文) 125

BULLETIN
OF THE
EARTHQUAKE RESEARCH INSTITUTE
TOKYO UNIVERSITY

VOL. 38

1960

東京大学
地震研究所彙報
第 38 号

昭和 35 年

CONTENTS.

Vol. 38.

Part 1. March, 1960.

Papers and Reports.

Page

1. T. YUKUTAKE, Stability and Non-Steady State of Self-Exciting Dynamos. I. (in English) 1
2. T. MATUMOTO, On the Spectral Structure of Earthquake Waves.—The Relation between Magnitude and Predominant Period—(in English) 13
3. E. SHIMA, Theoretical and Experimental Approach to the Designs and Calibrations of Electro-magnetic Seismograph: I. Voltage Sensitivity of the Moving-coil Type Seismometer. (in English) 29
4. T. YUKUTAKE and I. TANAOKA, Magnetic Survey on Hakone Volcano by Use of a Proton Magnetometer. (in English).... 41
5. I. MURAI, On the Mud-flows of the 1926 Eruption of Volcano Tokachi-daké, Central Hokkaido, Japan. (in English) 55
6. S. MIYAMURA, Local Earthquakes in Kii Peninsula, Central Japan. Part 4.—Location of Earthquakes by the Temporary Network of Stations near Wakayama—(in Japanese) 71
7. A. OKADA, Land Deformation of the Southern Part of the Kii Peninsula, South-western Japan. (in Japanese)..... 113
8. Research Group for Proton Magnetometer, Proton Magnetometers. (in Japanese)..... 125
9. S. YAMAGUTI, On the Changes in the Heights of Mean Sea-levels, before and after the Great Earthquakes. (in English) 145

Part 2. June, 1960.

10. S. ASANO, Reflection and Refraction of Elastic Waves at a Corrugated Boundary Surface. Part I. The Case of Incidence of SH Wave. (in English)..... 177
11. K. HÔRAI and S. UYEDA, Studies of the Thermal State of the Earth. The Fifth Paper: Relation between Thermal Conductivity of Sedimentary Rocks and Water Content. (in English) 199

12. K. KASAHARA, An Attempt to Detect Azimuth Effect on Spectral Structures of Seismic Waves (The Alaskan Earthquake of April 7, 1958). (in English) 207
13. T. A. SANTÔ, Observation of Surface Waves by Columbia-type Seismograph Installed at Tsukuba Station, Japan. (Part 1)—Rayleigh Wave Dispersions across the Oceanic Basin.—(in English) 219
14. T. A. SANTÔ, The Observation of Microseisms at a Wave Gauge Station. — On the Origin of Microseisms (Part III). — (in English) 241
15. T. ICHIMURA, Geological Investigations on the Zaō Volcanoes. V Kumano Volcano. (in English) 255
16. E. MINAMI and Y. MATSUI, Composition of the Main Chemical Components in the Rocks from Hotoke-iwa Volcanic Body of Mt. Asama. (in English) 291
17. I. MURAI, Pyroclastic Deposits distributed on the East Foot of Volcano Myôkô. (in English) 307
18. T. RIKITAKE and I. TANAOKA, A Differential Proton Magnetometer. (in English) 317
19. G. NISHIMURA and M. SUZUKI, Aseismic Properties of a Wooden House (III). (in English) 329
20. H. MATUMOTO, A Transistor Amplifier for Seismographs. (in Japanese) 345
21. S. MIYAMURA and A. OKADA, Results of Levelling Resurvey between Wakayama and Gobō, Wakayama Prefecture. (in Japanese) 355

Part 3. September, 1960.

22. R. YOSHIYAMA, Propagation of Surface Waves and Internal Friction. (in English) 361
23. Y. SATÔ and R. YAMAGUCHI, Coupling Effect of Shear Vibrations of the Structure with Elastic Foundations, and the Maximum Response of Rocking Motion. (in English) 369
24. T. A. SANTÔ, Rayleigh Wave Dispersions across the Oceanic Basin around Japan (Part II). (in English) 385
25. T. RIKITAKE and K. HÔRAI, Studies of the Thermal State of the Earth. The Fourth Paper: Terrestrial Heat Flows related to Possible Geophysical Events. (in English) 403

26. S. UYEDA and K. HÔRAI, Studies of the Thermal State of the Earth. The Sixth Paper: Terrestrial Heat Flow at Innai Oil Field, Akita Prefecture and at Three Localities in Kanto-District, Japan. (in English) 421
27. T. YUKUTAKE, Stability and Non-Steady State of Self-Exciting Dynamos. II. (in English) 437
28. I. MURAI, Pumice-flow Deposits of Komagatake Volcano, Southern Hokkaido. (in English)..... 451

Part 4. December, 1960.

29. R. YOSHIYAMA, Stability of Waves through a Heterogeneous Medium and Apparent Friction. (in English)..... 467
30. T. ICHIMURA, Xenoliths Included in Granitic Rocks of the Sekine-Azusayama District, Yamagata Prefecture. (in English)..... 479
31. T. MINAKAMI, Fundamental Research for Predicting Volcanic Eruptions. (Part 1) Earthquakes and Crustal Deformations originating from Volcanic Activities. (in English) 497
32. E. SHIMA, Note on the Magnetic Circuit of the Moving-coil Type Seismometer. (in Japanese)..... 545

目　　次

第 38 号

第 1 冊　　昭和 35 年 3 月

論文及報告

頁

1. 非定常ダイナモ (1) (英文) ..... 行武毅 1
2. 地震波のスペクトル構造—マグニチュードと卓越周期の関係—
(英文) ..... 松本利松 13
3. 電磁式地震計の理論的実験的研究 その1 電圧感度について
(英文) ..... 嶋悦三 29
4. プロトン磁力計による箱根火山の磁気測量 (英文) ..... 行武毅・棚岡巌 41
5. 北海道，十勝岳火山の泥流について (英文) ..... 村井勇 55
6. 紀伊半島の局地地震 (第4報)—臨時観測網による震源位置の
決定—(邦文) ..... 宮村摂三 71
7. 紀伊半島南端部附近の地殻変動について (邦文) ..... 岡田惇 113
8. プロトン磁力計の試作研究 (続報) (邦文) ..... 文部省科学試験研究費研究班 125
(代表者 力武常次)
9. 大地震前後の平均海水面変化について (英文) ..... 山口生知 145

第 2 冊　　昭和 35 年 6 月

10. 褶曲境界面における弾性波の反射，屈折
(第1報) SH 波入射の場合 (英文) ..... 浅野周三 177
11. 地球熱学 (第5報) 堆積岩における熱伝導度と含水量の関係 (英文) ..... 宝来帰一・上田誠也 199
12. 大地震発震スペクトルの方位特性に関する一つの試み
(アラスカ地震の場合) (英文) ..... 笠原慶一 207
13. コロンビア型地震計による表面波の観測 (第一報)
—海洋底を伝わるレーリー波の分散— (英文) ..... 三東哲夫 219
14. 脈動源について (第三報)—波浪観測点における脈動観測—
(英文) ..... 三東哲夫 241
15. 蔵王火山の地質学的研究 (第5報) (英文) ..... 市村毅 255
16. 浅間山仏岩火山体岩石の主化学成分組成 (英文) ..... 南英一・松井義人 291
17. 妙高火山東麓に分布する火砕堆積物 (英文) ..... 村井勇 307

18. プロトン磁力計による地磁気傾度計（英文）……力武常次・棚岡巌 317
19. 木造家屋の耐震性（第3報）（英文）……西村源六郎・鈴木正治 329
20. 地震計用トランジスター増幅器（邦文）……松本英照 345
21. 和歌山—御坊間水準測量結果（邦文）……宮村摂三・岡田惇 355

第 3 冊　昭和 35 年 9 月

22. 表面波と地球の内部摩擦（英文）……吉山良一 361
23. 構造物の剪断振動と弾性地盤の相互作用
附：ロッキングの最大倍率（英文）……佐藤泰夫・山口林造 369
24. 海洋底を伝わるレーリー波の分散（第二報）（英文）……三東哲夫 385
25. 地球熱学（第4報）マントル内熱対流その他に伴なう熱流量（英文）……力武常次・宝来帰一 403
26. 地球熱学（第6報）秋田県院内油田，および，関東地方三地点における地殻熱流量（英文）……上田誠也・宝来帰一 421
27. 非定常ダイナモ（2）（英文）……行武毅 437
28. 北海道，駒ケ岳火山の軽石流堆積物（英文）……村井勇 451

第 4 冊　昭和 35 年 12 月

29. 不均質な媒質内を伝る弾性波の安定性について　—見掛けの内部摩擦係数—（英文）……吉山良一 467
30. 山形県関根・梓山地方の花崗質岩に含まれる捕獲岩（英文）……市村毅 479
31. 噴火予知に関する基礎的研究（I）
火山活動に関連する地震と地殻変動（英文）……水上武 497
32. 電磁式地震計の磁気回路について（邦文）……嶋悦三 545

昭和36年1月5日印刷
昭和36年1月10日発行

東京都文京区本富士町一番地
東京大学構内
編纂兼発行者　東京大学地震研究所

東京都新宿区山吹町一八四番地
印刷者　笠井康頼

東京都新宿区山吹町一八四番地
印刷所　株式会社国際文献印刷社

売捌所
東京都中央区日本橋通二丁目六番地
丸善株式会社

Sold by Maruzen Co., Ltd., Nihonbashi-dôri, Chûô-ku, Tôkyô.
Price of this copy: 302 Yen. (Postage exclusive.)

BULLETIN OF

THE EARTHQUAKE RESEARCH INSTITUTE

UNIVERSITY OF TOKYO

Vol. 38, Part 4. December, 1960.

Contents.

Papers and Reports.

Page

29. R. YOSHIYAMA, Stability of Waves through a Heterogeneous Medium and Apparent Internal Friction. (in English) 467
30. T. ICHIMURA, Xenoliths Included in Granitic Rocks of the Sekine-Azusayama District, Yamagata Prefecture. (in English) 479
31. T. MINAKAMI, Fundamental Research for Predicting Volcanic Eruptions. (Part 1) Earthquakes and Crustal Deformations originating from Volcanic Activities. (in English) 497
32. E. SHIMA, Note on the Magnetic Circuit of the Moving-coil Type Seismometer. (in Japanese) 545

Institute Notes.

Index.

(For the papers written in Japanese or in occidental languages, the abstracts are given in occidental languages or in Japanese respectively.)